DIGITAL ACCESS TO SCHOLARSHIP AT HARVARD
DASH.HARVARD.EDU

HARVARD LIBRARY
Office for Scholarly Communication

4d Spectra from BPS Quiver Dualities

The Harvard community has made this article openly available. Please share how this access benefits you. Your story matters

Citation	Espahbodi, Sam. 2013. 4d Spectra from BPS Quiver Dualities. Doctoral dissertation, Harvard University.
Citable link	http://nrs.harvard.edu/urn-3:HUL.InstRepos:11110428
Terms of Use	This article was downloaded from Harvard University's DASH repository, and is made available under the terms and conditions applicable to Other Posted Material, as set forth at http://nrs.harvard.edu/urn-3:HUL.InstRepos:dash.current.terms-of-use#LAA

4d Spectra from BPS Quiver Dualities

A dissertation presented

by

Sam Espahbodi

to

The Department of Physics

in partial fulfullment of the requirements

for the degree of

Doctor of Philosophy

in the subject of

Physics

Harvard University

Cambridge, Massachusetts

May, 2013

© 2013 - Sam Espahbodi

All rights reserved.

Dissertation Advisor: Professor Cumrun Vafa Sam Espahbodi

4d Spectra from BPS Quiver Dualities

Abstract

We attack the question of BPS occupancy in a wide class of 4d $\mathcal{N} = 2$ quantum field theories. We first review the Seiberg-Witten approach to finding the low energy Wilsonian effective action actions of such theories. In particular, we analyze the case of Gaiotto theories, which provide a large number of non-trivial examples in a unified framework. We then turn to understanding the massive BPS spectrum of such theories, and in particular their relation to BPS quivers. We present a purely 4d characterization of BPS quivers, and explain how a quiver's representation theory encodes the solution to the BPS occupancy problem. Next, we derive a so called mutation method, based on exploiting quiver dualities, to solve the quiver's representation theory. This method makes previously intractable calculations nearly trivial in many examples. As a particular highlight, we apply our methods to understand strongly coupled chambers in ADE SYM gauge theories with matter. Following this, we turn to the general story of quivers for theories of the Gaiotto class. We present a geometric approach to attaining quivers for the rank 2 theories, leading to a very elegant solution which includes a specification of quiver superpotentials. Finally, we solve these theories by an unrelated method based on gauging flavor symmetries in their various dual weakly coupled Lagrangian descriptions. After seeing that this method agrees in the rank 2 case, we will apply our new approach to the case of rank n.

Contents

1 Introduction **1**

2 Background **5**

2.1 Seiberg-Witten Solution to super Yang-Mills 5

2.2 BPS Particles in $\mathcal{N} = 2$ Field Theories 10

2.3 Gaiotto Theories 12

3 BPS Quivers **18**

3.1 Quivers and Spectra 19

3.1.1 From BPS Spectra to BPS Quivers 20

3.1.2 From BPS Quivers to BPS Spectra 23

3.1.3 Composing Maps - Insights from Geometric Engineering 26

3.2 Finding BPS Quivers Directly 28

3.3 Quiver Representations 29

3.4 Passing a Quiver through a Wall 32

3.4.1 Examples from Argyres-Douglas Theories 33

4 The Mutation Method **37**

4.1 Quiver Duality 39

4.1.1 Argyres-Douglas Revisited 42

4.1.2 Justification of Mutation 44

4.2 The Mutation Method: BPS Spectra from Quiver Dualities 48

5 $SU(2)$ Gauge Theories **55**

5.1 Pure $SU(2)$ 55

5.2 Adding matter 60

5.3 Massless $N_f = 1$ 61

5.4 Massive $N_f = 1$ 66

5.5 Massless $N_f = 2$ 67

5.6 Massless $N_f = 3$ 71

5.7 $N_f = 4$ . . . 72

6 $SU(N)$ Gauge Theories **74**

6.1 Construction of $SU(N)$ Quivers . . . 74

6.2 General ADE-type Gauge Group . . . 78

6.3 BPS Spectra of Pure $SU(N)$ SYM . . . 80

6.3.1 $SU(3)$ . . . 80

6.3.2 $SU(N)$ at Strong Coupling . . . 84

6.4 Adding Matter . . . 89

6.5 BPS States of SQCD . . . 91

6.6 Further ADE examples . . . 92

7 Complete Gaiotto Theories **93**

7.1 Triangulations from Special-Lagrangian Flows . . . 98

7.2 BPS Quivers from Ideal Triangulations . . . 103

7.3 The Superpotential . . . 107

7.4 $SU(2)$ Revisited . . . 111

7.4.1 Asymptotically Free Theories . . . 111

7.4.2 Conformal Theories . . . 113

8 Quiver Gauging and Non-Complete Gaiotto **115**

8.1 Flavor Symmetries and Gauging . . . 116

8.2 Quivers for Gaiotto Building Blocks . . . 119

8.3 Rank 2 Quivers . . . 120

8.4 Rank 3 Quivers . . . 124

8.5 $\mathcal{N} = 2^*$ . . . 128

Acknowledgements

I thank my advisor, Cumrun Vafa. His ability to cut to the essence of a problem is remarkable, and if I have learned even a small fragment of this ability, I will have gained much. Working with him on physics for the last several years has been a pleasure. I would also like to thank my other collaborators - Ashwin Rastogi, Clay Cordova, Babak Haghighat, Sergio Cecotti and Murad Alim - who have provided numerous ideas and insights.

To me the insane asylum always seemed counterproductive. Having lost touch with reality, what a poor remedy it must be to find oneself in a room with N different conceptions of it, all colored by a unique break from the world as it ought to appear. And yet, this formula has worked wonders in graduate school at Harvard. Insanity unappreciated is confusing, annoying. Insanity understood, however, is a beautiful thing.

To some fellow inmates, then, I give thanks: To Richard White, Dionysios Anninos, Frederik Denef, Ashwin Rastogi, Irene Bredberg, Tarek Anous, Lauren Hartle, Lauren Merrill, Nick Van-Meter, Sharon Traiberman, Tongyan Lin, Norman Yao, Jana Renee and Kelechi Adibe - thank you for your respective conceptions of the world. They have colored mine in ways I cherish.

For a few, I must take an unprecedented break from the parable of the rubber room. Richard, thank you for unwavering friendship in a bizarre world. Dio, for staying inspired in the face of anything; may you always have a cholula. Ashwin, thank you for the road traveled. And Frederik, for musings shared around a vision understood; may you always sample widely.

Finally, I thank my mother, father and sister Sara, who have put up with my inanity, batting only a few eyes.

Citations to Previously Published Work

Large portions of sections 3 to 6, as well as 8, have appeared in the following paper:

> "N=2 Quantum Field Theories and Their BPS Quivers," M. Alim, S. Cecotti, C. Cordova, S. Espahbodi, A. Rastogi, C. Vafa. hep-th/1112.3984

Chapter 7 has largely appeared in

> "BPS Quivers and Spectra of Complete N=2 Quantum Field Theories," M. Alim, S. Cecotti, C. Cordova, S. Espahbodi, A. Rastogi, C. Vafa. hep-th/1109.4941

Electronic preprints are available on the Internet at the following URL:

> `http://arXiv.org`

If a blind man leads a blind man, both will fall into a pit.

—Matthew 15:14

1 Introduction

Our story begins with the study of four dimensional quantum field theories which exhibit an enhanced spacetime symmetry group - namely, so called $\mathcal{N} = 2$ supersymmetry in four dimensions. One may ask why such theories are worthy of study. Indeed, while in recent history many have assumed the effective field theory of nature possesses (broken) $\mathcal{N} = 1$ supersymmetry in 4 dimensions, $\mathcal{N} = 2$ SUSY is usually ruled out because we observe chiral fermions in nature.

Thus, if we accept that the effective theory of nature does not have $\mathcal{N} = 2$ supersymmetry, why has the study of $\mathcal{N} = 2$ theories received so much attention and devotion? The justification we will adopt here is simply that field theories are hard, and in addition to studying perturbative aspects of low energy theories which are candidate theories for real world, it is inherently useful to study those examples in which we can gain deeper understanding. The reader who prefers more precise statements can here replace the word 'deeper' with 'non-perturbative.' Of course, if the physical aspects of these theories had no bearing on their less supersymmetric brethren, one might object to this reasoning. But we are lucky in that this is not the case. Indeed, many physical features are common in the space of all non-trivial field theories. Thus, we hope that if we find a deep understanding of this subset of field theories, to which the mathematics has granted tractability, it will shed light on features of those theories which are indeed viable effective theories of nature.

The study of $\mathcal{N} = 2$ theories is not a new phenomenon. Indeed, we are nearing the second decade after which great strides were made in understanding $\mathcal{N} = 2$ quantum field theories, namely by the so-called Seiberg-Witten solution to their low energy dynamics. While Seiberg and Witten (and vast quantities of subsequent work) solved for the structure of the quantum moduli spaces of large classes of $\mathcal{N} = 2$ examples, another question went unanswered in most complex examples. Namely, we can ask, at a given point in moduli space, which supersymmetric particles actually exist in the theory. In other words, which particles in the theory disintegrate, and which are stable against decay. The famous Kontsevich-Soibelman wall crossing formula partially addresses this question, by placing a constraint on possible answers.

Kontsevich-Soibelman is, of course, just one piece of the recent progress made both in mathematics and in physics, in understanding the universal rules that govern potential decay processes of BPS particles [4–7], and continuing progress in this subject [11–22, 24–26] suggests that there

are yet undiscovered structures lurking in the BPS spectra of field theories. However in spite of these dramatic developments, there exists no general method for calculating the BPS spectrum of a given field theory. The work that forms the body of this thesis presents a partial solution to the next step of the puzzle, by taking advantage of a construct known as a BPS quiver.

In particular, we study theories whose spectra of BPS states can be calculated from the quantum mechanics of an associated BPS quiver. Such quivers originally arose in string theory constructions of quantum field theories [27, 29–33, 35]. In that context, there is a natural class of BPS objects, namely D-branes, and a quantum mechanical description of the BPS spectrum is provided by the worldvolume theory of the relevant branes. This string theory setup provides a simple way of organizing the spectrum into elementary BPS branes and their bound states, and explains the non-abelian degrees of freedom needed in the quiver description.

While the geometric engineering perspective provides a useful source of examples, our focus in this work is on analyzing the theory of BPS quiver directly from the point of view of 4d quantum field theory. The class of BPS quiver theories is broad, and includes gauge theories coupled to massive hypermultiplets, Argyres-Douglas type field theories [36], and all theories defined by M5 branes on punctured Riemann surfaces [21,24,37–41,43]. For all of these theories, the quiver appears to provide a simple and unique characterization of the theory, and one of the aims of this work is to illustrate in a variety of examples how simple graphical features and operations at the level of quivers translate into physical properties and constructions such as flavor symmetries, gauging, decoupling limits, and dualities. As a particular highlight, in section 8 we study the quiver version of a strong coupling duality [44] given by the relationship between the theory of $SU(3)$ coupled to six fundamental flavors, and the E_6 Minahan-Nemeschansky theory [45] coupled via gauging an $SU(2) \subset E_6$ to $SU(2)$ Yang-Mills with an additional fundamental flavor (a duality we review in section 2.3).

We begin in section 2 by reviewing the concept of dualities in $\mathcal{N} = 2$ field theories. In particular, we begin by posing the famous monodromy problem for pure $SU(2)$, as discovered by Seiberg and Witten. We describe how the solution to this monodromy problem characterizes the low energy effective description of the theory. We then discuss the question of BPS states in the field theory, and demonstrate by a consistency analysis that one can discover which BPS particles are stable in each region of moduli space. Of course, this simple reasoning does not extend to more complex

theories, and later in the work we'll come back and solve the $SU(2)$ theory again with our more general methods. Before concluding our background material, we will discuss a very broad class of superconformal theories, which we will find especially interesting down the line.

In section 3 we turn to a detailed description of the way in which quiver quantum mechanics encodes the spectrum of BPS states. We then develop the theory of quiver representations, the holomorphic description of quiver quantum mechanics, and explain how quivers yield a concrete method for studying wall-crossing phenomenon. A significant feature of quiver description of the spectrum is that a fixed quiver typically describes the BPS particles only on a small patch of the moduli space of a given theory. A key role is then played by quantum mechanical dualities, encoded by quiver mutations, which relate distinct quivers valid in different regions of parameter space. These relationships between a priori distinct quantum mechanics are a one-dimensional version of Seiberg duality [46]. Their basic content is that the BPS spectrum can be decomposed into bound states of primitive particles in more than one way by suitable changes of the set of building block BPS states. In section 4 we discuss these dualities and analyze the constraints that they impose upon the BPS spectrum. Remarkably we find that these consistency conditions are so powerful that frequently they completely determine the BPS spectrum. This results in an algorithm, the mutation method, for calculating a spectrum, which is far simpler than a direct investigation of the quantum mechanics.

In sections 5 and 6, we study the BPS spectra of $SU(N)$ gauge theories, with and without matter. We begin by re-deriving the result for pure $SU(2)$, and then move on to much more interesting examples which were previously not understood. For example, in section 6 we construct the quiver for the pure $SU(N)$ theory, and then set up a computational apparatus to track the quiver as we move in moduli space. For $SU(3)$ we're able to follow the quiver from weak to strong coupling explicitly, and see quite directly our infinite weak coupling spectrum transform, as we pass through a wall, to a strongly coupled six state chamber.

In section 7 we turn to a specific class of theories termed complete. These are theories in which the central charges can locally be taken to be coordinates on moduli space. In particular, we study the intersection of the set of Gaiotto type theories and complete theories. Theories of this type admit a very elegant solution. The BPS quiver is encoded in combinatoric information governing flows on the Gaiotto surface which defines the theory. Results from the mathematics literature fix

a natural choice of superpotential for theories of this type. This is one of the few examples in which the BPS quiver superpotential is known explicitly.

Finally, in section 8 we turn to general theories of the Gaiotto type. The approach of section 7 does not extend to the general case, so we use a new approach. In particular, we analyze how one can gauge flavor symmetries in a quiver. Using results from [38] reviewed in section 2.3, we're able show how one can construct the quiver for a Gaiotto theory by starting with quivers for the building blocks (which we also derive).

Frequently our mutation method is powerful enough to determine the BPS spectrum in a strongly coupled chamber where there are only finitely many BPS states. Let $\mathcal{B}$ denote the set of BPS particles at strong coupling, and $|\mathcal{B}|$ the number of such particles. Then a summary of the gauge theories whose strong coupling spectra we determine is:

- $SU(N_c)$ gauge theory coupled to N_f fundamentals.

$$|\mathcal{B}| = N_c(N_c-1) + N_f(2N_c-1)$$

- $SO(2N_c)$ gauge theory coupled to N_v vectors.

$$|\mathcal{B}| = 2N_c(N_c-1) + N_v(4N_c+1)$$

- E_6 gauge theory coupled to $N_{\mathbf{27}}$ fundamental $\mathbf{27}$'s.

$$|\mathcal{B}| = 72 + 73N_{\mathbf{27}}$$

- E_7 gauge theory.

$$|\mathcal{B}| = 126$$

- E_8 gauge theory.

$$|\mathcal{B}| = 240$$

One elegant feature of the above results can be seen in the limit where there is no matter whatsoever so that one is considering the strong coupling BPS spectrum of pure super-Yang-Mills with an

arbitrary ADE gauge group. Then our results can be summarized by noting that the number of BPS particles is given simply by the number of roots in the associated Lie algebra.

2 Background

2.1 Seiberg-Witten Solution to super Yang-Mills

A requisite step in understanding the BPS occupancy of $\mathcal{N} = 2$ quantum field theories is understanding the structure of their moduli spaces. Thus, we will undertake a brief review of the breakthrough Seiberg-Witten solution which paved the way to this understanding in a huge class of theories. We begin with the same example that Seiberg and Witten did, pure $SU(2)$ SYM [1]. This seemingly simple example captures the essential insights which are quite universal in the analysis of this entire class of theories. Our aim is simply to remind the reader of the features which will be relevant in the present work.

The key notion that allows one to make progress in understanding this theory, and indeed all of the theories that we will consider, is that of duality. Naively, we might look for an electro-magnetic like duality of the UV theory above, but no such duality exists. Heuristically we can see this by noting that such a duality would act on the coupling, but as the coupling in this theory runs with energy scale, this is ill-defined. This then precludes the existence of such a duality in the UV.

Instead, for $\mathcal{N} = 2$ theories we will find that there are dualities in the description of the extreme infared physics. To be precise, we are interested in theory described by the Wilsonian effective action at extreme low energies, where all massive charged particles have been integrated out. We will see that the infared theory is a free $U(1)$ theory that exhibits an electro-magnetic like duality which acts on the complexified coupling.

To understand the moduli space of our theory, we start by examining its classical incarnation, determined by the form of the bosonic potential after the auxiliary fields have been integrated out. We find

$$S_{\text{pot}} = -\int d^4x \frac{1}{2}\text{tr}\left([\phi^\dagger, \phi]\right)^2$$

where ϕ is the complex scalar in the vector multiplet. We note that the field configurations which leave supersymmetry unbroken are those which lie in the Cartan subalgebra of our gauge group.

Classically, we therefore can parametrize gauge-inequivalent SUSY preserving vacua by $u = \mathrm{tr}\phi^2$.

While a VEV of ϕ in the Cartan does not break SUSY, it does break the gauge symmetry, $SU(2) \to U(1)$, and gives masses to the non-Cartan elements of the gauge field. It is clear by supersymmetry that it must also give masses to the corresponding fermions in the theory. Thus, in the infared Wilsonian picture, where particles with finite mass have been integrated out, we are left with a free $U(1)$ theory coupled to classical sources. The general $\mathcal{N} = 2$ two-derivative action with $U(1)$ gauge symmetry is given by

$$S = \frac{1}{16\pi} \mathrm{Im} \int d^4x \left[\int d^2\theta \mathcal{F}''(\Phi) W^\alpha W_\alpha + \int d^2\theta d^2\bar{\theta} \Phi^\dagger \mathcal{F}'(\Phi) \right]$$

where $\mathcal{F}$ is a holomorphic prepotential that thus encodes the Lagrangian. Thus, to understand the infared effective action, we must understand the structure of the moduli space (the geometry of the $\mathrm{tr}\phi^2$ manifold), and the functional form of the prepotential $\mathcal{F}$, which so far is only constrained to be holomorphic. It is the notion of duality that will accomplish for us this seemingly insurmountable task.

To see that this theory indeed has a duality, we define a dual field

$$\Phi_D = \mathcal{F}'(\Phi)$$

and a function $\mathcal{F}_D$, such that

$$\mathcal{F}'_D(\Phi_D) = -\Phi.$$

The action can be written

$$S = \frac{1}{16\pi} \mathrm{Im} \int d^4x \int d^2\theta \frac{d\Phi_D}{d\Phi} W^\alpha W_\alpha + \frac{1}{32\pi i} \int d^2\theta d^2\bar{\theta} \left(\Phi^\dagger \Phi_D - \Phi_D^\dagger \Phi \right),$$

which is (in the path integral) invariant under $Sl(2,\mathbb{Z})$ transformations of the pair $(\Phi_D, \Phi)^t$. We note that this $Sl(2,\mathbb{Z})$ acts on τ with the standard upper half-plane action. Thus, the duality group in particular contains the electro-magnetic like duality transformation $\tau \to -1/\tau$.[1]

So the theory possesses a duality - there are multiple Lagrangian descriptions of the same

[1] We note, however, that this will not turn out to be an element of the monodromy group below.

physics - but how does this help us understand the moduli space? We consider a simple thought experiment: Say we start at a given point on moduli space, and follow a given closed curve, tuning moduli as we go. When we finish traversing and return to our starting point, we must of course return to the same theory. Naively we would say that the theory is described by $(a_D, a)^t$, so that these quantities must return to themselves upon traversing the loop. But in reality, nothing says that we must return to the same Lagrangian description of the theory, that is, to the same a and a_D. We must simply return to the same physics, perhaps as described by a duality transformed a and a_D. Mathematically, we say that $(a_D, a)^t$ is not constrained to be a function on moduli space, but rather a section of a flat bundle.

Indeed, we will see that in the semi-classical region of large u, a monodromy around infinity acts non-trivially on $(a_D, a)^t$: The section is non-trivial. We will find the quantum moduli space by posing and solving the corresponding monodromy problem.

To derive the result at infinity, we note that the pure $SU(2)$ theory is asymptotically free, and if we turn on the Higgs field, the coupling of the theory stops running when the lightest charged particle is integrated out. Since the mass of charged particles is set by the VEV of ϕ, for large $u = \mathrm{tr}\phi^2$ (compared to the strong coupling scale Λ^2) the theory is weakly coupled, and the behavior in this region is understood. Namely, the theory has perturbative corrections up to one loop, as well as instanton corrections, of the form

$$\mathcal{F}(\Phi) = \frac{1}{2}\tau_0\Phi^2 + \frac{i}{\pi}\Phi^2 \log\frac{\Phi^2}{\Lambda^2} + \frac{1}{2\pi i}\Phi^2 \sum_{l=1}^{\infty} c_l \left(\frac{\Lambda}{\Phi}\right)^{4l}$$

This allows us to trivially compute the monodromy around a circle at infinity. In particular, we have

$$M_\infty = \begin{pmatrix} -1 & 4 \\ 0 & -1 \end{pmatrix}.$$

The semi-classical expansion allows us to understand the moduli space near infinity, but what form does it take in the interior of the complex plane? Once again we first ask the question about the classical moduli space. Classically, we expect there to be a singularity in the moduli space at $u = 0$ because this point corresponds to turning off the VEV of the complex scalar. Turning off the Higgs VEV sends the mass of the charged particles (for example, the W^+ and W^-) to zero,

which means that our $U(1)$ Wilsonian effective action does not have enough degrees of freedom to describe the theory at this point. Thus from the perspective of our infared description, we have a singularity in the moduli space at this point.

However, it turns out that no solution with only two singularities in the quantum moduli space gives a theory which is everywhere unitary. Instead, Seiberg and Witten considered the possibility that there are points in the quantum moduli space where, instead of electrically charged particles becoming massless, BPS dyons became massless. A BPS particle is one that saturates the BPS bound, $|Z| \leq M$. In the $SU(2)$ theory these states are specified by their electric and magnetic quantum numbers, (q, g), and have central charge $Z = qa + ga_D$. At a point where such a particle goes massless, it is known that there is a monodromy of the form [94]

$$M = \begin{pmatrix} 1 + qg & q^2 \\ -g^2 & 1 - qg \end{pmatrix}$$

It is ultimately irrelevant which dyon we choose to go massless (simply shift by a global redefinition), so we will take a magnetic monopole to go massless at $u = \Lambda^2$. Since the product of monodromies is constrained, if we assume only 3 singularities,[2] the particle which goes massless at the second point in the interior of $\{u\}$ will be determined.

To find a solution to this monodromy problem, we will introduce a so-called spectral surface, which is fibered over our moduli space. At this point, this surface merely appears as a tool for solving the 4d field theory, but we will see that it is intimately related to changes in the properties of BPS particles as we vary moduli. From a 4d field theory perspective, it is a little bewildering that a such an essential feature of the theory has a geometric character, unrelated to the 4d geometry. It turns out that this geometrical structure pops out beautifully from string theory.

For the $SU(2)$ theory, the monodromy group gives us a hint as to what surface might be relevant; namely, the monodromies form a subgroup of $Sl(2, \mathbb{Z})$, the modular group of the torus. Thus we take the surface described by

$$y^2 = (x^2 - u)^2 - \Lambda^4,$$

which is a torus, except at $u = \pm\Lambda^2$, where the curve becomes singular. We recall that in the

[2]Indeed, it can be shown that this is the only solution.

moduli space of a geometry that includes singularities, basis cycles on the geometry undergo a well-defined transformation as we tune moduli in cycles around the singularities. This is natural, since at a singularity where a cycle vanishes, there is no change when we add some copies of that cycle to other, non-vanishing cycles. The precise transformation that arises is called Picard-Lefschetz monodromy. This is very similar to the transformation of a and a_D around singularities in the physical moduli space of our theory. Indeed, if we can express our 4d quantities a and a_D as period integrals of some 1-form on our auxiliary surface, we can be hopeful that we will be able to reconstruct the Lagrangian transformations we are looking for from Picard-Lefschetz monodromy.

A hint as to precisely what a and a_D should be identified with is provided by the fact that the torus provides a natural quantity to serve as the effective coupling of the 4d theory (which must have positive imaginary part for all moduli). Namely, this is just the period of the torus. If we take two cycles, α and β which define a basis for $H_1(T^2)$, with intersection $\alpha \cdot \beta = 1$, and ω is the holomorphic differential

$$\omega = \frac{1}{\sqrt{2}\pi}\frac{dx}{y},$$

then we can define

$$\tau = \frac{\oint_\beta \omega}{\oint_\alpha \omega}.$$

Since $\mathrm{Im}\tau$ is positive on the moduli space of complex structures of the torus, this will guarantee that the field theory is everywhere unitary.[3] From here we can work backwards, and find that a and a_D can also be defined as period integrals over α and β of the so-called Seiberg-Witten differential,

$$\lambda = \frac{1}{\sqrt{2}\pi}x^2\frac{dx}{y},$$

which is meromorphic on T^2.

Finally, since our central charge function is given by $Z = ga_D + qa$, we can express the central charge of the state (g, q) by

$$Z = g\oint_\beta \lambda + q\oint_\alpha \lambda = \int_\nu \lambda$$

where $\nu = g\beta + q\alpha$. Thus we see that it is natural to identify BPS states with cycles on spectral

[3]If not already evident, we note that the moduli space of complex structures will be identified with the physical moduli space of the theory.

surface. Indeed, if we do this one can check that the vanishing cycles precisely correspond to the 4d particles which go massless at $\pm\Lambda^2$. Thus the picture is consistent, and has given us what from field theory appears an odd relation between BPS states and cycles on an auxiliary spectral surface.

To explicitly calculate $\mathcal{F}$, we can use Picard-Fuchs equations to give differential equations for the dual form of the Lagrangian which is weakly coupled in the region of interest. However, this is not the direction of interest for us. Instead, we will recap what we have found, and then move on to a more detailed discussion of the BPS particles themselves.

We have seen that the moduli space of the extreme infared theory is equivalent to the moduli space of complex structures of an auxiliary spectral surface.[4] This surface comes equipped with a Seiberg-Witten differential - a meromorphic form which relates the monodromy of cycles on the surface to the monodromy of the Lagrangian description of the infared field theory. Additionally, massive BPS states can be associated with cycles on this Riemann surface. Periods of the Seiberg-Witten differential then give the central charges of these particles. The question that remains unanswered is this: Which cycles correspond to states that exist and are stable against decay in the 4d field theory? This question is the focus of our work.

2.2 BPS Particles in $\mathcal{N} = 2$ Field Theories

As we mentioned in the previous section, there is a collection of distinguished particles, referred to as BPS, which saturate the central charge bound of the $\mathcal{N} = 2$ algebra, $|Z| \leq M$. For the $SU(2)$ theory, these states are labeled by a pair of integers (q, g).[5] We saw in the previous section that for a given pair of integers, (q, g), we could assign a central charge by integrating our Seiberg Witten differential λ along the cycle $\nu = q\alpha + g\beta$.

However, just because we calculate such a central charge does not mean that it corresponds to the charge of some stable particle in the theory. Indeed, we can ask whether a given slot in the central charge lattice is actually occupied in our theory or not. This is the question of BPS spectroscopy, and the question we quite broadly aim to answer in this work.

For the pure $SU(2)$ theory, we can find a rather simple solution by considering a consistency

[4]Indeed, this is quite general, and is explained by string constructions, as we describe in section 3.1.3.

[5]More precisely, the charge should also be considered a section of our flat bundle. Thus there is some ambiguity in labeling our states by integers.

check on the Seiberg-Witten solution. We will find that the moduli space is divided into two chambers. Namely, there is a weak coupling chamber, which includes the semi-classical limit of large u, in which there is an infinite spectrum, including the W bosons and a tower of dyons. There is also a strong coupling chamber, in which only two BPS states are stable. These two chambers are separated by a curve, called the curve of marginal stability, which we can explicitly describe.

In a general $\mathcal{N} = 2$ field theory, the moduli space is higher dimensional, and there will be many codimension one hypersurfaces which divide our moduli space into different chambers. By a chamber, we mean a region in which the set of occupied BPS states is constant (of course, the charges of these states vary locally as we tune moduli; it is the occupancy we're referring to). These hypersurfaces are known as walls of marginal stability. In general the chamber structure for a theory is quite complex. The pure $SU(2)$ theory, however, has the advantage of being, relatively, quite simple.

A key quantity in the $SU(2)$ theory is the ratio a_D/a. If this is not real, the lattice of possible BPS states is non-degenerate. In particular, for q and g relatively prime, conservation laws prevent a state (q, g) from decaying if we stay in a region $a_D/a \in \mathbb{R}$. Thus, we can define a curve $\mathcal{C} = \{\text{Im } a_D/a = 0\}$; this will be our curve of marginal stability. One can numerically calculate $\mathcal{C}$ from the Seiberg-Witten solution. One finds that it is a near ellipse, passing through $\pm\Lambda^2$ [3]. For any points that are connected by some path not intersecting $\mathcal{C}$, the occupancy of BPS states must be identical. That's because one can start at either of the points, tune moduli to the arrive at the other, and at no point did any states have the opportunity to decay. However, nothing tells us that the two regions separated by this curve of marginal stability must have an identical spectrum.

The key insight is to note that for a particle that is massless, $|qa + ga_D| = 0$. Clearly, for any choice of $q, g \in \mathbb{Z}$, the ratio $a_D/a = -q/g$ will be real at such a massless point. Thus, particles can only become massless on the curve $\mathcal{C}$. It becomes quite interesting then to calculate which values a_D/a actually takes on on $\mathcal{C}$. In [3] it is found that a_D/a takes on all values in $[-1, 1]$. Thus, if we start with any state in the weak coupling region with $-q/g \in [-1, 1]$, it will become massless at some point on $\mathcal{C}$. Of course, we recall that a massless BPS particle will be seen as a singularity in the $U(1)$ Wilsonian effective description. These singularities were precisely determined by solving the monodromy problem. Thus, in this case, we will be able to use consistency of the Seiberg-Witten solution to determine the spectrum. Of course, a state that's massless on $\mathcal{C}$ must exist on

both sides, because it can't decay, being the only massless charged particle. Thus, we immediately conclude that the monopole and dyon that become massless on $\mathcal{C}$ must exist in both chambers.

Now we will ask what other particles are stable on each side. This requires two tricks. The first is the use of a $\mathbb{Z}_2$ symmetry the theory admits, which takes $u \to -u$. With some work [3], one can show that this symmetry is manifest on the BPS spectrum, relating the particles at u to those at $-u$. The second piece of the puzzle is noting that if one undergoes a monodromy that does not pass through a wall of marginal stability, it implies a symmetry of the BPS spectrum. Thus, for example, the monodromy at infinity implies the existence of the tower of dyons in the weak coupling spectrum. With these two transformations, one can then essentially determine if a particle is in the theory by doing some monodromy and $\mathbb{Z}_2$ transformations until getting to a charge that would become massless on $\mathcal{C}$. If this particle is one of the two singularities, the original particle should be in the spectrum. If not, it is not.

Putting these pieces together, one finds that the particle spectrum at weak coupling can contain only the W bosons and the towers of dyons, while at strong coupling we simply have the monopole and dyon. We will return to the question of the pure $SU(2)$ spectrum in section 5.1 using our own methods, and find agreement with this result.

2.3 Gaiotto Theories

In section 2.1, we explored a very simple $\mathcal{N} = 2$ quantum field theory, possessing a single $SU(2)$ gauge group, with no additional matter beyond that required by $\mathcal{N} = 2$ supersymmetry. As we saw in the following section, the BPS structure of this theory is already understood using a simple consistency check. In this work, we aim to attack a much broader set of field theories, however, and we'll need a more sophisticated approach. In the sections that follow, we will see that an intricate structure emerges to characterizes the BPS spectrum.

Before we get ahead of ourselves, however, we would be well served by considering examples of some more complicated field theories. Seiberg and Witten themselves, after describing the pure $SU(2)$ theory, went on to describe $SU(2)$ gauge theories with additional matter, in [2]. Of course, when trying to produce examples of complicated gauge theories through UV Lagrangians, we are not limited to specifying more complicated matter content; we can also complicate our gauge group. Indeed, many papers in the tradition of Seiberg and Witten went on to analyze higher rank $SU(n)$

gauge groups, and other groups of the ADE type [90–94].

Of course, obvious constraints limit us from discussing the complete details of all the various theories that have been analyzed, and to which our methods will apply. Indeed, in section 3 when we discuss our construction, we will list the generic inputs that are required from any $\mathcal{N} = 2$ theory to which our method applies, and see that we can propose a solution in a general way, regardless of many of the individual details at play in each example.

However, there is a special class of theories we will be especially interested in, which admits a unified description. Let us give a brief preview to clarify this point: These theories will be described by complex surfaces. Surfaces which describe theories in this class can be glued together to give a surface describing another such theory. It turns out that this glueing rule can be applied in a systematic way to the structures describing the BPS spectra of the theories, resulting in a structure describing the resultant BPS spectrum. We will explore this in section 8, and see how it allows us to solve for the BPS spectra of quite mystifying theories. Another feature of this class of theories is that, if decoupling limits are included, it contains a large fraction of the individual gauge theory examples we mentioned above. Thus it is clear that understanding these theories in a general way will be quite fruitful. These theories have recently been termed "theories of the Gaiotto type," after the analysis of their duality structure in [38].

In this section we will study these Gaiotto type theories. Our aim is two-fold: First, we hope to convey that the notion of duality plays an important role in the description of a general $\mathcal{N} = 2$ theory, and not just in the pure $SU(2)$ case. Second, our review in this section will lay the foundation for our discussion of the BPS spectra of these theories in section 8.

Theories of the Gaiotto type are superconformal. In their weakly coupled descriptions, this means that the gauge groups in the theories are all coupled to enough matter so that their beta functions vanish. In the case of an $SU(N)$ gauge group coupled to fundamental matter, this takes $N_f = 2N$ generations. The key insight of Gaiotto was that many seemingly different theories, defined by Lagrangians with different gauge and matter content, are in fact different weakly coupled cusps of a single $\mathcal{N} = 2$ theory defined by wrapping M5 branes on a Riemann surface. This fundamental insight can be intuitively discovered from 4d by considering S-dualities similar to dualities we saw present in the pure $SU(2)$ theory.

We will begin by considering 4d theories with gauge groups $SU(2)^n$. The theory with $n = 1$

(recall that superconformality then imposes $N_f = 4$) was studied in [2]. The moduli space of this theory is given by $\mathbb{H}/Sl(2,\mathbb{Z})$, and features a single cusp where the theory becomes arbitrarily weakly coupled. The novel feature for us is that this theory has a flavor symmetry. Indeed, such flavor symmetries will be fundamental to our discussion here and in section 8. Since the fundamental of $SU(2)$ is pseudoreal, the naive $SU(4)$ flavor symmetry in this theory is enhanced to $SO(8)$. It will be fruitful for us to consider the $SO(4) \times SO(4)$ subgroup, which we describe by $SU(2)_a \times SU(2)_b \times SU(2)_c \times SU(2)_d$. From [2], we know that S-duality acts not only on τ, but also on the flavor symmetry SO(8) by triality. By considering how the different 8 dimensional reps of SO(8) decompose under the $SU(2)^4$ subgroup, we find that this S-duality action effectively permutes the labels $\{a, b, c, d\}$.

Of course, our real interest is in what happens to more complicated examples that have multiple $SU(2)$ gauge groups. Let's consider a theory with three, which we label $SU(2)_1 \times SU(2)_2 \times SU(2)_3$, coupled linearly by bifundamentals. Of course, for superconformality we must couple two additional fundamentals each to $SU(2)_1$ and $SU(2)_3$. The reader may recognize this as a simple linear quiver gauge theory. We have an $SU(2)^6$ flavor symmetry; the bifundamentals each contribute an $Sp(1) \cong SU(2)$ because they lie in real representations of the gauge group. Lets label these a through f, from "left to right". Now we may ask, what are the dualities? Seiberg and Witten haven't solved this theory for us, so it's not obvious how to proceed.

We will make a reasonable, intuitive guess from 4d (which is validated in the M-theory construction in [38]). Namely, if turn off all but one gauge coupling, the theory would reduce to the case of one $SU(2)$ gauge group with $N_f = 4$, discussed above, and we would have a known $Sl(2,\mathbb{Z})$ action. We will assume that as we push the same gauge couplings arbitrarily close to their weakly coupled cusps, this same duality will apply. Let's do this to $SU(2)_1$ and $SU(2)_3$. The matter coupled to $SU(2)_2$ is in the rep

$$(2_2 \otimes 2_1 \otimes 2_c) \oplus (2_2 \otimes 2_3 \otimes 2_d).$$

(c and d label the $SU(2)$ factors associated to the bifundamentals.) We saw that S-dualities will permute the flavor symmetries as seen by this gauge group. Namely, the $\{1, c, 3, d\}$ labels will be permuted. There is a particularly interesting permutation which doesn't just return a relabeled version of original linear quiver theory. Namely, we can arrive at the theory in which the matter

at $SU(2)_2$ is described by

$$(2_2 \otimes 2_1 \otimes 2_3) \oplus (2_2 \otimes 2_c \otimes 2_d).$$

This leaves us a very interesting theory, which [38] labels a "generalized quiver theory." In particular, we have matter, a so called block of four hypermultiplets, that is charged under all three gauge groups. The block of four hypermultiplets can be thought of on its own as a superconformal theory with no marginal gauge couplings. This theory has $SU(2)^3$ flavor symmetry,[6] and we call it $\mathcal{T}_2$. We can then think of the theory we've arrived at as being constructed by taking 4 copies of $\mathcal{T}_2$. We gauge one $SU(2)$ in 3 of the 4 copies, gauge all three $SU(2)$s of the remaining $\mathcal{T}_2$, and identify them each with one of the former.

The theory we started with, on the other hand, was (naively) quite different. We again had 4 $\mathcal{T}_2$ theories, but this time we laid them in a line and diagonally gauged $SU(2)$s between each neighboring pair. That these generalized quivers with quite different topologies are linked by duality is quite remarkable. In fact, it turns out that all such generalized quivers with a fixed number n of $SU(2)$ flavor symmetries and fixed genus, g, correspond to different weak coupling duality frames of a single 4d $\mathcal{N} = 2$ theory called $\mathcal{T}_{n,g}[A_1]$. The general theory can be described by a string compactification on the surface

$$x^2 = \phi_2(z) + uv$$

where (x, z, u, v) are coordinates on a bundle over a Riemann surface with n punctures, and ϕ_2 is a quadratic differential on this surface, with poles at the punctures (see section 7 for additional details). Each puncture corresponds to a flavor symmetry factor. One can also easily turn on mass deformations and give a similar description. Forgetting the analytic structure of the surface yields the SW curve for the theory, and indeed with mass deformations turned on, the integral of the SW differential around the punctures yields the corresponding mass parameter m.

A careful analysis of the structure of the surface reveals that in the limit where a tube in the surface is pinched off, it splits into two surfaces,[7] each with an additional puncture, with equal residues. If we are at a point in moduli space where the theory can be interpreted as a weakly coupled generalized quiver theory, this degeneration corresponds to going to the weakly coupling

[6] Though this symmetry acts on half-hypermultiplets, a fact which will become important in section 8.

[7] Or, with $g \geq 0$ possibly a single connected genus $g - 1$ surface is left.

cusp of a gauge group. This gauge group decouples, leaving its $Tr\Phi^2$ as the mass deformation seen on either side of the remaining theories' newfound $SU(2)$ flavor symmetries.

Of course, there are gauge groups more complicated than $SU(2)^n$. We move next to include factors of $SU(3)$. We begin again with a single $SU(3)$ gauge group coupled to $N_f = 6$ hypermultiplets. The moduli space of this theory contains, as in the $SU(2)$ case, a weakly coupled cusp. But it also includes something more interesting - a strongly coupled one. At this cusp, there is a dual description of the theory which is weakly coupled. Remarkably, though, this weakly coupled dual description does not have gauge group $SU(3)$, it has gauge group $SU(2)$.

To understand this dual description we must understand the E_6 Minahan-Nemeschansky theory [45]. This is an interacting superconformal theory with E_6 global symmetry. The theory is isolated in the sense that it has no marginal gauge couplings. It does, however, have a nontrivial moduli space parametrized by a dimension 3 operator. So, what is the entire theory that gives the dual description to $N_f = 6$ $SU(3)$? We gauge an $SU(2)$ subgroup of our E_6 flavor symmetry which commutes with an $SU(6) \subset E_6$, and attach an additional fundamental to the $SU(2)$ gauge group.

This is known as Argyres-Seiberg duality, and was discussed in [44]. As evidence for this duality, we can check that the moduli spaces and marginal deformations match on the two sides. The $SU(3)$ has a single marginal gauge coupling, as does the $SU(2)$ theory (since the E_6 theory is isolated). Further, the $SU(3)$ theory is parametrized by one two dimensional and one three dimensional operator. The two dimensional operator matches $\mathrm{tr}\Phi^2$ in the $SU(2)$, while the three dimensional operator matches the three dimensional operator in the interacting E_6 theory.

We can now follow a similar story as in the $SU(2)^n$ case, by considering S dualities at a node in a generalized quiver when the other gauge groups are at weakly coupled cusps. It is clear that the story is slightly more complicated to begin with, in that there is more than one type of flavor factor. Bifundamentals contribute $U(1)$ factors, while, for example, 6 fundamentals will contribute $U(6)$. Consider what happens, in a setup similar to before, to a linear quiver theory with three $SU(3)$ gauge groups. Again, let us take the left and right nodes to weakly coupled cusps.

Now we take the middle node to our strongly coupled cusp in moduli space, and assume the $SU(3) - SU(2)$ duality holds. In terms of the middle node, before duality there was an $SU(3) \times SU(3)$ subgroup of the flavor symmetry which was gauged by the neighboring gauge groups. After duality, we are left with a $U(1) \times SU(6)$ flavor symmetry. $SU(3) \times SU(3) \subset SU(6)$ must be

gauged, and so have a $U(1) \times U(1)$ flavor symmetry. These are a mixture of the two bifundamental $U(1)$ factors in the original duality frame. Again, we see that we have arrived at a very different looking generalized quiver theory, in which an $SU(2) \times SU(3) \times SU(3)$ subgroup of the E_6 Minahan-Nemeschansky theory is gauged.

We can now ask if the E_6 theory plays the same role in the rank 3 case as the $\mathcal{T}_2$ building block played in the rank 2 case. Indeed, from the above, it's not clear that the theory can be symmetrically attached to three gauge factors. But in fact it can be, and we can see this by turning off the $SU(2)$ gauge group above. From an analysis of the representation theory, one finds that when the $SU(2)$ is turned off, an $SU(3)$ flavor symmetry is restored. This is just the $SU(3)^3$ subgroup of E_6, where two of the $SU(3)$ factors have been gauged by the neighboring gauge groups. Thus the E_6 theory, which we call $\mathcal{T}_3$, is indeed a building block for the rank 3 generalized quiver gauge theories.

Indeed, a very similar general picture emerges in the rank 3 case. Namely, there are many generalized quivers which correspond to different weakly coupled cusps of a single 4d $\mathcal{N} = 2$ theory, called $\mathcal{T}_{(n,m),g}[A_2]$. Each puncture can now be one of two kinds. In the weakly coupled picture it's very simple - they can either correspond to an $SU(2)$ or an $SU(3)$ flavor factor. As before, a surface describing a theory can degenerate. The $SU(3)$ punctures are referred to as "punctures of the second kind." When we pinch off a tube in our surface, the surface degenerates and leaves behind two of these punctures of the second kind. Thus, we see that pinching a tube corresponds to going to the decoupling limit of an $SU(3)$ gauge factor.

The Seiberg-Witten curve has a similar form as before, described by

$$x^3 = \phi_2(z)x + \phi_3(z)$$

where, as before, we have a quadratic differential ϕ_2 defined on a punctured Riemann surface, but now also a cubic differential ϕ_3. This cubic differential distinguishes the type of puncture, with simple poles at punctures of the first kind and double poles at punctures of the second kind. The mass deformed case is also analyzed in [38].

There is in fact a general story for theories of the Gaiotto type, where types of punctures are classified by Young tableaux, but we will be most interested in the rank 2 and 3 cases. We will

construct descriptions of the BPS spectra for the $\mathcal{T}_2$ and $\mathcal{T}_3$ theories in section 8, and then see how to glue them together in much the same way that the surfaces of the theories themselves can be glued together. Now we turn to the general framework for understanding the BPS structure of an $\mathcal{N} = 2$ quantum field theory.

3 BPS Quivers

In the previous section we explored in great detail the pure $SU(2)$ SYM theory, and explained how Seiberg and Witten solved for its non-perturbative infared structure. We also explained how one can use a consistency argument to discover which particles in the theory, as a function of moduli, are stable against decay, and which are not.

In this section we will propose a new, more constructive path to this solution. The utility in our construction is that it will apply not just to $SU(2)$, but to a wide class of $\mathcal{N} = 2$ theories. For example, we will explicitly construct a solution to the Gaiotto-type theories introduced above. Most of these theories cannot be solved by any analogous consistency analysis.

First, we will review the features of the $SU(2)$ theory that are essential to our construction. As we do so, we will explain how these features generalize to the arbitrary theory to which our method applies.

In pure $SU(2)$, we had a complex manifold which served as our moduli space. We could think of a point in this space as a specification of a VEV for the Higgs field. In the general theory we now want to consider, we will also have some moduli space we call $\mathcal{U}$. We work on the Coulomb branch of theory, and we include in $\mathcal{U}$ the freedom to tune the bare masses and and UV coupling constants.

In the $SU(2)$ case, a generic (non-singular) value of the moduli produced, in the extreme infared, a $U(1)$ field theory. The moduli space had point singularities on which this description broke down, because there weren't enough degrees of freedom in the IR model. The singularity structure of the moduli space of a general theory is more interesting. Classically, we have hypersurfaces on which a non-Abelian subgroup of the gauge group is left unbroken. Then such hypersurfaces can intersect in interesting ways, producing an intricate singularity structure. However, here we are concerned with a generic point in the moduli space, away from singular hypersurfaces, in which the infared

theory has a $U(1)^r$ gauge symmetry, and also a $U(1)^f$ flavor group. Charges under these $U(1)$'s will then serve to label our BPS particles in the usual way: In the $SU(2)$ case we had a 2d lattice (e, m) of electric and magnetic charges of BPS particles. Correspondingly, in the generic case we will have a lattice that we call Γ, of dimension $2r + f$, that describes the electric, magnetic and flavor charges of BPS particles.

The crucial quantities in the $SU(2)$ theory, in terms of which the Wilsonian effective action could be expressed, were a and a_D. Note that these are identical, as sections of a flat bundle on moduli space, to the central charges of the 2-tuples $(1, 0)$ and $(0, 1)$, respectively. Indeed, the Wilsonian effective action was encoded in central charge function $\mathcal{Z}_u$.[8] This central charge function is fundamental in the general case as well. We simply have, in general, a linear central function $\mathcal{Z}_u : \Gamma \to \mathbb{C}$. Central charges which couple to the electric and magnetic charges encode the effective coupling and theta angle of the infrared physics (as in the $SU(2)$ case), while the central charges that couple to the flavor symmetries sample possible bare masses of matter in the theory. In general, as in the $SU(2)$ theory, the extreme IR effective action is determined by the behavior of the central charge function. The piece of the puzzle we attempt to solve is the question of the massive BPS spectrum in these theories, the so called BPS occupancy problem.

3.1 Quivers and Spectra

We now proceed to discuss a general solution to the BPS occupancy problem. Central to this solution is the notion of a quiver, and a connection between the BPS spectra of 4d $\mathcal{N} = 2$ theories and quantum mechanical quiver theories. This connection is not our discovery; in fact, it has been explored at length in [27, 29–33, 35]. However, we will flesh out the connection, and find a novel use by exploiting a duality on the quantum mechanical quiver theory. This procedure, which we term the mutation method, will lead to a plethora of new results. Once the method is established, we will first return and apply it to the $SU(2)$ case, and then to many other examples.

To make the connection very explicit, we will begin by constructing two maps. The first is rather straightforward: Given a BPS spectrum and a point in moduli space, we will construct a

[8] Note that the central charge function is indeed a function, and not a section. This is because the charge labels of BPS particles are in fact not integers, but themselves flat sections of the bundle. The transformations of these two quantities under monodromy then precisely cancel to leave one with an honest function on moduli space for the central charge of a fixed particle.

decorated quiver. The second map goes the other way: Given a decorated quiver, we will construct a BPS spectrum - that is, we will specify the occupancy of a charge lattice. We will then give arguments that show that, in a large class of theories, these two maps compose to the identity. For these theories, the quiver will encode everything that is known about the BPS spectrum.

The notion of a quiver serves as more than a bookkeeping device, however. We will see that there are many ways of attaining the quiver for a theory. A quiver at one point in moduli space, for example, is intimately tied to the quiver at another point. Even more striking, operations on the level of theories, such as gauging a flavor symmetry, often are manifest as elegant graphical operations on the quivers. We will give an overview of such techniques in 3.2, and use them throughout our examples.

If we attain the quiver through some alternate means, then in principle we have discovered the spectrum for our theory. There is one hiccup, however, which has likely been the been the historical impediment to progress in this direction: While the second map is in principal easy to define, its definition essentially amounts to the statement "solve the following complicated linear algebra problem and use its solution." We will see later in this section that this problem becomes quite complicated even for an example as simple as the Argyres-Douglas A_3 theory.

It turns out, however, that there is a quiver duality waiting to be found. As with the dualities we have seen so far, exploiting it will be immensely fruitful. We will lay out the framework for doing this in section 4, and repeatedly take advantage of it thereafter.

3.1.1 From BPS Spectra to BPS Quivers

Let us begin by fixing a point $u \in \mathcal{U}$ in the moduli space of our theory. We wish to describe a map from the BPS spectrum to a decorated quiver, so we assume the occupancy at this point in moduli space is known. We will give an explicit algorithm for constructing the quiver, when it exists.

To begin, we split the BPS spectrum into two sets: particles and antiparticles. Every particle has some complex central charge assignment. We define particles to be those BPS states whose central charges lie in the upper half of the complex $\mathcal{Z}$ plane, and antiparticles those in the lower. CPT invariance ensures that for each BPS particle of charge γ, there is an antiparticle of charge $-\gamma$. Thus the full BPS spectrum consists of the set of BPS particles plus their associated CPT conjugate antiparticles. We will use the occupancy of the particles to construct a quiver.

Among the particles, we choose a minimal basis set of hypermultiplets. Since the lattice Γ has rank $2r + f$, our basis will consist of $2r + f$ BPS hypermultiplets. While the spectrum may indeed contain higher spin particles, these cannot be taken as elements of our basis. Let us label the charges of these basis hypermultiplets γ_i. The particles in the basis set should be thought of as the elementary building blocks of the entire spectrum of BPS states. As such they are required to form a positive integral basis for all occupied BPS particles in the lattice Γ. This means that every charge γ which supports a BPS particle satisfies

$$\gamma = \sum_{i=1}^{2r+f} n_i \gamma_i. \quad n_i \in \mathbb{Z}^+ \tag{1}$$

We emphasize that the basis need not span Γ, but only the subset of occupied states in Γ. We will see in section 3.1.2 that this equation can be interpreted as saying that the BPS particle with charge γ can be viewed as a composite object built up from a set of elementary BPS states containing n_i particles of charge γ_i.

It is important to notice that the requirement that a set of states form a positive integral basis for the entire spectrum of BPS particles is quite strong, and in particular uniquely fixes a basis when it exists. To see this, we suppose that $\{\gamma_i\}$ and $\{\widetilde{\gamma}_i\}$ are two distinct bases. Then there is a matrix n_{ij} relating them

$$\widetilde{\gamma}_i = n_{ij}\gamma_j; \qquad \gamma_i = (n^{-1})_{ij}\widetilde{\gamma}_j. \tag{2}$$

However since both $\{\gamma_i\}$ and $\{\widetilde{\gamma}_i\}$ form positive integral bases, the matrix n_{ij} and its inverse must have positive integral entries. It is easy to see that this forces both matrices to be permutations. Thus the two bases can differ only by a trivial relabeling.

Now, given the basis of hypermultiplets $\{\gamma_i\}$ there is a natural diagram, a *quiver*, which encodes it. This quiver is constructed as follows:

- For each element γ_i in the basis, draw a node, decorated by the charge γ_i.
- For each pair of charges in the basis compute the electric-magnetic inner product $\gamma_i \circ \gamma_j$. If $\gamma_i \circ \gamma_j > 0$, connect corresponding nodes γ_i and γ_j with $\gamma_i \circ \gamma_j$ arrows, each of which points from node j to node i.

We will now illustrate this map by using it to construct a decorated quiver for the pure $SU(2)$

theory at a large value of the Higgs VEV $\mathrm{tr}\phi^2$, where the theory is governed by semi-classical physics. As we saw above, in terms of their associated electric and magnetic charges (e, m), the occupied BPS states in this chamber are given by:

$$\begin{gathered}\text{Vector multiplet } W-\text{boson}: (2,0), \\ \text{Hypermultiplet dyons}: (2n,1),\ (2n+2,-1)\ n \geq 0.\end{gathered} \tag{3}$$

Choosing the particle half-plane represented in Fig. 1a,[9] the unique basis is given by the monopole $(0,1)$ and the dyon $(2,-1)$. The inner product of these particles is trivial to calculate, and so we very easily draw the quiver for this theory, at this point. The spectrum and resulting quiver are shown in Figure 1.

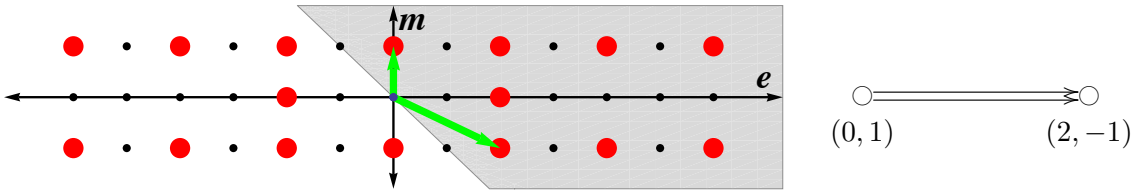

(a) BPS Spectrum (b) BPS Quiver

Figure 1: The spectrum and BPS quiver of $SU(2)$ Yang-Mills. In (a) the weak-coupling BPS spectrum, both particles and antiparticles, is plotted in the (e, m) plane. Red dots denote the lattice sites occupied by BPS states. The green arrows show the basis of particles given by the monopole and dyon. We have represented our choice of particle central charge half-plane by the gray region. In (b) the BPS quiver is extracted from this data. It has one node for each basis vector, and the double arrow encodes the symplectic product.

At this stage, we pause to point out important subtleties in the general procedure we have outlined. The first is that our identification of arrows as being determined by the Dirac inner product glosses over the possibility of having arrows between nodes which point in opposite directions. In fact, what the Dirac product truly captures is the net number of arrows. It is a fortunate feature of all of the field theory examples discussed in this work, with the exception of section 6.2, that there are in fact no opposing arrows in the theories' quivers. Further analysis of this issue occurs in our discussion of superpotentials in section 4.

A second important subtlety is that there exist field theories for which there is no BPS quiver

[9]Technically this requires a global rotation of the central charge function, but we will see below it is useful to extend the definition of the quiver map to allow the choice of an arbitrary half plane for splitting particles and anti-particles.

whatsoever. To illustrate this, note that one assumption thus far was that we could find a basis of hypermultiplets in the upper half of the central charge plane. By linearity of the central charge function, this gives a constraint on the occupied subset of Γ. In particular, since the set $\{\gamma_i\}$ forms a basis, we have for an arbitrary BPS particle of charge γ,

$$\gamma = \sum_i n_i \gamma_i \Longrightarrow \mathcal{Z}_u(\gamma) = \sum_i n_i \mathcal{Z}_u(\gamma_i). \quad n_i \geq 0 \tag{4}$$

Since $\mathcal{Z}(\gamma_i)$ all lie in the upper half-plane, (4) implies that the central charges of all BPS particles lie in a cone in the upper half of the central charge plane, bounded by the left-most and right-most $\mathcal{Z}(\gamma_i)$.

One can see that many theories do not even have such a cone, and therefore don't have an associated BPS quiver. The simplest example is $\mathcal{N} = 4$ Yang-Mills with gauge group $SU(2)$. Because of S-duality, this theory has a spectrum of dyons with charges (p, q), for p and q arbitrary coprime integers. It follows that the phases of the central charges of these dyons form a dense set in the unit circle in the central charge plane. In particular, there is no cone of particles and hence no quiver.

We can state the problem with $\mathcal{N} = 4$ Yang-Mills from the $\mathcal{N} = 2$ perspective: there is an adjoint hypermultiplet which is forced to be massless. The $\mathcal{N} = 2^*$ theory, where the adjoint is given a mass, *does* admit a BPS quiver, given in section 5. This situation is typical of gauge theories that become conformal when all mass deformations are turned off. A conformal field theory has no single particle states at all, let alone BPS states. A quiver description is therefore only possible when sufficiently many massive deformations of the theory exist and have been activated.

3.1.2 From BPS Quivers to BPS Spectra

We will now construct the more complicated of our two maps - given a decorated quiver, we will furnish a BPS spectrum. That is, we will specify a subset of a charge lattice, with multiplicities and spins, that can serve to describe the occupied BPS spectrum of our theory at a given point in moduli space.

We simply define our charge lattice as $\Gamma = \text{span}\{\gamma_i\}$. Then we must say, for a given charge

$$\gamma = \sum_i n_i \gamma_i, \tag{5}$$

whether any particles of this charge exist in the theory, and if so, what their degeneracies and spins are. Naively, the quiver appears to contain very little information, and so even a proposal for such a map seems difficult. However, the quiver actually encodes a non-trivial physical theory - namely, a four supercharge supersymmetric quiver quantum mechanics. To see this, let i index nodes of the quiver, and a its arrows. Then we introduce a gauge group $U(n_i)$ for each node, and a bifundamental field B^a_{ij} for each arrow which points $i \to j$, producing a theory with

$$\text{Gauge Group} = \prod_{\text{nodes } i} U(n_i), \qquad \text{Matter} = \bigoplus_{\text{arrows } a} B^a_{ij}. \tag{6}$$

To asses the existence of a BPS particle with charge γ, we look for supersymmetric ground states on the Higgs branch of this quiver theory. These depend on two data which we must still specify:

- Fayet-Iliopoulos Terms

  Since the gauge groups at each node are given by $U(n_i)$, the overall $U(1)$ at each node can couple to an independent FI-term θ_i. These parameters are fixed by the central charges $\mathcal{Z}_u(\gamma_i)$ of the constituent particles. We state this identification in the case that all the central charges point in nearly the same direction in the complex plane. Then let $\mathcal{Z}_u(\gamma)$ denote the central charge of a state with charge γ, and set

  $$\theta_i = |\mathcal{Z}_u(\gamma_i)| \left(\arg(\mathcal{Z}_u(\gamma_i)) - \arg(\mathcal{Z}_u(\gamma)) \right). \tag{7}$$

  For each node i in the quiver there is then a D-term equation of motion

  $$\sum_{\substack{\text{arrows} \\ \text{starting at } i}} |B^a_{ij}|^2 - \sum_{\substack{\text{arrows} \\ \text{ending at } i}} |B^a_{ki}|^2 = \theta_i. \tag{8}$$

  When the central charges are not nearly aligned, the identification of the FI parameters is

more involved, and for now the reader should assume that the moduli are such that this approximation is valid.[10] Later in section 3.3 we will see an elegant way of rephrasing our problem that completely avoids this issue.

- Superpotentials

  Whenever there are non-trivial oriented cycles in the BPS quiver, the quantum mechanics theory admits a non-trivial gauge invariant superpotential $\mathcal{W}$ which is a holomorphic function of the bifundamental fields. Our procedure for producing a quiver does not fix a superpotential; it is an independent datum of our construction which must be computed by alternative means. Later in section 4 we will see general constraints on $\mathcal{W}$. For now, we simply assume that $\mathcal{W}$ is given. This superpotential yields F-term equations of motion

$$\frac{\partial \mathcal{W}}{\partial B^a_{ij}} = 0. \tag{9}$$

Having fully fixed the quantum mechanics, we now turn to the moduli space of supersymmetric ground states with charge γ, $\mathcal{M}_\gamma$.[11] This space is simply the solution to the equations of motion described above, quotiented by the action of the unitary gauge groups.

$$\mathcal{M}_\gamma = \left\{ B^a_{ij} \left| \frac{\partial \mathcal{W}}{\partial B^a_{ij}} = 0, \sum_{\substack{\text{arrows} \\ \text{starting at } i}} |B^a_{ij}|^2 - \sum_{\substack{\text{arrows} \\ \text{ending at } i}} |B^a_{ki}|^2 = \theta_i \right. \right\} / \prod_i U(n_i). \tag{10}$$

If $\mathcal{M}_\gamma$ is non-empty, then there exists a BPS particle in the spectrum with charge γ. To determine spins and degeneracy from $\mathcal{M}_\gamma$, we examine the structure of its cohomology. Specifically, since $\mathcal{M}_\gamma$ is the moduli space of a theory with four supercharges, it is a Kähler manifold, and as such its cohomology automatically forms representations of Lefschetz $SU(2)$. For each such irreducible Lefschetz $SU(2)$ representation, we obtain a supersymmetric BPS multiplet. The spacetime spin of

[10] Alternatively one may tune the central charges to near alignment. Since this involves no crossing of walls of marginal stability the spectrum is stable under this motion.

[11] From now on, whenever we refer to supersymmetric ground states of the quiver quantum mechanics, we will always mean on the Higgs branch. The Coulomb branch can also be studied and gives rise to equivalent results for BPS spectra. [35]

a multiplet is then determined by tensoring the Lefschetz spin with an overall $\mathcal{N} = 2$ hypermultiplet,

$$\text{Spin} = \text{Lefschetz} \otimes \left(\left[\frac{1}{2} \right] + 2\,[0] \right). \tag{11}$$

In practice the most important application of (11) is to distinguish vector multiplets from hypermultiplets. The latter are associated to Lefschetz multiplets of length zero, as would naturally occur if, say, $\mathcal{M}_\gamma$ were a point. Meanwhile vector multiplets are associated to Lefschetz multiplets of length two, the canonical example of which is $\mathcal{M}_\gamma \cong \mathbb{P}^1$. In complete generality the formula (11) tells us that if $\mathcal{M}_\gamma$ has complex dimension d then there is guaranteed to be a BPS multiplet of spin $\frac{d+1}{2}$ with charge γ in the spectrum. Naive parameter counting gives the expected dimension of the $\mathcal{M}_\gamma$ as

$$d = \sum_{B_{ij}^a} (n_i n_j) - \sum_{\text{nodes } i} n_i^2 - (\#\,\text{F-term constraints}) + 1. \tag{12}$$

Here we have simply counted the degrees of freedom of the bifundamental fields, B_{ij}^a, and subtracted the gauge degrees of freedom and the F-term constraints. The addition of 1 is for the overall diagonal gauge group $U(1)_d \subset \prod_i U(1) \subset \prod_i U(n_i)$. Since all fields are bifundamental, no field is charged under the simultaneous $U(1)$ rotation of all gauge groups, so this gauge degree of freedom is actually redundant.

In summary, given a quiver we have defined a supersymmetric quantum mechanics problem, and then used the cohomology of the moduli spaces of grounds states of this quantum mechanics to define an occupancy of BPS states. This is precisely our definition of the map from decorated quivers to BPS spectra.

3.1.3 Composing Maps - Insights from Geometric Engineering

One may well ask what the significance of the two maps we have proposed above are. Naively, we have given an arbitrary prescription for producing a quiver from a BPS spectrum, and a seemingly unrelated prescription for producing a BPS spectrum from a quiver. Indeed, these constructions are useful precisely when the the second map, when applied to the quiver produced by the theory's spectrum, returns the same spectrum.

Clearly, in that case, the quiver encodes the information of the BPS spectrum. We will say

that such theories (at our implicit choice of moduli) admit a BPS quiver. We will see throughout this work that a great class of theories admit BPS quivers. In fact, in the theories we consider, the failure of the theory to admit a quiver is usually the result of the first map itself becoming ill defined, rather than a more subtle failure of the composition property.

Thus, we should expect there to be some physical justification for this remarkable property, and indeed there is [35]. The justification is opaque from a 4d field theory perspective, however. Indeed, this prescription can be motivated most easily when the four-dimensional field theory is engineered in string theory. In particular, we work in the IIB framework, and compactify our theory on an ALE fibration, then decouple gravity, also keeping the 4d particle states at finite mass and making extended objects in 4d infinitely massive. It is a remarkable fact of $\mathcal{N} = 2$ supersymmetry that hypermultiplets cannot correct the Coulomb branch. Realizing that g_s falls into a 4d hypermultiplet, we are then free to work at tree level in the string theory. A priori we ought to still be concerned with instanton corrections, but it is another amazing fact that these play no role. Indeed, when IIB is reduced to 4 dimensions, the Kahler moduli fall into a hypermultiplet, and it is the complex structure moduli which fall into a vector multiplet. The complex structure moduli of a Calabi-Yau are encoded by the volumes of 3-cycles. However, in IIB there is no 3 (world-volume) dimension object to wrap the 3-cycle, so there can be no instanton contributions to the 4d theory. Indeed, the situation is different in IIA, where it is the Kahler moduli that fall into a vector multiplet, and we must indeed include instanton corrections to engineer the non-perturbative 4d theory.

We emphasize the remarkable property we have just described: tree level type IIB string theory with no instanton corrections has encoded the full non-perturbative quantum field theory in 4d. Indeed, the Seiberg-Witten surface is none other than a dimensional reduction of our Calabli-Yau 3-manifold. The Seiberg-Witten differential is simply the volume 3-form on the Calabi-Yau integrated over 2-cycles in the extra dimensions. While in section 2 we derived the Seiberg-Witten curve through a consistency argument, considering monodromies, in the string theory construction it simply emerges directly.

Further, in string theory we know where our massive particles in 4d arise from - charged 4d BPS states are simply supersymmetric bound states of D-branes wrapping cycles in the Calabi-Yau. This is why the quiver description works: The nodes of our quiver correspond to a collection of basic

supersymmetric branes, and the arrows are bifundamental fields that arise at brane intersections. We recall that arrows in the quiver were defined in 4d by the electro-magnetic intersection product of charges. This was equivalent to the intersection product of cycles on the Seiberg-Witten curve, which in turn is equivalent to the intersection of 3-cycles the D-branes wrap in the Calabi-Yau. The gauge groups in the quantum mechanics simply result from the world-volume theory on the branes, which has $\mathcal{N} = 1$ supersymmetry in 4d, hence 4 supercharges when it is reduced to 0+1 dimensions.

Finally, equation (11) can be intuitively understood by thinking about the worldvolume theory of a BPS particle. This worldvolume theory supports four supercharges and hence has an R-symmetry group of $SU(2)$ which is none other than the Lefschetz $SU(2)$ of the moduli space. On the other hand, the R-symmetry group of a brane, in this case our particle, can be identified with the group of rotations transverse to the worldvolume, which in turn controls the angular momentum of the state. Thus the Lefschetz $SU(2)$ computes the orbital angular momentum of the state, and the overall shift by $1/2$ in (11) simply takes into account the intrinsic spin contribution.

3.2 Finding BPS Quivers Directly

Thus far we have seen how a BPS quiver can be used as a convenient way for encoding the complete BPS spectrum of a theory. However, this isn't particularly exciting. While it would be a nice bookkeeping device, we are really interested in discovering previously *unknown* spectra. Indeed, we will see that we have other means of attaining the BPS quiver for a theory whose spectrum at some point is unknown, giving us access to previously unknown results.

One way we can do this is by taking advantage of the fact that our construction of BPS quivers is completely local in the Coulomb branch moduli space $\mathcal{U}$. Given the BPS spectrum at a single point in moduli space, we can construct the BPS quiver for that point. However, as we will see in section 4, quivers for various points in moduli space are not unrelated. Indeed, there are well defined transformations, called mutations, that quivers undergo as we tune moduli. This has great utility. For example, if we knew the spectrum of some theory at weak coupling from semi-classical techniques, we could construct the quiver at a weak coupling point using the first map. We could then tune moduli to a point of strong coupling, doing the necessary quiver mutations as we go. At strong coupling we could then apply our second map to discover the theory's strong coupling

spectrum. Indeed, we will explicitly do this for the pure $SU(N)$ SYM theories to discover the spectrum of their minimal strongly coupled chamber.

Even more striking is the fact that BPS quivers can frequently be deduced by alternative geometric methods in various contexts in string theory, even when the BPS spectrum is unknown for any value of the moduli. The existing literature on the techniques used to extract BPS quivers is by now very vast. In the following we outline some of the various interrelated approaches:[12]

- Building on the original orbifold construction of quiver gauge theories of [27] refs. [29–31, 48] provided the identification of the quiver nodes with a basis of BPS states obtained from fractional branes, these BPS quivers were further explored in [32, 33].

- The relation of the $4d$ quivers with the soliton spectrum in $2d$ [49] was studied in various places, see for example [50–52], more recently this $2d/4d$ correspondence and the associated construction of BPS quivers was discussed in [16].

- The toric methods of [53, 54] and the relation to dimer models [55] were used in [56] to construct a large class of quivers, their construction using mirror symmetry was studied in [57].

- Based on the geometric study of BPS states in SW theories pioneered in [60] and further studied in [12, 61], the BPS quivers can be obtained from triangulations of Riemann surfaces as described in [21, 24] using the relation of triangulations and quivers of [62]. Given a pair of M5-branes wrapping a Riemann surface $\mathcal{C}$, an ideal triangulation of $\mathcal{C}$ can be used to determine the BPS quiver. We discussed this in great detail in section 7. There is reason to believe that these techniques can be generalized to larger numbers of M5-branes and we initiate this analysis in section 8.

3.3 Quiver Representations

In the previous section, we presented a map from BPS quivers to BPS spectra that defined the 4d spectrum associated with a quiver through the solution to a supersymmetric quantum mechanics

[12] See also [47] and references therein for an excellent recent exposition of the mathematical structures used to describe to D-branes which in includes in particular the associated quiver representation theory.

problem. While our supersymmetric quantum mechanics is precisely the correct construction, it is useful in practice to work in the language of quiver representation theory instead. Here the problem of determining the ground states of the supersymmetric quantum mechanics gets recast in a mathematically elegant framework.

Our ability to rephrase the problem in terms of quiver representation theory arises from the fact that a supersymmetric moduli space of a theory with four supercharges, such as $\mathcal{M}_\gamma$, can be presented in two ways:

- As the solution to the F-term and D-term equations of motion modulo the action of the unitary gauge groups (this is what has been stated in (10)).
- As the solution to the F-term equations modulo the action of the complexified gauge group $\prod_i Gl(n_i, \mathbb{C})$, augmented by a stability condition.

It is the second notion of $\mathcal{M}_\gamma$ that makes use of quiver representation theory.

To begin, we note that in a zero energy field configuration of supersymmetric quantum mechanics, the bifundamental fields are constants and hence their expectation values can be viewed as linear maps between vector spaces $\mathbb{C}^{n_i}$ associated to each node. These expectation values are constrained by the condition that they must solve the F-term equations of motion $\partial\mathcal{W}/\partial B^a_{ij} = 0$. A quiver representation is by definition precisely a choice of complex vector spaces $\mathbb{C}^{n_i}$ for each node, and linear maps $B^a_{ij} : \mathbb{C}^{n_i} \longrightarrow \mathbb{C}^{n_j}$ for each arrow in a quiver subject to the F-term equations. So the data of a classical zero energy field configuration completely specifies a quiver representation (see [47] and references therein).

A basic notion in quiver representation theory is that of a morphism of quiver representations. We will be interested in a particular kind of morphism: That which defines a subrepresentation of a quiver representation. Given a quiver representation R, defined by vector spaces $\mathbb{C}^{n_i}$ and maps B^a_{ij}, a subrepresentation S is defined by a choice of vector subspaces $\mathbb{C}^{m_i} \subset \mathbb{C}^{n_i}$ for each node and maps $b^a_{ij} : \mathbb{C}^{m_i} \longrightarrow \mathbb{C}^{m_j}$ for each arrow, such that all diagrams of the following form commute:

$$\begin{array}{ccc} \mathbb{C}^{n_i} & \xrightarrow{B^a_{ij}} & \mathbb{C}^{n_j} \\ \uparrow & & \uparrow \\ \mathbb{C}^{m_i} & \xrightarrow{b^a_{ij}} & \mathbb{C}^{m_j} \end{array} \tag{13}$$

This notion of subrepresentation is fundamental to the definition of a stability condition in the representation theory that ensures that a given quiver representation R is related to a solution of the D-term equations in the quiver quantum mechanics. To motivate the stability condition, note that a quiver rep R with vector spaces $\mathbb{C}^{n_i}$ is related to the description of a particle with charge $\gamma_R = \sum n_i \gamma_i$. Then heuristically, a subrepresentation S of R can be thought of as a bound state of smaller charge which may, in principle, form one of the constituents of a decay of a particle of charge γ_R. To prohibit such a decay, we must restrict our attention to *stable* quiver representations. To define this notion of stability we let $\mathcal{Z}_u(R)$ denote the central charge of a representation,[13]

$$\mathcal{Z}_u(R) \equiv \mathcal{Z}_u(\gamma_R) = \sum_i n_i \mathcal{Z}_u(\gamma_i). \tag{14}$$

By construction, the central charge vector lies in the cone of particles in the upper half of the central charge plane. Then R is called stable if for all subrepresentations S, other than R and zero, one has

$$\arg(\mathcal{Z}_u(S)) < \arg(\mathcal{Z}_u(R)). \tag{15}$$

We will refer to any subrepresentation S that violates this condition as a destabilizing subrepresentation. This condition is denoted Π-stability, and was studied in [30]. We take this to be the requisite notion of stability at general points in moduli space. One important consistency check on this choice is that when all the central charges are nearly aligned, the stability condition (15) reduces to the D-term equations of motion presented earlier [30, 64].

Given this notion of stability, we can now formulate the moduli space $\mathcal{M}_\gamma$ as set of stable quiver representations modulo the action of the complexified gauge group.

$$\mathcal{M}_\gamma = \left\{ R = \{B^a_{ij} : \mathbb{C}^{n_i} \to \mathbb{C}^{n_j}\} \,\middle|\, \frac{\partial \mathcal{W}}{\partial B^a_{ij}} = 0,\ R \text{ is } \Pi - \text{stable} \right\} / \prod_i Gl(n_i, \mathbb{C}). \tag{16}$$

This is a completely holomorphic description of $\mathcal{M}_\gamma$, and in many examples is explicitly computable.

As a very elementary application, we note that the nodes of a quiver are always Π-stable reps. That is, consider γ_j as the representation given by choosing $n_i = \delta_{ij}$. This is always stable since it

[13] When we speak of the central charge of a representation, we are always referring to the central charge of the bound state associated to that representation.

has no non-trivial subrepresentations, and thus in particular no destabilizing subreps. Furthermore, since there is only one non-zero vector space, all maps must be chosen zero; thus the moduli space $\mathcal{M}_{\gamma_j}$ is given by a single point. We find that each node of a quiver gives a multiplicity one hypermultiplet BPS state.

3.4 Passing a Quiver through a Wall

So far we have focused exclusively on utilizing BPS quivers to encode the spectrum of an $\mathcal{N} = 2$ quantum field theory at a specific point u on the Coulomb branch $\mathcal{U}$. BPS states are stable under infinitesimal variations of the modulus, and thus our description can be viewed as local theory of BPS particles adequate on a patch in $\mathcal{U}$. Now we begin to ask, what happens to the quiver description as the moduli is tuned over a finite region in $\mathcal{U}$?

In the quiver representation theory problem, the moduli u enter the calculation through the central charge function $\mathcal{Z}_u$. From the perspective of quiver representation theory, these are changes in the stability conditions. For small deformations of the stability condition, the set of stable representations, and hence the BPS spectrum, is unchanged. However, at certain real codimension one loci in moduli space we encounter walls of marginal stability where a supersymmetric particle decays. At the wall, the central charges of some representation R and its subrep S become aligned. On one side of the wall, $\arg \mathcal{Z}(S) < \arg \mathcal{Z}(R)$ so that R stable, and hence some corresponding BPS particle exists. On the other side of the wall, the phases have crossed, and the stability condition has changed. We will have $\arg \mathcal{Z}(S) > \arg \mathcal{Z}(R)$, so the representation R is no longer stable, and the associated particle has disappeared from the BPS spectrum.

It is a virtue of the description of the spectrum in terms of stable quiver representations that these wall-crossing processes are completely explicit. Indeed, the BPS quiver gives us a way to calculate directly the BPS spectrum on either side of a wall. One can then simply compare the answer on both sides, and see that properties such as the Kontsevich-Soibelman wall-crossing formula hold. In this section we study these wall crossing phenomena in the context of the Argyres-Douglas conformal theories.

3.4.1 Examples from Argyres-Douglas Theories

We will find it useful, for our first example of wall crossing, to consider a theory even simpler than pure $SU(2)$. We consider the Argyres-Douglas A_2 theory, whose quiver is given by two nodes, connected by a single arrow [16]. We will denote by $\mathcal{Z}_i$ the central charges of the two basis particles,

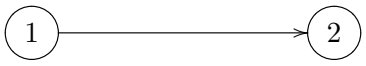

(17)

No matter what the value of the central charges, the basis particles described by the nodes of the quiver are stable. Thus the spectrum always contains at least two hypermultiplets. Now let us search for a bound state involving n_1 particles of type γ_1 and n_2 particles of type γ_2. According to the general theory developed in the previous sections we are to study a quiver representation of the following form

$$\mathbb{C}^{n_1} \xrightarrow{B} \mathbb{C}^{n_2} \tag{18}$$

To determine stability we investigate subrepresentations. Let's start with a subrepresentation of the form

$$\begin{array}{ccc} \mathbb{C}^{n_1} & \xrightarrow{B} & \mathbb{C}^{n_2} \\ \uparrow & & \uparrow \\ 0 & \xrightarrow{0} & \mathbb{C} \end{array} \tag{19}$$

There is no condition on the field B for this diagram to commute; it is always a subrepresentation. Thus, stability of our bound state requires

$$\arg(\mathcal{Z}_2) < \arg(n_1\mathcal{Z}_1 + n_2\mathcal{Z}_2) \Longrightarrow \arg(\mathcal{Z}_2) < \arg(\mathcal{Z}_1). \tag{20}$$

Next we consider a similar decay involving the first basis particle

$$\begin{array}{ccc} \mathbb{C}^{n_1} & \xrightarrow{B} & \mathbb{C}^{n_2} \\ \uparrow & & \uparrow \\ \mathbb{C} & \xrightarrow{0} & 0 \end{array} \tag{21}$$

If this is a subrepresentation, then stability demands that $\arg(\mathcal{Z}_1) < \arg(\mathcal{Z}_2)$, so (20) cannot be satisfied. Thus, to ensure the existence of a bound state we must forbid this subrepresentation, and hence we must choose B so that the diagram in (21) does not commute. Thus B should have no kernel, and in particular, we have $n_1 \leq n_2$.

Finally we consider a decay involving the subrepresentation

$$\begin{array}{ccc} \mathbb{C}^{n_1} & \xrightarrow{B} & \mathbb{C}^{n_2} \\ \uparrow & & \uparrow \\ \mathbb{C} & \xrightarrow{b} & \mathbb{C} \end{array} \tag{22}$$

It is clear that b can be chosen in such a way that this is always a subrepresentation. Then stability demands that the central charges satisfy

$$\arg(\mathcal{Z}_1 + \mathcal{Z}_2) < \arg(n_1\mathcal{Z}_1 + n_2\mathcal{Z}_2). \tag{23}$$

However, given that $n_1 \leq n_2$, and that $\mathcal{Z}_2$ has smaller phase than $\mathcal{Z}_1$, it is not possible to satisfy the above inequality. It follows that the only possibility for a bound state is that (22) is not a subrepresentation, but an isomorphism of representations. So we only have the possibility of non-trivial moduli spaces for $n_1 = n_2 = 1$.

In summary, when $\arg(\mathcal{Z}_2) < \arg(\mathcal{Z}_1)$ this theory supports a bound state with charge $\gamma_1 + \gamma_2$. The moduli space of representations of this charge is given by the quotient of a single non-zero complex number B modulo the action of the complexified gauge group. Clearly this moduli space is just a point, and so this representation describes a single hypermultiplet. The complete spectrum for this example is depicted in Figure 2, and agrees with the known result for this theory [61]. This basic 2-3 decay process is known in various contexts as a primitive decay [5]. In formalism of Kontsevich and Soibelman this wall-crossing gives rise to the pentagon identity of quantum dilogarithms.

As another example of quiver representation theory and wall-crossing we consider a quiver involving a non-trivial superpotential $\mathcal{W}$. The quiver, known to be related to the A_3 Argyres-Douglas theory is given by

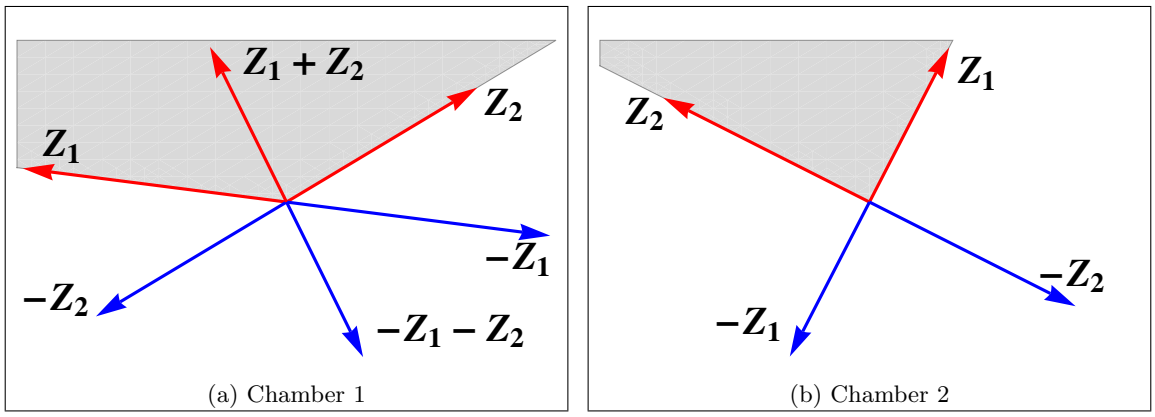

(a) Chamber 1 (b) Chamber 2

Figure 2: The chambers of the A_2 Argyres-Douglas theory. The BPS spectrum is plotted in the central charge plane. Particles are shown in red, antiparticles in blue. The cone of particles is the shaded gray region. In (a) the particles form a bound state. In (b) the bound state is unstable and decays.

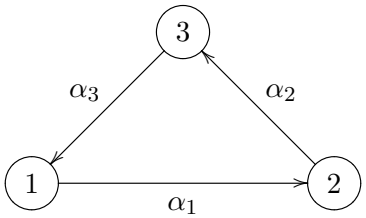

(24)

We let α_i indicate the bifundamental field map exiting node i and $\mathcal{Z}_i$ the central charge of node i. The quiver is equipped with a superpotential

$$\mathcal{W} = \alpha_3\alpha_2\alpha_1. \tag{25}$$

Minimization of $\mathcal{W}$ implies that in any allowed field configuration all compositions of pairs of maps vanish

$$\alpha_2 \circ \alpha_1 = 0, \qquad \alpha_3 \circ \alpha_2 = 0, \qquad \alpha_1 \circ \alpha_3 = 0. \tag{26}$$

We will show that this quiver has, up to relabeling the nodes, exactly two chambers with four or five BPS hypermultiplets respectively.

First, we note that as usual all of the node representation where the dimensions n_i of the associated vector space are given by $n_i = \delta_{ij}$ for $j = 1, 2, 3$ are stable and hence yield three hypermultiplets. Further, when one of the n_i vanishes, then two of the maps α must also vanish and the analysis reduces to the A_2 case considered in the previous section. This yields two or

one bound states depending on whether the phases of the $\mathcal{Z}_i$ are or are not cyclically ordered. To conclude the analysis of this quiver, we now wish to illustrate that there are no further bound states that arise from representations

$$\mathbb{C}^{n_1} \xrightarrow{\alpha_1} \mathbb{C}^{n_2} \xrightarrow{\alpha_2} \mathbb{C}^{n_3} \quad \text{with } \alpha_3 : \mathbb{C}^{n_3} \to \mathbb{C}^{n_1} \tag{27}$$

with all n_i non-zero.

We begin by considering possible subrepresentations corresponding to node vectors, $(1,0,0)$, $(0,1,0)$, and $(0,0,1)$. These are only subrepresentations when α_i has a kernel for $i = 1,2,3$ respectively. Clearly not all of these can be subreps simultaneously or else the representation would already be destabilized. It follows that at least one of the α_i, say α_1 is injective and hence in particular $n_1 \leq n_2$.

Now we apply the F-term equations (26). From the fact that $\alpha_1 \circ \alpha_3 = \alpha_2 \circ \alpha_1 = 0$ and the fact that α_1 is injective we learn that both α_2 and α_3 have non-vanishing kernels. This means that both the node representations $(0,1,0)$ and $(0,0,1)$ are subreps so we deduce that $\mathcal{Z}_1$ must have largest phase for stability, and $\arg \mathcal{Z}_2, \arg \mathcal{Z}_3 < \arg(n_1\mathcal{Z}_1 + n_2\mathcal{Z}_2 + n_3\mathcal{Z}_3)$.

However now we consider a subrepresentation with dimension vector $(1,1,0)$.

$$\begin{array}{ccccc} \mathbb{C}^{n_1} & \xrightarrow{\alpha_1} & \mathbb{C}^{n_2} & \xrightarrow{\alpha_2} & \mathbb{C}^{n_3} \\ {\scriptstyle i}\uparrow & & {\scriptstyle j}\uparrow & & {\scriptstyle 0}\uparrow \\ \mathbb{C} & \xrightarrow{\beta_1} & \mathbb{C} & \xrightarrow{\beta_2} & 0 \end{array} \quad \text{with } \alpha_3 : \mathbb{C}^{n_3} \to \mathbb{C}^{n_1}, \ 0 : 0 \to \mathbb{C} \tag{28}$$

This is a subrep exactly when the image of α_1 meets the kernel of α_2 non-trivially, which it does by the F-terms. Thus we learn that

$$\arg(\mathcal{Z}_1 + \mathcal{Z}_2) < \arg(n_1\mathcal{Z}_1 + n_2\mathcal{Z}_2 + n_3\mathcal{Z}_3). \tag{29}$$

Given the conditions on the $\mathcal{Z}_i$ and the fact that $n_1 \leq n_2$, the above is impossible.

Thus we have arrived at a contradiction. It follows that for this quiver with the given superpotential there are no states with all n_i non-vanishing. Note that this conclusion is altered when the superpotential is turned off. In that case it is easy to check that the representation $(1,1,1)$ with

all maps non-zero provides a stable hypermultiplet at all moduli. This completes our analysis of this quiver.

4 The Mutation Method

We have seen how wall crossing is encoded into our quiver quantum mechanics picture. Walls of marginal stability correspond to hypersurfaces in which two central charges become aligned. The stability condition will differ on the two sides of this wall, and therefore there may be some representations which are stable on one side but not the other. There is in fact another type of hypersurface in moduli space that is strikingly relevant in our picture: hypersurfaces across which a fixed quiver quantum mechanics description of the BPS spectrum may break down entirely. Following [10] we will refer to these as walls of the second kind.

The situation is less dire than it may seem; we will be able to find another quiver description, valid on the other side of the wall. We will argue that the transformation of a quiver across a wall of the second kind is given by a canonical procedure, known as *quiver mutation*, which describes a quantum mechanical duality relating the ground state spectra of two distinct quivers. Once the rule for transforming quivers at such walls is understood, we will be able to start with a quiver description at any point in moduli space and arrive at any other point by following an arbitrary path connecting them, doing the necessary mutations along the way.[14] Further, in section 4.2 we will revisit this procedure and see that the same transformation can be made on quivers at a fixed point in moduli space, and in this case the transformation will take us between quivers that describe the same physics. We will then immediately exploit this duality to circumvent the computations involved in solving the representation theory problem.

Recalling that the nodes of a quiver all correspond to particles, and must therefore have central charges which lie in the upper half-plane, we see what can go wrong. As we tune moduli, our central charge function changes, and as we cross some real co-dimension 1 subspace in $\mathcal{U}$, the central charge of one of the nodes may exit the half-plane. This behavior defines the walls of the second kind. They are the loci in moduli space (including as usual masses and couplings) where the central

[14] This is not strictly true, as we may find ourselves faced with an infinite sequence of mutations.

charge of a basis particle becomes real

$$\mathcal{Z}_u(\gamma_i) \in \mathbb{R}. \tag{30}$$

Let us study the process of crossing such a wall in more detail. Consider the central charge configuration illustrated in Figure 3a where the BPS particles are described by the quiver Q. As moduli are varied, the central charge of one of the basis elements, $\mathcal{Z}_1$ rotates out of the upper half-plane and we arrive at the new configuration illustrated in Figure 3b.

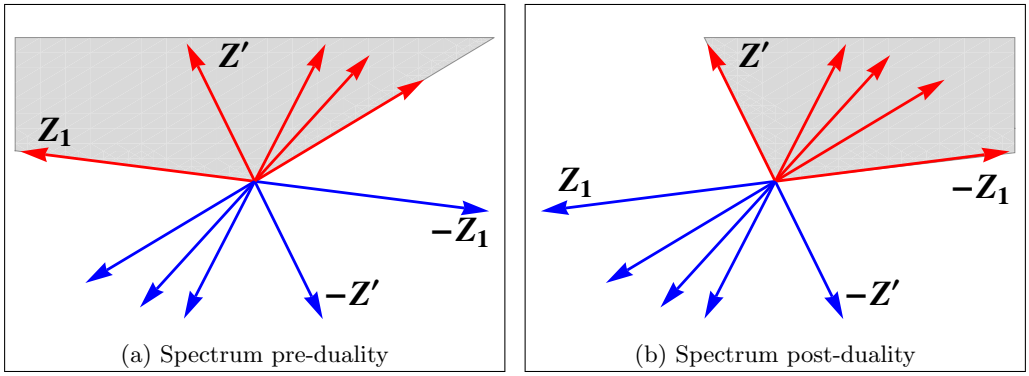

Figure 3: A discontinuity in the quiver description results in a quantum mechanical duality described by quiver mutation. In both diagrams the BPS spectrum is plotted in the central charge plane. Red lines denote particles while blue lines denote antiparticles. The gray shaded region indicates the cone of particles. In passing from (a) to (b) the particle with central charge $\mathcal{Z}_1$ changes its identity to an antiparticle. The cone of particles jumps discontinuously and a new quiver description is required.

The first thing to notice about this process is that, since no central charges align, no walls of marginal stability are crossed, and hence the total BPS spectrum (consisting of both particles and antiparticles) is the same in Figures 3a and 3b. On the other hand, from the point of view of the quiver, this process is discontinuous. After $\mathcal{Z}_1$ has rotated out of the upper half of the central charge plane, it has changed its identity from a particle to an antiparticle. Then the original basis of particles encoded by the quiver Q is no longer acceptable. Specifically, in passing from Figure 3a to Figure 3b, the cone of particles has jumped discontinuously and as a result the original quiver description of the BPS spectrum is no longer valid.

To remedy this deficiency we must introduce a new quiver $\widetilde{Q}$ that encodes the BPS spectrum in the region of moduli space described by Figure 3b. Since the total spectra of particles and antiparticles in Q and $\widetilde{Q}$ are identical, the physical relation between them is that of a duality: they are equivalent descriptions of the same total spectrum of BPS states. In the moduli space $\mathcal{U}$ the

regions of validity of $\mathcal{Q}$ and $\widetilde{\mathcal{Q}}$ are sewn together smoothly along the loci where the central charge of an elementary basis particle is real. This sewing is illustrated in Figure 4

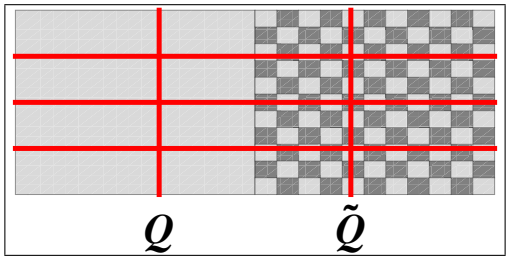

Figure 4: A cartoon of the moduli space and its relation to various BPS quiver descriptions. The red lines denote walls of marginal stability where the BPS spectrum jumps. The gray shaded region is the domain in moduli space where $\mathcal{Q}$ describes the BPS spectrum. The gray checkered region is the domain where $\widetilde{\mathcal{Q}}$ describes the spectrum. The two descriptions are glued together smoothly away from the walls of marginal stability. Their interface is a wall of the second kind.

In section 4.1 we define the operation of mutation on a given quiver $\mathcal{Q}$ to produces the quiver $\widetilde{\mathcal{Q}}$, valid on the other side of the wall of the second kind. In section 4.2 we explain how the existence of the mutation operation, when interpreted as duality between different quiver descriptions, leads to a powerful and striking method for determining BPS spectra.

4.1 Quiver Duality

As the preceding discussion indicates, a global description of the BPS spectrum across the entire Coulomb branch will require many quivers, all glued together in the fashion described above. In this subsection we describe the algorithmic construction of this set of quivers by a graphical process known as quiver mutation. In the following subsection we justify these rules using arguments from quiver representation theory.

To define mutation, let us suppose that node γ_1 is the BPS particle in the quiver whose central charge $\mathcal{Z}_1$ is rotating out of the half-plane. We then seek to describe the dual quiver $\widetilde{\mathcal{Q}}$ with corresponding nodes $\{\widetilde{\gamma}_i\}$. Of course, since we have determined that a given spectrum of BPS particles admits at most one basis of BPS states, both $\widetilde{\mathcal{Q}}$ and $\{\widetilde{\gamma}_i\}$ are uniquely fixed. What's more, the quiver $\widetilde{\mathcal{Q}}$ can be described in a simple graphical way starting from $\mathcal{Q}$. [50,51,65–69]. The

new basis is given by

$$\widetilde{\gamma}_1 = -\gamma_1 \tag{31}$$

$$\widetilde{\gamma}_j = \begin{cases} \gamma_j + (\gamma_j \circ \gamma_1)\gamma_1 & \text{if } \gamma_j \circ \gamma_1 > 0 \\ \gamma_j & \text{if } \gamma_j \circ \gamma_1 \leq 0. \end{cases} \tag{32}$$

To construct $\widetilde{Q}$ graphically we follow the steps below:

1. The nodes of $\widetilde{Q}$ are in one-to-one correspondence with the nodes in Q.

2. The arrows of $\widetilde{Q}$, denoted $\widetilde{B}^a_{ij}$, are constructed from those of Q, denoted B^a_{ij} as follows:

   (a) For each arrow B^a_{ij} in Q draw an arrow $\widetilde{B}^a_{ij}$ in $\widetilde{Q}$.

   (b) For each length two path of arrows passing through node 1 in Q, draw a new arrow in $\widetilde{Q}$ connecting the initial and final node of the length two path

   $$B^a_{i1}B^b_{1j} \longrightarrow \widetilde{B}^c_{ij}. \tag{33}$$

   (c) Reverse the direction of all arrows in $\widetilde{Q}$ which have node 1 as one of their endpoints.

   $$\widetilde{B}^a_{i1} \longrightarrow \widetilde{B}^a_{1i}; \qquad \widetilde{B}^a_{1j} \longrightarrow \widetilde{B}^a_{j1}. \tag{34}$$

3. The superpotential $\widetilde{\mathcal{W}}$ of $\widetilde{Q}$ is constructed from the superpotential $\mathcal{W}$ of Q as follows:

   (a) Write the same superpotential $\mathcal{W}$.

   (b) For each length two path considered in step 2(b) replace in $\mathcal{W}$ all occurrences of the product $B^a_{i1}B^b_{1j}$ with the new arrow $\widetilde{B}^c_{ij}$.

   (c) For each length two path considered in step 2(b) $B^a_{i1}B^b_{1j}$ there is now a new length three cycle in the quiver $\widetilde{Q}$ formed by the new arrow created in step 2(b) and the reversed arrows in step 2(c)

   $$\widetilde{B}^a_{1i}\widetilde{B}^c_{ij}\widetilde{B}^b_{j1}. \tag{35}$$

   Add to the superpotential all such three cycles.

As a simple example of this procedure we consider the A_3 quiver of section 3.4.1 shown on the left and its mutation at node 1 shown on the right.

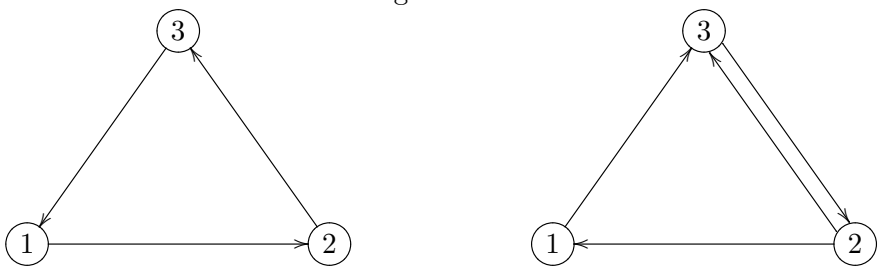

(36)

$$\mathcal{W} = B_{12}B_{23}B_{31} \qquad\qquad \mathcal{W} = \widetilde{B}_{32}\widetilde{B}_{23} + \widetilde{B}_{32}\widetilde{B}_{21}\widetilde{B}_{13}$$

As the above example illustrates, the process of quiver mutation in general creates cycles of length two in our new quiver. From a physical perspective these are fields in the quiver quantum mechanics which admit a gauge invariant mass term. In the example above such mass terms are present in the quadratic piece of the potential $\widetilde{B}_{32}\widetilde{B}_{23}$. As is typical in physical theories, the massive fields decouple from the analysis of ground states and hence do not affect the BPS spectrum. We may therefore integrate them out. Thus to our list of quiver mutation rules we append the following final steps:

4. For each two-cycle in $\widetilde{Q}$ for which a quadratic term appears in $\widetilde{W}$, delete the two associated arrows.

5. For each deleted arrow $\widetilde{B}^a_{ij}$ in step 4, solve the equation of motion

$$\frac{\partial \widetilde{W}}{\partial \widetilde{B}^a_{ij}} = 0. \tag{37}$$

   Use the solution to eliminate $\widetilde{B}^a_{ij}$ from the potential.

In the example illustrated above, the only two cycle has quadratic terms in the superpotential and is therefore deleted from the quiver. This results in a vanishing superpotential and a quiver of the following form.

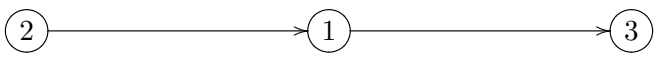

(38)

As a general rule, the study of BPS quivers is greatly complicated by the existence of pairs of opposite arrows whose associated fields cannot be integrated out from the superpotential. When this is never the case, that is when the potential $\mathcal{W}$ is strong enough to integrate out to all opposite bifundamental fields after an arbitrary sequence of mutations, the potential is said to be *non-degenerate*. It is a fortunate simplification that for the vast majority of BPS quivers related to quantum field theories that we discuss in this paper the potential will turn out to be non-degenerate. However exceptions to this general rule do arise. For example in section 8.3 we will see that the the quiver for the $\mathcal{T}_2$ theory, defined by a free trifundamental half-hypermultiplet of a flavor group $SU(2) \times SU(2) \times SU(2)$, involves opposing arrows and a potential which is too degenerate to integrate out all the associated bifundamental fields. In the following, unless otherwise stated, we avoid this complication and assume that all of our quivers involve non-degenerate superpotentials. However, even when this is not the case, one may still apply the mutation rules written above. Mutation at a node supporting a pair of canceling arrows then results in adjoint fields at the mutated node.

4.1.1 Argyres-Douglas Revisited

To put the above theory of quiver mutation in perspective, it is useful to consider the simplest example where the phenomenon of wall of the second kind occurs. This is the A_3 theory, whose representation theory was investigated in section 3.4.1. There are in fact four distinct quivers for the A_3 theory, all related by mutation. These make up the following set:

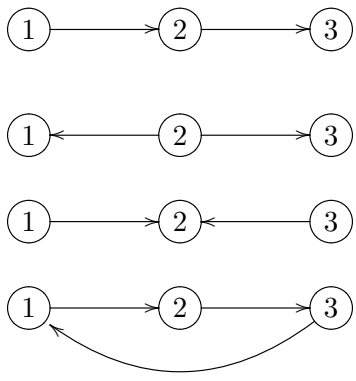

Let us name these four quivers respectively L, O, I and C. The representation theory of the C quiver was worked out in section 3.4.1. In particular, we determined that C supports 4 to 5

Chamber	Phase Conditions	Number of BPS States
L_1	$\theta_3 > \theta_2 > \theta_1$	3
L_2	θ_2 smallest, and $\theta_1, \theta_3 > \theta_{12}$	4
L_3	θ_2 largest, and $\theta_{23} > \theta_1, \theta_3$	4
L_4	$\theta_1 > \theta_{12} > \theta_3 > \theta_2$	5
L_5	$\theta_2 > \theta_1 > \theta_{23} > \theta_3$	5
L_6	$\theta_1 > \theta_2 > \theta_3$	6
O_1	θ_2 smallest	3
O_2	θ_2 intermediate	4
O_3	θ_2 largest, and $\theta_{12} < \theta_3$ or $\theta_{23} < \theta_1$	5
O_4	θ_2 largest, and $\theta_{12} > \theta_3$ and $\theta_{23} > \theta_1$	6
I_1	θ_2 largest	3
I_2	θ_2 intermediate	4
I_3	θ_2 smallest, and $\theta_3 < \theta_{12}$ or $\theta_1 < \theta_{23}$	5
I_4	θ_2 smallest, and $\theta_3 > \theta_{12}$ and $\theta_1 > \theta_{23}$	6
C_1	not cyclically ordered e.g. $\theta_2 > \theta_1 > \theta_3$	4
C_2	cyclically ordered e.g. $\theta_1 > \theta_2 > \theta_3$	5

Table 1: The chambers of the A_3 quivers before mutation equivalences are imposed. For each quiver labeled with node charges Z_i, θ_i denotes the argument of Z_i while θ_{ij} denotes the argument of $Z_i + Z_j$.

BPS states, depending on moduli. The representation theory of the other quivers is also readily calculated. One finds that L has 6 distinct chambers, while both I and O have 4. If we denote by θ_i the phase of $\mathcal{Z}_i$ and θ_{ij} the phase of $\mathcal{Z}_i + \mathcal{Z}_j$, then the complete list of chambers is given in table 1.

In the global theory of A_3 these chambers are connected together across walls of the second kind, where the quiver changes by a mutation. To understand the structure of the mutations, we then represent each chamber as a node in a graph, and connect mutation equivalent quivers with directed arrows. For example we define the expression

$$Q_i \longrightarrow \widetilde{Q}_j \ , \tag{39}$$

to mean that mutation in chamber i of quiver Q on the leftmost boundary ray leads to chamber j in the quiver $\widetilde{Q}$. With these conventions, the complete structure of walls of the second kind in the

A_3 theory is encoded in the following diagrams.

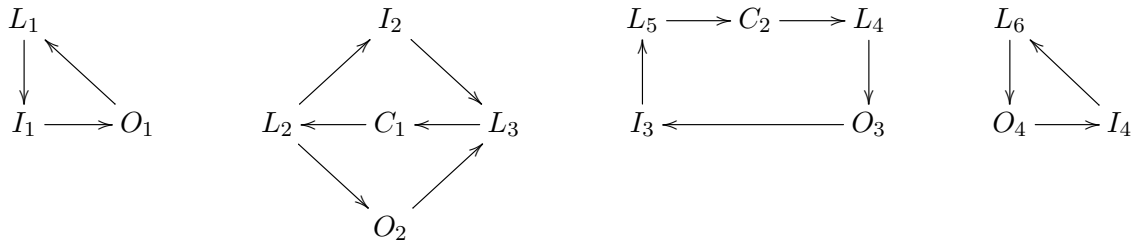

(40)

In the above, some chambers have two arrows leaving them because one can change the leftmost ray without crossing a wall.

4.1.2 Justification of Mutation

The previous subsection gives a straightforward recipe for producing, from a given quiver Q, all of its related duals by considering mutations at various nodes. However we have not yet explained why this mutation rule is in fact correct. In this subsection we fill in this gap. Specifically our goal will be to derive the mutation rule, given the assumption that a quiver description $\widetilde{Q}$ exists after the transition illustrated by Figure 3.

The basic point is that the new elementary basis particles $\widetilde{\gamma}_i$, are interpreted from the point of view of Q as certain bound states of the original basis particles γ_i. The key step is to identify which bound states.

Consider again the cone geometry illustrated in Figure 3. A special role is played by the two particles whose central charge rays form the boundary of the cone. Such particles must always be included in the basis because, as their central charges are on the boundary of the cone, there is no way to generate these states by positive linear combinations of other rays in the cone. Thus in Figure 3b the two states with central charges $\mathcal{Z}'$ and $-\mathcal{Z}_1$ must appear as nodes of the quiver $\widetilde{Q}$. Of these, the latter is easy to identify as the antiparticle of the mutated node, $-\gamma_1$, and hence this charge must be in the new basis. Meanwhile, in the following argument we will prove that the left-most ray, which we frequently refer to as the extremal ray, $\mathcal{Z}'$, is always a two particle bound state which may be identified explicitly.

To begin, we consider all connected length two subquivers of Q which involve the node γ_1. For

a given node γ_i there are k_i arrows pointing either from γ_i to γ_1 or from γ_1 to γ_i.

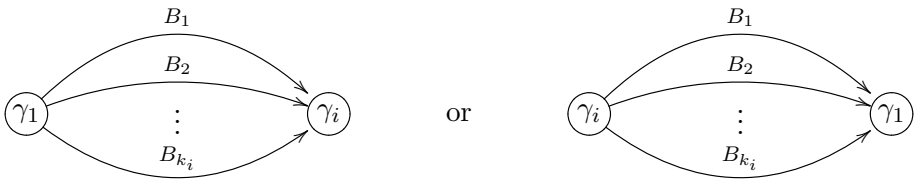

(41)

Let us describe the leftmost bound state supported by these two node quivers. In the case on the right of (41), γ_1 appears as a sink. Then, since $\mathcal{Z}(\gamma_1)$ has largest phase by hypothesis, γ_1 by itself is a destabilizing subrep of any possible bound state; thus no bound states can form.

On the other hand, in the case on the left of (41), where γ_1 appears as a source, bound states can exist. We consider a general representation of the form

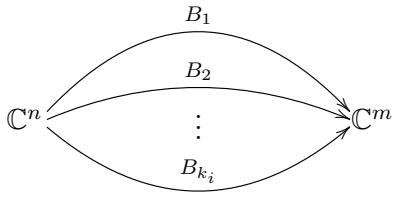

(42)

To make a bound state with largest possible phase we wish to make a representation where n/m is as large as possible. However, it is not difficult to see that the ratio n/m is bounded. Indeed, since $\mathcal{Z}(\gamma_1)$ has largest phase, there is a potentially destabilizing subrepresentation involving only the particle γ_1. Such a subrepresentation is described by k_i commutative diagrams of the form

$$\begin{array}{ccc} \mathbb{C}^n & \xrightarrow{B_j} & \mathbb{C}^m \\ \uparrow & & \uparrow \\ \mathbb{C} & \xrightarrow{0} & 0 \end{array} \tag{43}$$

In other words, the potential destabilizing subrepresentation is nothing but a non-zero vector which is simultaneously in the kernel of all of the maps B_j. But then a simple dimension count shows that

$$\text{dimension}\left(\bigcap_{j=1}^{k_i} \ker(B_j)\right) \geq n - k_i m. \tag{44}$$

And so in particular when the right-hand side of the above is positive, the subrepresentation (43)

exists and hence the bound state is unstable. Thus we learn that stability requires

$$\frac{n}{m} \leq k_i. \tag{45}$$

Finally, it is not difficult to find a stable representation R which saturates the above bound. Indeed let us take $n = k_i$ and $m = 1$. Then the maps B_j are simply projections to a line. The stability constraint that the B_j have no common kernel implies that, up to gauge transformation, B_j can be taken to be the dual vector to the jth basis element in the vector space attached to γ_1. So defined, the representation R is stable and has no moduli. Thus it gives rise to a hypermultiplet with charge

$$\gamma_i + k_i\gamma_1. \tag{46}$$

This completes the required analysis of quivers with two nodes. To summarize, in the region of parameter space where $\mathcal{Z}(\gamma_1)$ has largest phase, we have determined the extremal bound state of all two-node subquivers involving γ_1. The charges of the extremal bound states are:

- If $\gamma_i \circ \gamma_1 < 0$ then the extremal bound state is simply γ_i.
- If $\gamma_i \circ \gamma_1 > 0$ then the extremal bound state is $\gamma_i + (\gamma_i \circ \gamma_1)\gamma_1$.

Now we claim that in the quiver Q with an arbitrary number of nodes, one of the two particle bound states we have identified above will still be the left-most extremal ray after $\mathcal{Z}(\gamma_1)$ exits the upper half-plane. To see this, we consider an arbitrary stable representation R of Q. We write the charge of R as

$$\gamma_R = n\gamma_1 + \sum_{\gamma_i \circ \gamma_1 > 0} m_i\gamma_i + \sum_{\gamma_j \circ \gamma_1 \leq 0} l_j\gamma_j \tag{47}$$

Let us focus in on the representation R near the node γ_1. There are now many nodes connected to the node 1 by various non-zero maps. For those connections with $\gamma_i \circ \gamma_1 \leq 0$, the node γ_1 appears as a sink, for those with $\gamma_i \circ \gamma_1 > 0$, γ_1 appears as a source.

Our strategy is again to test whether R is stable with respect to decays involving the subrepresentation S with charge γ_1. As in the two node case, in such a situation the connections where γ_1 is a sink are irrelevant. On the other hand, if S is really a subrepresentation then for each node link in the representation where node 1 is a source, we have commutative diagrams of the form (43).

Given that $\mathcal{Z}(\gamma_1)$ has largest phase, stability of R means that we must obstruct the existence of S. As in the analysis of the two node quivers we see that S will be a subrepresentation provided that the kernels of all maps exiting the node γ_1 have nonzero intersection. However, just as in (44) we can see that this leads to an a priori bound on n, the amount of γ_1 contained in the representation R. Explicitly we have

$$\text{dimension}\left(\bigcap_{\gamma_i\circ\gamma_1>0}\bigcap_{j=1}^{k_i}\ker(B_j)\right)\geq n-\sum_{\gamma_i\circ\gamma_1>0}k_i m_i. \tag{48}$$

Hence to obstruct the existence of the subrepresentation S we deduce the bound

$$n\leq\sum_{\gamma_i\circ\gamma_1>0}k_i m_i. \tag{49}$$

But now we can directly see that R cannot be extremal. We have

$$\begin{aligned}\arg\left(\mathcal{Z}(R)\right) &= \arg\left(nZ_1+\sum_{\gamma_i\circ\gamma_1>0}m_iZ_i+\sum_{\gamma_j\circ\gamma_1\leq 0}l_jZ_j\right) \\ &\leq \arg\left(\sum_{\gamma_i\circ\gamma_1>0}m_i(k_iZ_1+Z_i)+\sum_{\gamma_j\circ\gamma_1\leq 0}l_jZ_j\right).\end{aligned} \tag{50}$$

But the final expression in (50) is manifestly contained in the positive span of the two node extremal bound states, $k_i\gamma_1+\gamma_i$, that we identified in our analysis of two node quivers. In particular, this means that R cannot be a boundary ray and hence is not extremal.

Thus we deduce that the left-most ray after mutation is one of the two particle bound states that we have identified in our analysis of two node quivers. Extremality then ensures that our new basis must include this two particle bound state. But finally we need only notice that the central charges of all the two node extremal bound states that we have discovered are independent parameters. Indeed letting the central charges vary in an arbitrary way, our conclusion is in fact that *all* the two node bound states which we have determined must in fact be in the new basis. In particular this means that the new basis of charges after mutation is completely fixed and we may

write the transformation as follows:

$$\widetilde{\gamma}_1 = -\gamma_1 \tag{51}$$

$$\widetilde{\gamma}_j = \begin{cases} \gamma_j + (\gamma_j \circ \gamma_1)\gamma_1 & \text{if } \gamma_j \circ \gamma_1 > 0 \\ \gamma_j & \text{if } \gamma_j \circ \gamma_1 \leq 0 \end{cases} \tag{52}$$

As one can easily verify, the graphical quiver mutation rules described in the previous section are a direct consequence of computing the new BPS quiver $\widetilde{Q}$ from the symplectic products of the new basis of charges $\{\widetilde{\gamma}_i\}$. This completes our argument justifying the mutation rules.

4.2 The Mutation Method: BPS Spectra from Quiver Dualities

We saw above that at walls of the second kind, we were forced to change our quiver description because the central charge of some state exited the upper half of the complex half-plane, thereby turning from a particle to an antiparticle. We might also consider what happens if we fix a modulus $u \in \mathcal{U}$ and then consider a different definition of the particle half-plane, $\mathcal{H}$. If we imagine continuously changing our choice from one $\mathcal{H}$ to another, the situation is precisely the same as above; there is some parameter which we are tuning, and at some critical value the central charge of some state becomes such that it switches from particle to antiparticle.

In this case, however, we are remaining at a fixed point in moduli space, and so all of these quivers describe precisely the same physics. That is, they are dual descriptions of the BPS spectrum. In fact, there is a whole class of quivers related to each other by duality at each point in moduli space. We will now exploit this fact to produce for us, in many cases, the entire spectrum for free.

First, let us reiterate that a single form of the quiver already in principle determines exactly which BPS states in the theory are occupied, including their spin and multiplicity. To find the answer, one can solve the representation theory of the quiver with superpotential, which amounts to the linear algebra problem described in section 3.3. However, in practice this problem can become quite intractable. The mutation method we propose gets rid of all of the unsightly work required in solving the problem directly, and instead produces the spectrum using chains of dualities through different quiver descriptions of the theory.

Recall our first application of quiver rep theory in section 3.3, where we checked that nodes

of the quiver always correspond to multiplicity one hypermultiplets. This fact, together with an examination of which states are forced to be nodes for various choices of half-plane $\mathcal{H}$, is at the heart of what we call the mutation method. Imagine that for our initial choice of $\mathcal{H}$, with BPS basis $\{\gamma_i\}$, γ_1 is the node such that $\mathcal{Z}(\gamma_1)$ is left-most in $\mathcal{H}$.[15] Say we then rotate our half-plane past it, and do the corresponding mutation to arrive at a new quiver description of the theory. This mutation includes an action on the charges of the quiver γ_i, as given in equation (3.2)-(3.3). Since this new quiver is a description of the BPS states of the same theory, its nodes are also multiplicity one hypermultiplets. Consequently, we have discovered some subset of states in the 4d theory which we can say must exist. In particular, we generate some new BPS states of the form $-\gamma_1, \gamma_i + (\gamma_i \circ \gamma_1)\gamma_1$. Of course, $-\gamma_1$ is just the antiparticle of the state γ_1, so this is no additional information. However, the states $\gamma_i + m_i\gamma_1$ are completely new. To discover these same states from the original quiver would have involved solving the non-trivial representation theory problem studied in the previous subsection. We are able to avoid this headache by observing that, because of duality, these states must be in the spectrum for consistency.

So we have found that duality will trivially produce some subset of the spectrum as nodes of various dual quivers. But in fact it does much more: in many cases, mutation produces the full spectrum in this way. Imagine we're in a chamber with finitely many BPS states, and pick an arbitrary state γ which is a hypermultiplet of the 4d theory. Then we can rotate the half-plane $\mathcal{H}$ so that γ is left-most. As usual, since the nodes of the quiver form a positive basis for states in $\mathcal{H}$, γ must itself be a node. Therefore, if we start with any quiver description, and start rotating $\mathcal{H} \to e^{-i\theta}\mathcal{H}$ until γ becomes left-most, we will go through a corresponding sequence of mutations, after which γ will simply be a node of the quiver.

It is then easy to see how to systematically generate the spectrum in any finite chamber. We start with any quiver description which is valid at our given point in moduli space, and start rotating the half-plane. Since there are only finitely many states, we will only pass through finitely many mutations before we return to the original half-plane $\mathcal{H} \to e^{2\pi i}\mathcal{H}$.[16] The key point is every state in the chamber is left-most at some point during this rotation, so every state will indeed show

[15] From now on we will abuse verbiage slightly and simply say that "γ_1 is left-most."

[16] Recall that for a given choice of $\mathcal{H}$, the quiver description is actually unique - there is a unique positive integral basis for the lattice of occupied BPS states, up to permutation. So we will also return to the original quiver up to permutation when $\mathcal{H}$ undergoes a full rotation.

up as a node of one of the dual quivers. Since rotating past a state corresponds to mutating on the node corresponding to that state, if we do the entire sequence of mutations and record each state we've mutated on, we will have exhausted all states in the chamber.

We can save a bit of work by making use of CPT: for any state γ in the spectrum, $-\gamma$ is also occupied. So instead of taking $\mathcal{H} \to e^{2\pi i}\mathcal{H}$, we can just rotate half-way, $\mathcal{H} \to e^{i\pi}\mathcal{H}$, ending up at the quiver which describes all the antiparticles.[17] If we record every state γ we mutate on as $\mathcal{H}$ is rotated, and then add all antiparticles $-\gamma$, we will have precisely the spectrum of the 4d theory. Note that we must repeat this procedure for each chamber, by doing mutations in some different order, as prescribed by the ordering of the phases of the central charges in that region of moduli space. As we discussed above any given quiver generally only covers some subset of moduli space; therefore, for different chambers, it will generally be necessary to apply this procedure to different mutation forms of the quiver.

Let's try an example. The representation theory for the Argyres-Douglas A3 theory was worked on in detail in section 3.4.1. We will see how to reproduce it with much less work in the present framework. We will assume that we are at a point in moduli space covered by the cyclic three node quiver. Imagine that γ_1 is leftmost. After the first mutation, the mutation that follows will depend on the ordering of γ_3 and $\gamma_1 + \gamma_2$. Suppose that γ_3 is to the left. Then the particle half-plane, $\mathcal{H}$

[17] By a similar argument as above, the final quiver will have nodes $-\gamma_i$.

and associated quiver before (i) and after (ii) the first mutation at γ_1 are

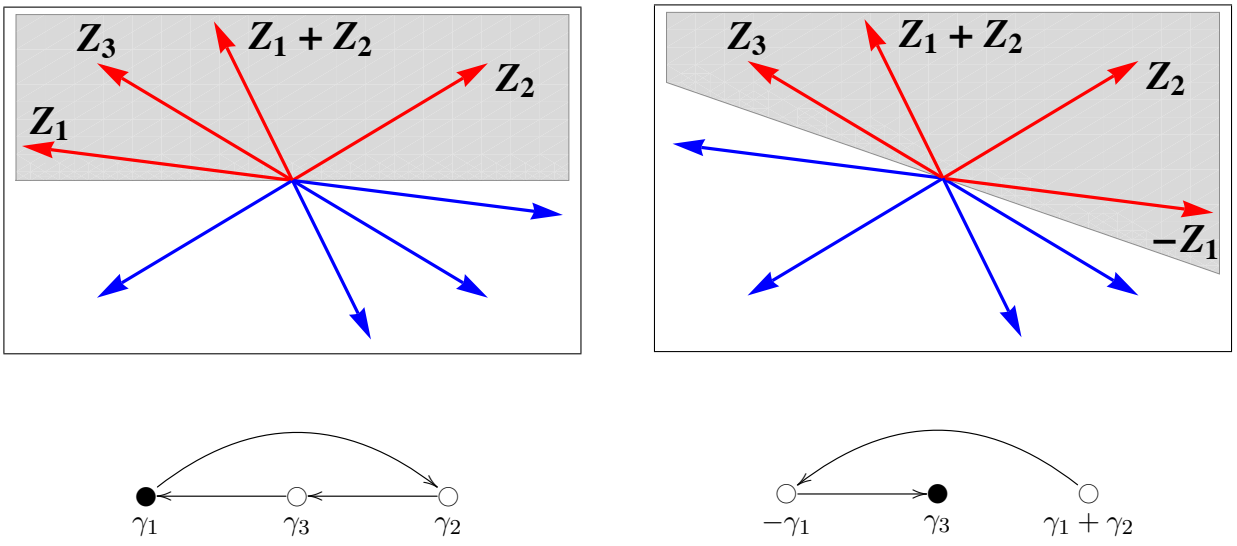

(i) (ii)

In the above diagrams, we denote the left-most particle state in each quiver, which indicates the next node to be mutated, by drawing the corresponding node in black, ●. Now since the γ_i were in the original half-plane $\mathcal{H}$ to begin with, it must be that $\gamma_1 + \gamma_2$ is to the left of $-\gamma_1$ and $-\gamma_3$ in the current half-plane. This is true in general: one never mutates on negative nodes in going through a π-rotation of $\mathcal{H}$ from a quiver to its antiparticle quiver. The remaining mutations are completely

fixed, and we find (iii,iv,v)

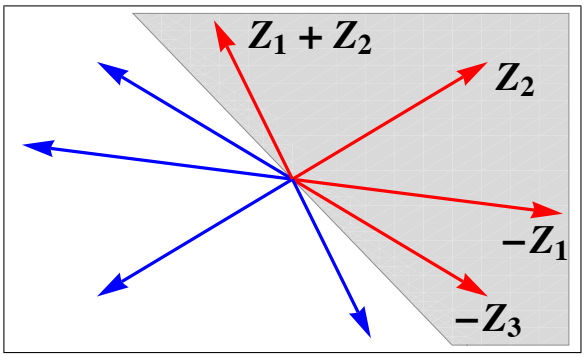

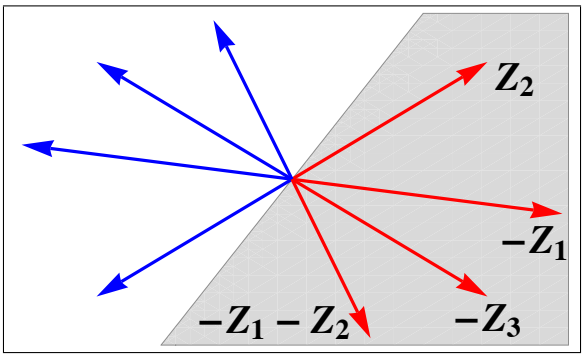

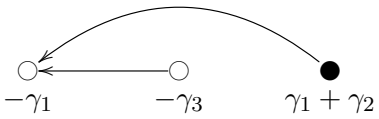

(iii)

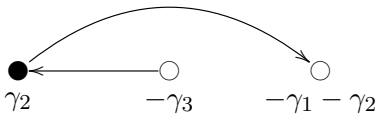

(iv)

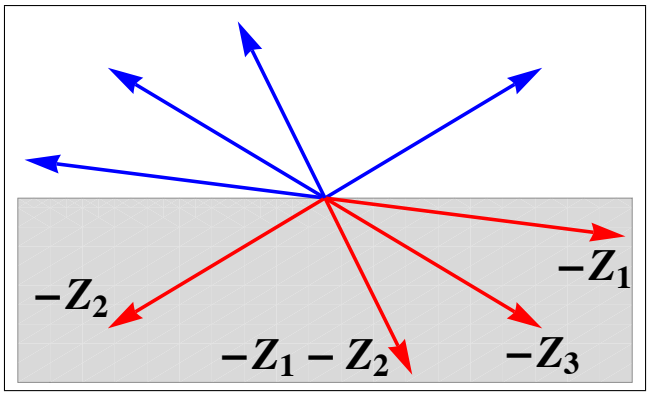

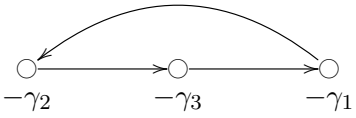

(v)

So we've arrived at the antiparticle quiver, which at the level of quiver without charges is the same, because the antisymmetric product is not affected by an overall sign on charges.[18] Therefore we've discovered a chamber with the states γ_1, γ_2, γ_3 and $\gamma_1 + \gamma_2$. This indeed agrees with one of the

[18] If you try to label nodes and keep track of them, which the drawings may subliminally suggest you do, in general you will return to $(-1)\times$permutation.

chambers found in 2.3.2. All of the chambers can similarly be mapped out, without ever doing the linear algebra analysis.

We pause here to emphasize two important points. The first is to recall that a quiver from the mutation class generically only covers a subset of moduli space. Therefore to map out all chambers, one must carry forth the above with the starting quiver being any one of the quivers in the mutation class. The second point is that, using the above method, one will not find any chamber covered by the cyclic quiver which contains the state $\gamma_1 + \gamma_2 + \gamma_3$. In the analysis of section 2.3.2, it was found that the $\gamma_1 + \gamma_2 + \gamma_3$ state was there in the quiver without superpotential, but killed when the (unique) non-degenerate superpotential was included. Thus we see that this mutation method knows about the associated non-degenerate superpotential indirectly. This is expected, because a non-degenerate superpotential is required for the mutation rule written above to be sensible.

There are some simple non-trivial statements which we can immediately make based on this method. One is that any finite chamber can only contain hypermultiplets, with multiplicity one. The argument here is simply that any state in a finite chamber can be made into a node of some dual quiver, and nodes, as we've mentioned, can never correspond to higher spin objects or higher multiplicity hypers. Therefore, it would be inconsistent with duality to ever have a higher spin or higher multiplicity object in a finite chamber.

Now let's consider infinite chambers. An additional layer of complexity, as compared to the finite case, is that two dual quiver descriptions may be separated by an infinite sequence of mutations. This is because, as we rotate between two choices of $\mathcal{H}$, we will generically have infinitely many BPS states which rotate out to the left. Our method above depended on our ability to keep track of the sequence of mutations which happens as $\mathcal{H} \to e^{i\pi}\mathcal{H}$. Now the infinitude of states in some sense blocks us from competing this sequence of mutations. For example, if we start with a given quiver description, we can't explore beyond the closest accumulation ray in the $\mathcal{Z}$-plane. Because of this difficulty, we can't make a similarly definite statement about the method as it applies to infinite chambers. Indeed, for certain theories, such as $\mathcal{N} = 2^*$ $SU(2)$ (the mass deformed $\mathcal{N} = 4$ theory), it appears that the method isn't sophisticated enough to exhaust the spectrum.[19]

However, as we will see in several examples, infinite chambers may also be understood by

[19]Of course we can always produce some arbitrarily large subset of states of the theory by mutating until exhaustion (of the mutator, that is).

this method. Infinitude of the chamber is often due to higher spin objects, and we can often make progress by being just a bit clever. Note that any higher spin object must in fact be an accumulation ray of states in the central charge plane: If it weren't, we could rotate $\mathcal{H}$ so that it was left-most, and as above, in this dual quiver description our higher spin state would be a node. Of course this is a contradiction - nodes are always multiplicity one hypers. Higher multiplicity hypers must similarly be accumulation rays, a fact which may be less intuitive outside of this framework.

Before going on to examples and applications, we make some additional technical notes about the actual implementation of the mutation method. As we have described it here, we choose a point of the physical moduli space, compute central charges at that point, and mutate on the nodes in the order given by the ordering of phases of the central charges, as we tune $\mathcal{H} \to \mathcal{H}_\pi$. Instead, when exploring the possible BPS spectra, it is sometimes more practical to simply mutate on the nodes in any order, and then check two things: (1) that the ordering chosen is consistent, and (2) that the ordering chosen is realized somewhere in physical moduli space. By consistent, we mean that there exists some choice of central charges $\mathcal{Z}(\gamma_i)$ that correspond to the ordering chosen. As it turns out, there is no need to check the first point: as long as we mutate only on nodes whose charges are given by positive linear combinations of the original γ_i, then the ordering is consistent. Of course, we expect to only mutate on positive nodes since we are only rotating by π through the particle half-plane, and all particles should be given by positive integer linear combinations of the initial γ_i. Note that the only condition for consistency is that $\arg \mathcal{Z}(\gamma_1 + \gamma_2)$ lie between $\arg \mathcal{Z}(\gamma_1), \arg \mathcal{Z}(\gamma_2)$. In fact, the mutation method protects us from making inconsistent choices. Fix $\arg \mathcal{Z}(\gamma_1) > \arg \mathcal{Z}(\gamma_2)$, and suppose we have already mutated past γ_1, but not yet γ_2. Thus $-\gamma_1$ is in the positive integral span of the mutated quiver basis. Suppose both $\gamma_1 + \gamma_2$ and γ_2 to appear as nodes; this is an immediate contradiction with the fact that the nodes form a basis, since now γ_2 is both a basis element and a non-trivial linear combination of basis elements $(\gamma_1 + \gamma_2) + (-\gamma_1)$. So only one of these can appear as nodes and be mutated on next. If it is $\gamma_1 + \gamma_2$, there we are safe, and there is no inconsistency. If it is γ_2, let's mutate past so that both $-\gamma_1, -\gamma_2$ are in the positive integral span of the mutated quiver basis; now it is impossible for $\gamma_1 + \gamma_2$ to appear as a node of the quiver, or else we can construct 0 as a non-trivial linear combination of basis elements $\gamma_1 + \gamma_2 + (-\gamma_1) + (-\gamma_2)$.

Therefore we can apply the mutation method by simply mutating on the positive nodes in any

order we like, until we arrive at a quiver with all nodes labeled by negative charges, indicating that we have completed the rotation $\mathcal{H} \to \mathcal{H}_\pi$. It remains to be checked whether the ordering we have applied is actually physically realized in moduli space. We can dispense of this final check when the physical moduli space has complex dimension equal to the number of nodes. Then as we move in moduli space, it is possible to tune all central charges of nodes however we wish. These theories are known as *complete* theories, studied and classified in [21]. In section 7, we will study the application of these techniques to the class of complete theories. In the more general case of non-complete theories, existence of the desired charges in the physical moduli space must be checked, though one can argue that there exist UV completions of the same IR theory which fill out the moduli space and allow arbitrary choices of central charges.

5 $SU(2)$ Gauge Theories

We will now return to where we started - the $SU(2)$ SYM theory. We will make quick work of understanding the BPS spectrum of this theory in a constructive way, without using the consistency trick we demonstrated in section 2. We will then quickly transition to more complicated examples by adding matter to our theory, hypermultiplet by hypermultiplet, until it is no longer asymptotically free.

5.1 Pure $SU(2)$

The quiver for pure $SU(2)$ gauge theory has been worked out in various papers [14, 16, 21, 33, 35]. Here we will content ourselves to fix it based on the known weak coupling spectrum, as was done in section 3.1. We will verify that the quiver, in turn, generates the correct spectrum at weak coupling, as discussed in section 3.1.3.

We recall that the quiver takes the form

(53)

While directly solving for the representation theory of this quiver is a relatively difficult task, the mutation method applies quite simply. We first look at the strong coupling chamber, which is given

by $\arg \mathcal{Z}(\gamma_2) > \arg \mathcal{Z}(\gamma_1)$. To apply the mutation method, we rotate $\mathcal{H}$, which gives the following sequence of mutations:

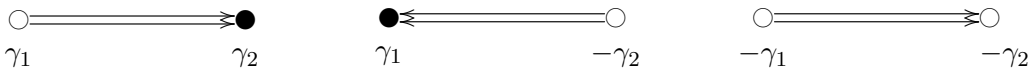

(54)

(i) (ii) (iii)

We see that we end with the antiparticle quiver, and that the only states in this chamber are γ_1 and γ_2. Thus we have found the same result as we found with our consistency argument in section 2. Namely, only the dyon and monopole are stable inside the strong coupling region.

Now we can check that the quiver reproduces the input spectrum at weak coupling, where $\arg \mathcal{Z}(\gamma_1) > \arg \mathcal{Z}(\gamma_2)$. We begin with the usual sequence of mutations

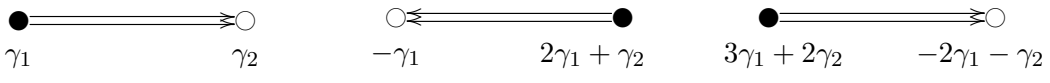

(i) (ii) (iii)

(55)

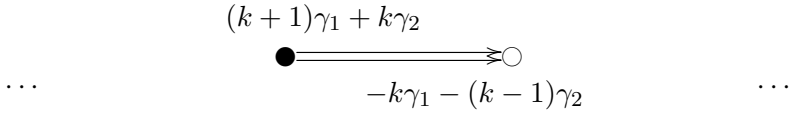

(k+1)

It is quite clear that we are in an infinite chamber. The entire sequence we'll find is obvious: we will have $(k+1)\gamma_1 + k\gamma_2$ for $k \geq 0$, with charge $(2k, 1)$. In the $\mathcal{Z}$ plane these limit to the ray $\alpha \mathcal{Z}(\gamma_1 + \gamma_2)$. Notice that the (e, m) charge of $\gamma_1 + \gamma_2$ is $(2, 0)$. We're finding the expected

accumulation ray associated with the vector, the W boson, in the weak coupling spectrum. In terms of rotating the half-plane, W is protected from being a node because it is an accumulation ray of hypermultiplet dyons. In terms of the mutations, the "quiver with W as a node" is infinitely many mutations away in the space of dualities, preventing a contradiction. As mentioned above, this accumulation ray is blocking us from exploring the states lying in the rest of the central charge plane. We expect to only find one vector in the pure $SU(2)$ theory, but we have not yet found all the dyons. We would expect another set of dyons, $(2k, -1)$ which decompose as $k\gamma_1 + (k+1)\gamma_2$ for $k \geq 0$. These would all lie to the right of the W boson, $\gamma_1 + \gamma_2$; thus we need some method for exploring that region of the $\mathcal{Z}$-plane.

In this case, and in any case where there is only a single accumulation ray, we can get around this problem easily. To do so, we recall that our mutation rule came from rotating the half-plane clockwise, $\mathcal{H} \to e^{-i\theta}\mathcal{H}$. We'll refer to this as left-mutation, because it is associated with states rotating out of the left of $\mathcal{H}$. There should of course be a similar mutation rule corresponding to rotating the half-plane counter-clockwise instead, $\mathcal{H} \to e^{i\theta}\mathcal{H}$, which we will call right-mutation. Both of these rules can be expressed as an action of a linear operator on the set of charges γ_i which label the nodes of the quiver. If we call the usual left-mutation action on charges M_L, and the right-mutation action M_R, then we should have the obvious relations

$$M_L M_R = M_R M_L = Id_{\{\gamma\}} \tag{56}$$

One can check that the transformation which satisfies the above identities (for γ_1 rotating out of $\mathcal{H}$) is simply

$$\widetilde{\gamma}_1 = -\gamma_1 \tag{57}$$

$$\widetilde{\gamma}_j = \begin{cases} \gamma_j + (\gamma_1 \circ \gamma_j)\gamma_1 & \text{if } \gamma_1 \circ \gamma_j > 0 \\ \gamma_j & \text{if } \gamma_1 \circ \gamma_j \leq 0. \end{cases} \tag{58}$$

Pictorially, mutation to the left (on node 1) acts non-trivially on those nodes which 1 points to, while right mutation acts non-trivially on nodes which point to 1. With this new rule in hand,

we can start with the quiver and begin mutating "to the right". Then we'll explore the BPS states starting from the right side of $\mathcal{H}$, as these are the ones leaving the half-plane. If there is only a single accumulation ray in $\mathcal{H}$, left and right-mutation together will allow us to explore both sides of it, filling out the entire $\mathcal{Z}$-plane except for the ray of the accumulation point.

Let's apply right mutation starting from the original $SU(2)$ quiver to find the remaining states. Now we use $\otimes$ to indicate the right-most node which will be right-mutated next.

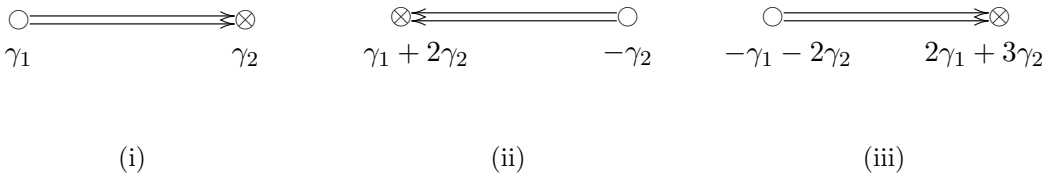

(59)

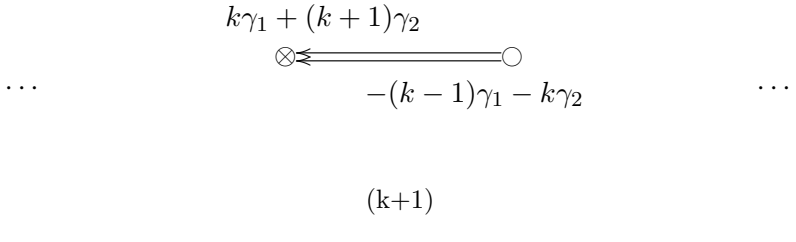

We have generated the states $k\gamma_1 + (k+1)\gamma_2 = (2k, -1)$. So mutation to the right obtains the dyons that we didn't see before, namely the ones lying on the other side of the vector. Since these states limit to the same ray in the $\mathcal{Z}$ plane, $\mathcal{Z}(\gamma_1 + \gamma_2)$, we have understood the stability of all states except those lying on this ray. To complete the analysis, in principle one should do the representation theory for states along the ray $\gamma_1 + \gamma_2$. At a generic choice of parameters, the only particles that may exist along this ray are of the form $n(\gamma_1 + \gamma_2)$.[20] It turns out that there is indeed a single vector present with the expected charge. This seems slightly obnoxious, because we still have to do some representation theory, but keep in mind that the work has been drastically reduced

[20]This statement heavily relies on the fact that this theory is complete. If the central charges of nodes cannot be varied independently, and the theory is thus incomplete, then there are non-trivial relations satisfied by the central charges of nodes at all points of parameter space. For example, there may be a relation of the form $\gamma_k = \gamma_1 + \gamma_2$, satisfied for all parameter choices. Then the general particle at the ray $\mathcal{Z}(\gamma_1 + \gamma_2)$ is of the form $n(\gamma_1 + \gamma_2) + m\gamma_k$. We will see how this may come about in section 5.3.

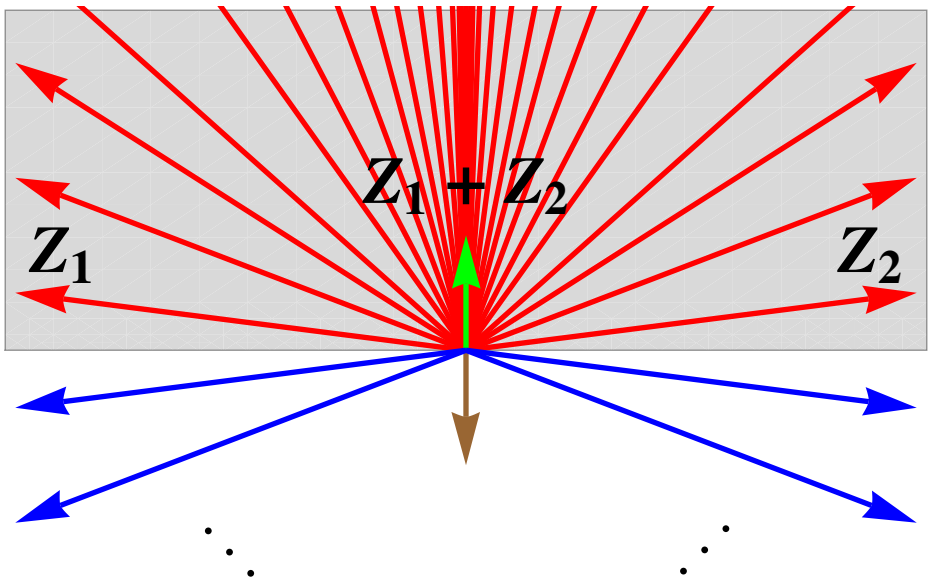

Figure 5: The BPS spectrum of pure $SU(2)$ gauge theory, plotted in the central charge $\mathcal{Z}$-plane. The spectrum contains a vector state with charge $\mathcal{Z}_1 + \mathcal{Z}_2$ (plotted in green), which is forced to occur in the $\mathcal{Z}$-plane at an accumulation ray of hypermultiplet states. On either side of the vector state, there is an infinite sequence of dyons whose central charges asymptotically approach the ray on which the vector lies. The mutation method is able to capture the full spectrum of the theory by rotating the half-plane to the left (yielding particles on the left of the vector particle) and the to right (yielding particles on the right of the vector particle).

in that we only have to check for representations along this ray.

To summarize, we have found the strong coupling $SU(2)$ spectrum by a completely trivial application of the mutation method. For the weak coupling chamber, we introduced *right-mutation* to be able to explore the central charge $\mathcal{Z}$-plane on both sides of the accumulation ray at the W boson. Here we found, as expected, the W boson and the infinite tower of dyons. In Figure 5, we draw the spectrum in the $\mathcal{Z}$-plane to clarify how the mutation method is capable of obtaining all states of the theory. The well-known resulting spectra are summarized in the table below:

Strong coupling		**Weak coupling**	
Monopole:	$(0,1)$	Positive dyons:	$(2n,1)$
Dyon:	$(2,-1)$	Negative dyons:	$(2n+2,-1)$
		W boson:	$(2,0,0)$

5.2 Adding matter

The quiver of $SU(2)$ $N_f = 1$ was deduced using general considerations in [21]. We will briefly review the reasoning used. We expect $2r + f = 3$ nodes of the quiver. First we note that we can tune the mass of the quark to infinity. Then the massive quark fields should decouple from the theory, leaving the BPS states of pure $SU(2)$. This suggest that the quiver should consist of the pure $SU(2)$ quiver (with the usual monopole and dyon charges) along with an additional node. In the decoupled limit, there should be additional states with (e, m) charges $(\pm 1, 0)$; the third node should correspond to one of these two charges. However, we need to make the correct choice for third node that allows *both* of these new states to be generated by positive linear combinations of the nodes. If we take $(1, 0)$, all nodes of the quiver have positive electric charge, and the state $(-1, 0)$ cannot be generated; the correct choice is then $(-1, 0)$, which can be combined with the W boson $(2, 0)$ of the $SU(2)$ subquiver to form $(1, 0)$. Computing electric-magnetic inner products, we find the following quiver:

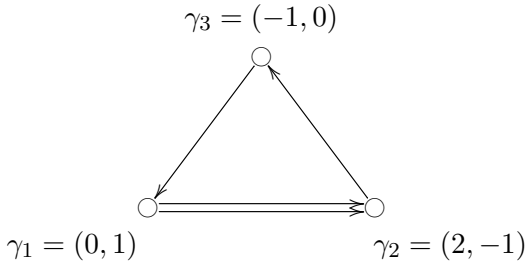

(60)

We can repeat this argument to add as many additional flavors as we like; the result is to produce N_f copies of the node γ_3 with different flavor charges.

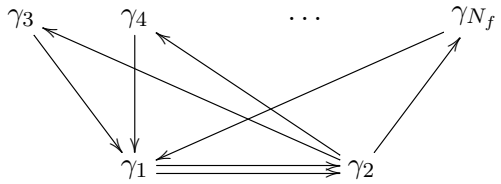

(61)

Alternatively, we can add hypermultiplet matter charged under other representations of the gauge group. If instead of a fundamental **2** of $SU(2)$ we consider a **j** rep of $SU(2)$, we find that γ_3 has charge $(-j, 0)$. Generalizing our analysis above, we conclude that if a quiver description of this

theory exists, it is given by a similar quiver with j arrows $\gamma_3 \to \gamma_1, \gamma_2 \to \gamma_3$

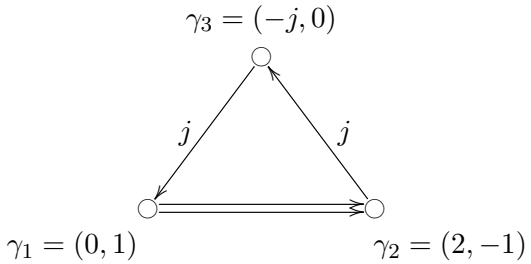

(62)

Certainly this quiver can generate the full **j** representation, raising the electric charge by adding the W boson. However, for $\mathbf{j} \neq \mathbf{2}$, it is possible that the quiver generates some additional representations of the gauge group. Indeed, it turns out that such a quiver will correspond to $SU(2)$ with a full $\otimes^j \mathbf{2}$ representation of the gauge group. We will see an explicit occurrence of this in section 8.5, where for $j = 2$ the quiver above (62) produces the matter representation $\mathbf{3} \oplus \mathbf{1}$.

5.3 Massless $N_f = 1$

Recall that a single quiver from the mutation class generally does not cover all of moduli space. If we start with a valid quiver description and move in moduli space, it may be that at some point the central charges $\mathcal{Z}(\gamma_i)$ no longer lie in a common half-plane. We deduced the $SU(2)$ with matter quivers in the decoupling limit of infinite quark mass, so there is no reason to expect it to cover the chamber with the bare mass of the quark set to zero. Actually, one can easily see that the massless chamber should have $\mathcal{Z}(\gamma_1 + \gamma_2 - 2\gamma_3) = 0$ for the charges given in (60). Thus we have $\mathcal{Z}(\gamma_3) = -\frac{1}{2}\mathcal{Z}(\gamma_1) + \mathcal{Z}(\gamma_2))$. There is no way that the three central charges can lie in a single half-plane.

It is easy to remedy this situation by properly applying mutations. Imagine beginning at a point of parameter space where the quiver above is valid. Then we consider tuning parameters until we reach the desired point. As we do this, we should keep track of any states leaving the half-plane, and perform the appropriate mutations. This sounds as though it involves detailed knowledge of the moduli space geometry, but that turns out to be completely unnecessary. There is no need to restrict our path to the physical parameter space; instead we are free to move throughout full space of central charges for the theory. In other words, we are free to pretend that the theory is complete

as we tune parameters.[21] This drastically simplifies the procedure. Now we may start with a valid quiver at a certain choice of parameters, and then tune the central charges one-by-one to produce the arrangement at the desired endpoint in parameter space.

For the $N_f = 1$ quiver (60), let's keep γ_1, γ_2 fixed in the central charge plane, and tune γ_3 from its initial value within the half-plane by rotating it to the right. It will exit on the right, inducing a right-mutation on γ_3. We should continue rotating γ_3 all the way to $\mathcal{Z}(\gamma_3) = -\mathcal{Z}(\gamma_1 + \gamma_2)$, and keep track of mutations of the charges of the mutated quiver. In this case, no additional mutations occur. This gives[22]

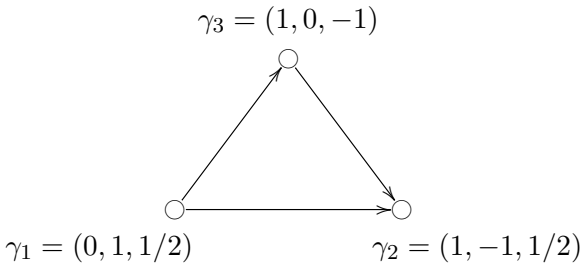

(63)

The flavor group for $N_f = 1$ is $SO(2) \cong U(1)$, so we label the charges of our states by their $U(1)$ charge f; the nodes then correspond to the electromagnetic and flavor charges (e, m, f) as given above. At zero bare mass, the central charge function only depends on the electric and magnetic charges of the states, so the third node is constrained as $\mathcal{Z}(\gamma_3) = \mathcal{Z}(\gamma_1) + \mathcal{Z}(\gamma_2)$. Thus, just as in the pure $SU(2)$ theory, there are only two distinct chambers, one with $\arg \mathcal{Z}(\gamma_1) > \arg \mathcal{Z}(\gamma_2)$, and the other with $\arg \mathcal{Z}(\gamma_2) > \arg \mathcal{Z}(\gamma_1)$. This will turn out to be a feature of all the massless examples we consider.

Let's start by exploring the chamber with $\mathcal{Z}(\gamma_2)$ ahead of $\mathcal{Z}(\gamma_1)$. We start by mutating on γ_2, after which we have the nodes γ_1, γ_3 and $-\gamma_2$. γ_3 is now left most, so we must mutate on it next,

[21] This theory actually *is* complete; however, in any other non-complete examples, the same approach is valid.

[22] The monopole and dyon acquire flavor charges [2], which we now include in the charge labels.

and so on.

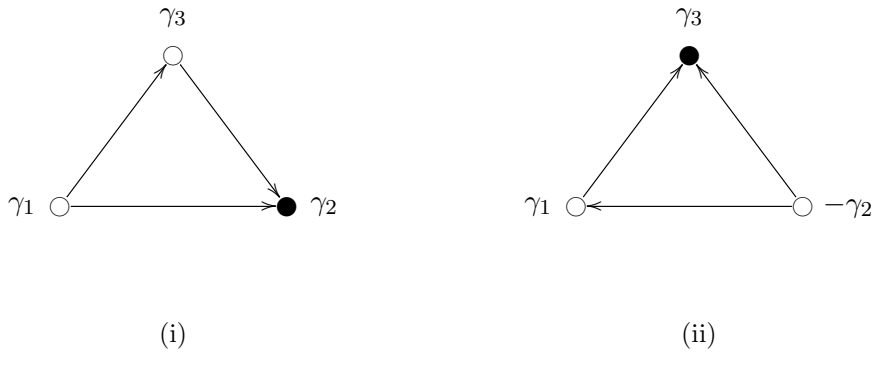

(i) (ii) (iii) (iv) (64)

We see the only states in this chamber were the nodes of the original quiver and their antiparticles. We've discovered the strong coupling chamber of the $N_f = 1$ theory, whose spectrum indeed coincides with these hypermultiplets.

Now let's explore the other chamber. Here we take $\mathcal{Z}(\gamma_1)$ ahead of $\mathcal{Z}(\gamma_2)$. We have the sequence

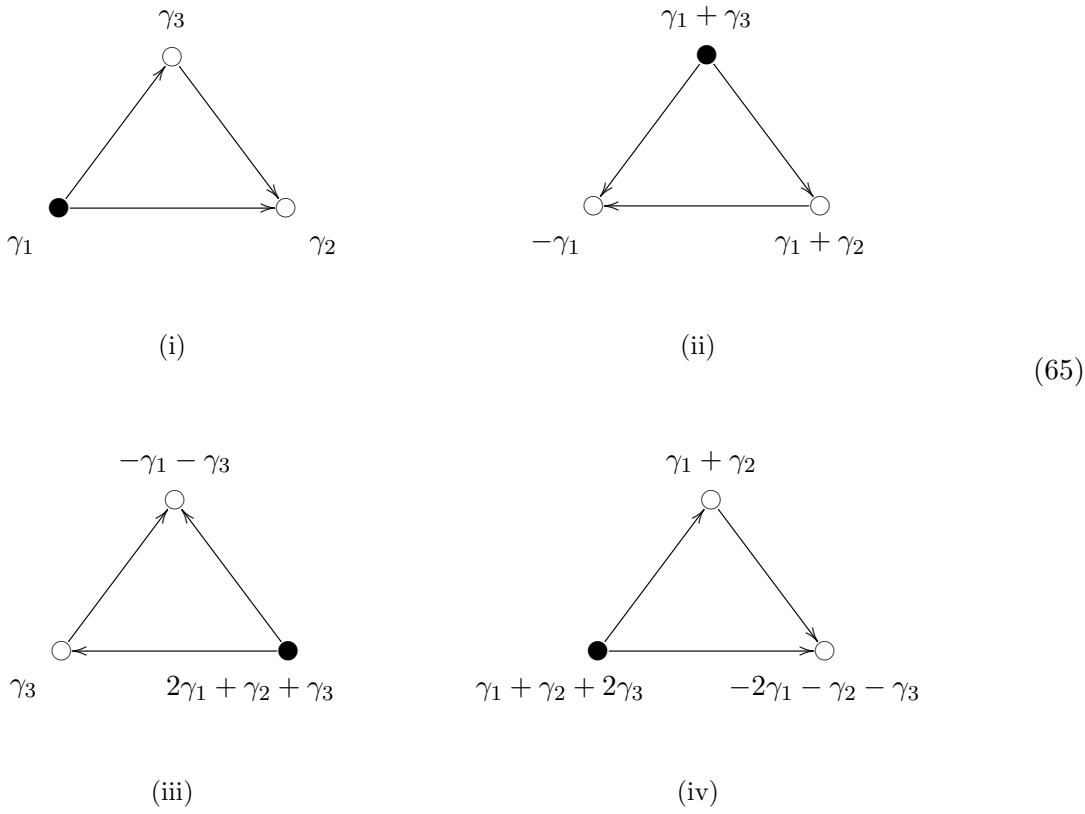

(65)

We're clearly in an infinite chamber. Continuing in this way, we see our spectrum includes the states

$$(n+1)\gamma_1 + n(\gamma_2+\gamma_3) = (2n, 1, 1/2)$$
$$(n+1)(\gamma_1+\gamma_3) + n\gamma_2 = (2n+1, 1, -1/2)$$

As in the weak chamber of the pure $SU(2)$ theory, we are seeing the accumulation ray which should contain the W boson of the theory. Here we are actually getting twice as many hypermultiplets as in pure $SU(2)$ since we have states of both even and odd electric charge. We will identify the odd electric charge states as quark-dyon bound states.

As before, let's start with the original quiver and mutate to the right to study the BPS states

on the other side of the accumulation ray. This generates the states

$$n(\gamma_1+\gamma_3)+(n+1)\gamma_2=(2n+1,-1,1/2)$$
$$n\gamma_1+(n+1)(\gamma_2+\gamma_3)=(2n+2,-1,-1/2)$$

This sequence of states also accumulate at the same ray in the central charge plane; between these two sequences of infinities, the only central charges that can appear are proportional to $\mathcal{Z}(\gamma_1+\gamma_2)$. We might again expect that these dyons limit to a single vector in the central charge plane. We could attempt to test this hypothesis by actually doing the representation theory along this ray, but instead let's appeal to some physical reasoning to see why this is indeed wrong. Namely, we're in the weak coupling chamber of the $N_f=1$ theory. We would expect that this theory indeed contains BPS states corresponding to the fundamental quark hypermultiplet, and at zero bare mass the central charge of this hyper lies directly at the same BPS phase as the W boson. This is precisely the non-generic situation we hinted at in footnote 20.

Actually, given the non-genericity, something special has happened in this example. This quarks, given by γ_3 and by $\gamma_1+\gamma_2$, appeared as nodes after a finite sequence of mutations. Note that we never mutated on these quark nodes, because the nodes we mutate on are left-most (or right-most) and being on an accumulation ray, the quark can never be made left-most (or right-most). Instead, they simply appeared as one of the other "interior" nodes in some of the dual quiver descriptions of the theory. This doesn't have to happen, and indeed won't happen in the undeformed $N_f=2,3$ cases below. We simply got lucky. If we hadn't seen the quark this way, we would have had to find it by hand. In either case, how can we be sure there are no other hypermultiplets lying on top of the vector, which aren't showing up as interior nodes elsewhere? One should consider a slightly deformed $N_f=1$ theory with $m\neq 0$ and check that there are no additional hypermultiplets (aside from those predicted by wall-crossing formulae). In this way, one can check that there are no additional hypermultiplets coinciding with the vector when $m\to 0$. In principle, it is irrelevant whether or not the deformation we take is physically realized - thus, even in a non-complete theory, the same strategy works for understanding the particles along an accumulation ray. Alternatively, of course, one could always directly use quiver representation theory to rule out other states with that BPS phase.

Putting everything together, we find the following possible spectra for massless $N_f = 1$.

Strong coupling		**Weak coupling**	
Quark:	$(1, 0, -1)$	Quarks:	$(1, 0, \pm 1)$
Monopole:	$(0, 1, 1/2)$	Positive dyons:	$(2n, 1, 1/2)$
Dyon:	$(1, -1, 1/2)$	Negative dyons:	$(2n + 2, -1, -1/2)$
		Quark-dyons:	$(2n + 1, \mp 1, \pm 1/2)$
		W boson:	$(2, 0, 0)$

where n ranges over integers $n \geq 0$. Along with their antiparticles, this collection agrees with the well known weak coupling spectrum of massless $SU(2)$ $N_f = 1$ ([73]).

5.4 Massive $N_f = 1$

For just one flavor, it is not too difficult to actually find all possible spectra of the theory with $m \neq 0$. It turns out that the acyclic quiver used in the previous subsection covers all chambers. Unfortunately, there is a great deal of redundancy in the full chamber spectrum - there are many distinct regions of moduli space that give the same spectrum due to dualities. By duality here, we mean the following: the spectrum depends only on the quiver and the central charges decorating the nodes, but not on the actual charge (e, m, f) labels themselves. Thus, there may be widely separated regions of moduli space that happen to have the same quiver and associated central charges, but different charge labels; consistency of this framework requires that such regions actually have spectra that are equivalent up to some appropriate $Sp(2r, \mathbb{Z})$ relabeling of charges. Here we will simply list the possible spectra, without choosing a particular point in moduli space or duality frame; the downside is that, as a result, we cannot give the charges of the states, since charge labels require a choice of duality frame.

- Minimal chamber: 3 nodes are the only BPS states.
- 4 state chamber: 3 nodes and 1 bound state hypermultiplet.
- 5 state chamber: 3 nodes and 2 bound state hypermultiplet.
- Weak coupling chambers, labelled by k. These consist of:

– 2 quark hypermultiplets,

– W boson vector multiplet,

– Infinite tower of dyon hypermultiplets,

– k additional quark-dyon bound state hypermultiplets, for $0 \leq k \leq \infty$.

This list exhausts the BPS spectra that can be supported by quivers in this mutation class. Embedded in this result are the two massless chambers, which correspond to the 3 state minimal chamber and the $k = \infty$ weak coupling chamber. It is a relatively straight-forward exercise to find all these chambers beginning with the minimal massless spectrum, by repeated application of the pentagon and $SU(2)$ wall-crossing identities.

5.5 Massless $N_f = 2$

The relevant quiver for massless $N_f = 2$ follows from analogous mutations of the decoupling limit quiver (61) as in section 5.2. Here we find that the quiver describing the massless theory is given by:

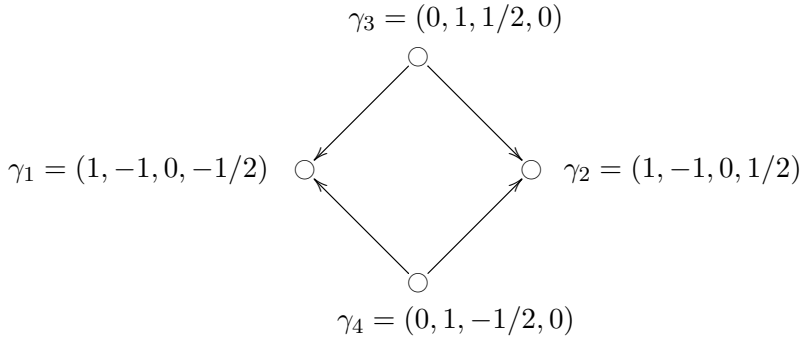

(66)

The flavor group is now $Spin(4) \cong SU(2) \times SU(2)$, and we will denote our states by (e, m, f_1, f_2), where f_i are the charges under the $U(1)$ contained in the ith $SU(2)$ factor. We see that there are only two distinct values for the central charge between the four nodes when the bare masses vanish. This means that there will again only be two chambers, given by the relative ordering of $\mathcal{Z}(\gamma_1) = \mathcal{Z}(\gamma_2), \mathcal{Z}(\gamma_3) = \mathcal{Z}(\gamma_4)$.

There is a small added subtlety that was absent for $N_f = 1$. Namely, we technically can't rotate the central charge of a single node out of the half plane by itself. All mutations will happen for two nodes simultaneously. Also, as mentioned above, we don't get lucky in this example - the quarks don't show up as interior nodes of any of the quivers as we start mutating. If we mass deform

the theory, however, the central charge of the quarks no longer coincides with the vector, and we will see them appear after a finite number of mutations. This tells us that there are the quark hypermultiplets lying on top of the vector when $m \to 0$, but no extra states. For simplicity, we will work out the $m = 0$ point and quote this result.

For strong coupling, we first mutate on nodes 1 and 2, and find

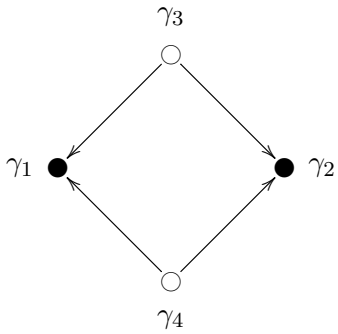

(i)

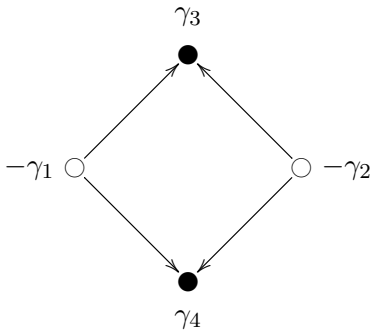

(ii)

(67)

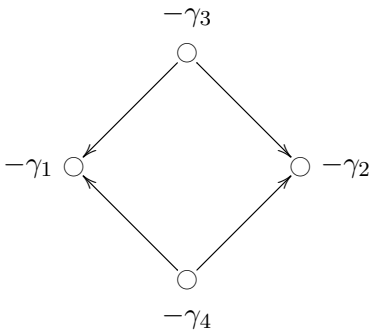

(iii)

Thus we see that this chamber contains no bound states, and the only states are hypermultiplets contributed by the nodes. We have one hypermultiplet of electromagnetic charge $(1, -1)$ in the $(\mathbf{1}, \mathbf{2})$ rep of $SU(2) \times SU(2)$, and one of charge $(0, 1)$ in the $(\mathbf{2}, \mathbf{1})$.

The other chamber is of course more interesting. We have the following sequence of mutations:

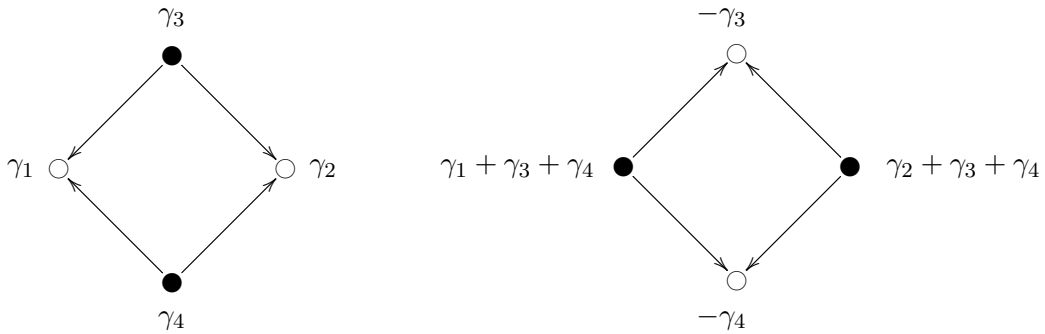

(i) (ii)

(68)

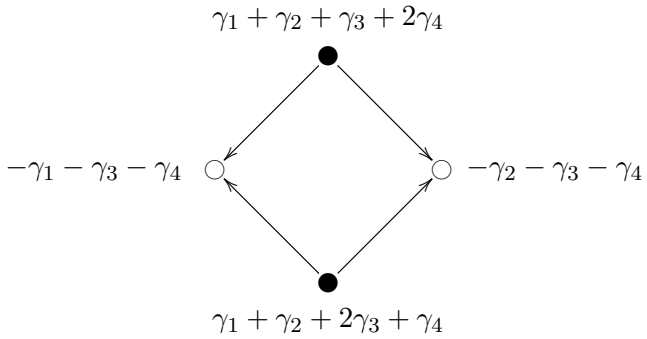

(iii)

Continuing in this way, we generate the states

$$n(\gamma_1+\gamma_2+\gamma_4)+(n+1)\gamma_3=(2n,1,1/2,0)$$

$$(n+1)\gamma_4+n(\gamma_1+\gamma_2+\gamma_3)=(2n,1,-1/2,0)$$

$$(n+1)(\gamma_1+\gamma_3+\gamma_4)+n\gamma_2=(2n+1,1,0,-1/2)$$

$$(n+1)(\gamma_2+\gamma_3+\gamma_4)+n\gamma_1=(2n+1,1,0,1/2).$$

On the other hand, mutating to the right gives the states

$$n(\gamma_1+\gamma_3+\gamma_4)+(n+1)\gamma_2 = (2n+1,-1,0,1/2)$$
$$n(\gamma_2+\gamma_3+\gamma_4)+(n+1)\gamma_1 = (2n+1,-1,0,-1/2)$$
$$(n+1)(\gamma_1+\gamma_2+\gamma_4)+n\gamma_3 = (2n+2,-1,-1/2,0)$$
$$n\gamma_4+(n+1)(\gamma_1+\gamma_2+\gamma_3) = (2n+2,-1,1/2,0).$$

These fill out dyons $(2n,\pm 1)$ in the $(\mathbf{2},\mathbf{1})$ and quark-dyons $(2n+1,\pm 1)$ in the $(\mathbf{1},\mathbf{2})$. Trapped between the two infinite sequences we have the vector boson $\gamma_1+\gamma_2+\gamma_3+\gamma_4 = (2,0,0,0)$, which we identify as the W. The quarks also lie at the same BPS phase, and are given by $\gamma_2+\gamma_4, \gamma_1+\gamma_4, \gamma_2+\gamma_3, \gamma_1+\gamma_3$.

The two spectra are tabulated below, where we now assemble the states into representations of the full $SU(2)\times SU(2)$ with charges given as $(e,m)_{\mathbf{f_1},\mathbf{f_2}}$:

Strong coupling		**Weak coupling**	
Monopole:	$(0,1)_{\mathbf{2},\mathbf{1}}$	Quarks:	$(1,0)_{\mathbf{2},\mathbf{2}}$
Dyon:	$(1,-1)_{\mathbf{1},\mathbf{2}}$	Positive dyons:	$(2n,1)_{\mathbf{2},\mathbf{1}}$
		Negative dyons:	$(2n+2,-1)_{\mathbf{2},\mathbf{1}}$
		Quark-dyons:	$(2n+1,\pm 1)_{\mathbf{1},\mathbf{2}}$
		W boson:	$(2,0)_{\mathbf{1},\mathbf{1}}$

This agrees with the well known weak coupling spectrum of the $SU(2)$ $N_f = 2$ theory.

5.6 Massless $N_f = 3$

The $N_f = 3$ quiver is given, after mutations to reach the massless chamber, as

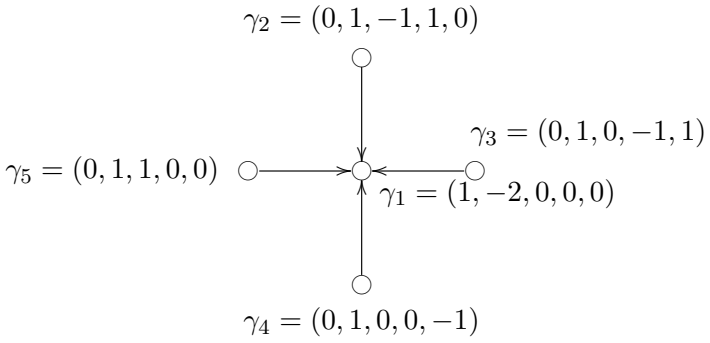

(69)

The flavor group is $SO(6) \cong SU(4)$ and the nodes of the quiver make up a monopole of electric/magnetic charge $(0, 1)$ in the **4** of $SU(4)$, and a dyon of charge $(1, -2)$ in the **1**. We have labeled the flavor charges as (e, m, q_1, q_2, q_3), where q_i are the eigenvalues under the respective generators of the Cartan of $SU(4)$. The central charge degeneracy we experienced in the $N_f = 2$ case is again present, among γ_i for $2 \leq i \leq 5$. Half the spectrum will come as sets of 4 simultaneous mutations.

There are again two chambers, one with $\arg \mathcal{Z}(\gamma_5) > \arg \mathcal{Z}(\gamma_1)$, and the other with $\arg \mathcal{Z}(\gamma_1) > \arg \mathcal{Z}(\gamma_5)$. The second chamber is strong coupling, and just includes the particles that correspond to the original nodes of the quiver. In the other chamber, the mutations generate the spectrum

$$\gamma_i + n(\gamma_2 + \gamma_3 + \gamma_4 + \gamma_5) + 2n\gamma_1 = (2n, 1, 1, 0, 0)$$
$$(n+1)(\gamma_2 + \gamma_3 + \gamma_4 + \gamma_5) + (2n+1)\gamma_1 = (2n+1, 2, 0, 0, 0)$$
$$-\gamma_i + (n+1)(\gamma_2 + \gamma_3 + \gamma_4 + \gamma_5) + (2n+1)\gamma_1 = (2n+1, 1, -1, 0, 0)$$

The states in which γ_i appears are repeated for $1 \leq i \leq 4$. Thus we see that we have a magnetic charge 2 dyon that is a singlet under flavor $SU(4)$, as well as magnetic charge 1 dyons in the $\bar{\mathbf{4}}$ and quark-dyons in the **4**.

As usual, the mutations to the right will fill out the dyons on the other side of the accumulation

ray. Right mutation generates:

$$n(\gamma_2+\gamma_3+\gamma_4+\gamma_5)+(2n+1)\gamma_1=(2n+1,-2,0,0,0)$$
$$\gamma_i+n(\gamma_2\gamma_3+\gamma_4+\gamma_5)+(2n+1)\gamma_1=(2n+1,-1,1,0,0)$$
$$-\gamma_i+(n+1)(\gamma_2+\gamma_3+\gamma_4+\gamma_5)+(2n+2)\gamma_1=(2n+2,-1,-1,0,0)$$

The vector W boson, is at an accumulation ray, and the subtlety about generating the quarks is the same as in the $N_f=2$ case. Here the quarks are given by $\gamma_1+\gamma_i+\gamma_j$, where $2\le i<j\le 5$.

Strong coupling		**Weak Coupling**	
Monopole:	$(0,1)_{\mathbf{4}}$	Quarks:	$(1,0)_{\mathbf{6}}$
Dyon:	$(1,-2)_{\mathbf{1}}$	Positive dyons:	$(2n,1)_{\mathbf{4}}$
		Negative dyons:	$(2n+2,-1)_{\bar{\mathbf{4}}}$
		$m=2$ dyons:	$(2n+1,\pm 2)_{\mathbf{1}}$
		Quark-dyons:	$(2n+1,-1)_{\mathbf{4}}$
			$(2n+1,1)_{\bar{\mathbf{4}}}$
		W boson:	$(2,0)_{\mathbf{1}}$

5.7 $N_f=4$

For $N_f=4$ the massless theory is conformal; mass deformations break conformality. The quiver in the decoupling $m\to\infty$ limit is given as[23]

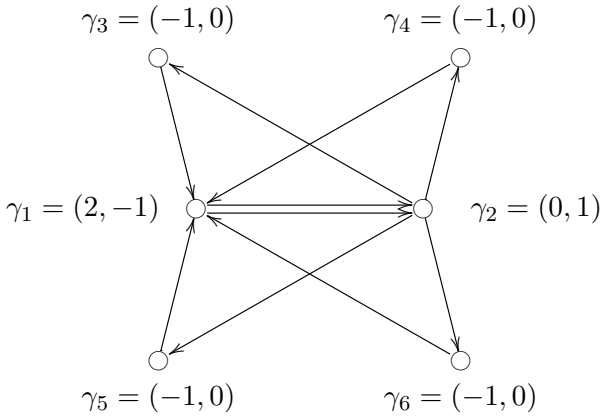

(70)

[23]Our analysis will break the $SO(8)$ flavor symmetry, so we suppress all flavor data.

There are many subtleties in the BPS spectrum of this theory, because it corresponds to a massive deformation of the conformal theory. In particular, there is no quiver that describes the $m \to 0$ limit; if we try to follow the strategy employed in the asymptotically free cases to trace the quiver from $m = \infty$ to $m = 0$, we find that any path goes through infinitely many mutations, preventing us from identifying a quiver for the $m = 0$ chamber.

Nonetheless, we may take a finite mass and find various chambers in which the mutation method can successfully compute BPS spectra. The following is an example of a finite chamber of this theory, with the BPS states listed in decreasing order of BPS phase:

$$\gamma_3, \gamma_4, \gamma_2, \gamma_1 + \gamma_3 + \gamma_4, \gamma_2 + \gamma_5, \gamma_2 + \gamma_6, \gamma_1 + \gamma_3, \gamma_1 + \gamma_4, \gamma_2 + \gamma_5 + \gamma_6, \gamma_1, \gamma_5, \gamma_6. \tag{71}$$

This theory is complete, so, as previously discussed, this chamber must occur in physical moduli space.

In principle, the BPS spectrum can be worked out in all of moduli space by applying the KS wall crossing formula to this chamber. However, the spectrum in some regions of moduli space becomes extremely complicated. To give a general sense of this, we will describe some wall crossings in this theory, which were first studied in [12].

Focus on the first three states, $\gamma_3, \gamma_4, \gamma_2$. If we move γ_2 all the way to the left, we will produce $\gamma_2, \gamma_2 + \gamma_3, \gamma_2 + \gamma_4, \gamma_2 + \gamma_3 + \gamma_4, \gamma_3, \gamma_4$. Separating the rest of the spectrum into similar consecutive sets of three, analogous wall crossings will produce a spectrum of 24 states.

$$\begin{aligned}
&\gamma_2, \gamma_2 + \gamma_3, \gamma_2 + \gamma_4, \gamma_2 + \gamma_3 + \gamma_4, \gamma_3, \gamma_4, \\
&\gamma_2 + \gamma_5, \gamma_2 + \gamma_6, \gamma_1 + 2\gamma_2 + \gamma_3 + \gamma_4 + \gamma_5 + \gamma_6, \gamma_1 + \gamma_2 + \gamma_3 + \gamma_4 + \gamma_6, \\
&\qquad \gamma_1 + \gamma_2 + \gamma_3 + \gamma_4 + \gamma_5, \gamma_1 + \gamma_3 + \gamma_4, \\
&\gamma_2 + \gamma_5 + \gamma_6, \gamma_1 + \gamma_2 + \gamma_3 + \gamma_5 + \gamma_6, \gamma_1 + \gamma_2 + \gamma_4 + \gamma_5 + \gamma_6, \\
&\qquad 2\gamma_1 + \gamma_2 + \gamma_3 + \gamma_4 + \gamma_5 + \gamma_6, \gamma_1 + \gamma_3, \gamma_1 + \gamma_4, \\
&\gamma_5, \gamma_6, \gamma_1 + \gamma_5 + \gamma_6, \gamma_1 + \gamma_5, \gamma_1 + \gamma_6, \gamma_1.
\end{aligned} \tag{72}$$

Now we can produce various vectors by crossing states between the four sets of six; for example, $(\gamma_1 + \gamma_3 + \gamma_4) \circ (\gamma_2 + \gamma_5 + \gamma_6) = -2$, so exchanging them will produce a tower of dyons and a vector

$\gamma_1 + \gamma_2 + \gamma_3 + \gamma_4 + \gamma_5 + \gamma_6 = (-2, 0)$, by the $SU(2)$ wall crossing identity. Similarly, exchanging γ_3, γ_4 with $\gamma_2 + \gamma_5, \gamma_2 + \gamma_6 =$ will produce a vector $2\gamma_2 + \gamma_3 + \gamma_4 + \gamma_5 + \gamma_6 = (-4, 2)$ along with two dyon towers and four additional hypers; this is just the wall crossing of massless $SU(2), N_f = 2$. Two more vectors will be generated by this procedure, $2\gamma_1 + \gamma_3 + \gamma_4 + \gamma_5 + \gamma_6 = (0, -2)$ and $\gamma_1 - \gamma_2 = (2, -2)$.[24] These four vectors have non-trivial electric-magnetic inner products, and so additional wall crossing of the vectors will produce some highly complicated spectrum with infinitely many vectors.

One would expect such wild BPS behavior in the massless conformal limit, where conformal dualities produce some infinite set of vectors dual to the familiar W boson. It is interesting to observe that this complicated structure begins to emerge even with finite mass, in regions of moduli space where the quiver description is perfectly valid.

6 $SU(N)$ Gauge Theories

6.1 Construction of $SU(N)$ Quivers

Quivers for pure $SU(N)$ gauge theory were constructed in [16] via the $2d/4d$ correspondence studied there. These BPS quivers have also been studied previously in [33]. That work identified as nodes of the quiver a set of fractional branes in an orbifold phase of the geometries used in the type IIA geometric engineering [59, 75].[25]

Here we will provide a purely $4d$ motivation for that result, and use it to extend the proposal to $SU(N)$ gauge theory with arbitrary matter. First we fix some notation. We have been using (e, m) for electric and magnetic charges of the $SU(2)$ theories. In $SU(N)$ theories, electric charges will naturally be associated to weights of the gauge group, and magnetic charges associated to roots. We denote simple roots α_i and fundamental weights ω_i; the appropriate inner product is given by $\alpha_i \cdot \omega_j = \delta_{ij}$.

[24] To obtain this last vector, we must rotate the half-plane, allowing γ_2 to exit and mutating on γ_2 in the quiver.

[25] Fractional branes as a basis of BPS quivers were studied in [29–31]. Their charges for $SU(N)$ were identified from a boundary CFT analysis in [76]. BPS particles with magnetic and electric charge in the IIA geometric engineering context correspond to even branes wrapped on cycles of the geometry. The fractional branes are identified with the monopoles and dyons which can become massless somewhere in moduli space, equivalently these states correspond to the vanishing cycles in the homology lattice of the Seiberg-Witten curves of these theories found in refs. [77–79]. See also [80] and references therein.

By the $2r + f$ counting, the quiver should consist of $2(N-1)$ nodes. Let us consider the mutation form of the quiver that covers the decoupling limits in which each W boson associated to a simple root α_i separately becomes infinitely massive. In order to separately decouple these vectors, the $N-1$ simple root W bosons must be disjointly supported as reps of the quiver. Since the reps supported on only one node cannot give vectors, and we only have $2(N-1)$ nodes, each W boson must be supported on two distinct nodes. So we have two nodes b_i, c_i, forming an $SU(2)$ subquiver associated to each simple root. Then we simply need to choose charge assignments within the $SU(2)$ subquivers. In order to obtain the associated W boson, the two nodes should have the charges of a consecutive pair of dyons, $((n_i+1)\alpha_i, -\alpha_i), (-n_i\alpha_i, \alpha_i)$. The most obvious choice is just $n_i = 0$, the appropriate monopole and dyon for each simple root. If we make this choice, the result is precisely the quiver computed by [16] using the 2d/4d correspondence:

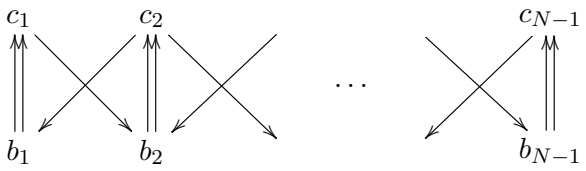

(73)

where $b_i = (0, \alpha_i)$ and $c_i = (\alpha_i, -\alpha_i)$.

The $SU(N)$ quivers we have deduced contain closed oriented cycles; thus the quiver requires a superpotential to be specified. The orbifold construction of [33] produces this superpotential by reducing the superpotential of the $\mathcal{N} = 4$ theory.[26] Explicitly, the appropriate superpotential is given as,

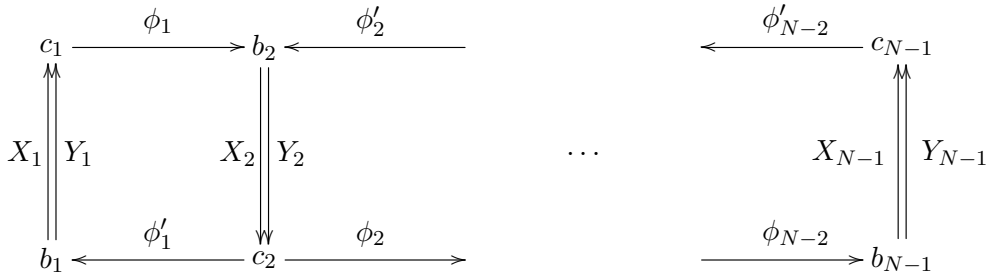

(74)

[26]The quiver (and superpotential) discussed on [33] is actually related by some mutations to the quiver we study here.

with

$$\mathcal{W} = \sum_{i=1}^{N-2} X_i \phi_i' X_{i+1} \phi_i - Y_i \phi_i' Y_{i+1} \phi_i. \tag{75}$$

Before going on, we will demonstrate a weak-coupling check on this superpotential. The quivers given above explicitly display W bosons associated to the simple roots; the ordering $\arg \mathcal{Z}(b_i) > \arg \mathcal{Z}(c_i)$ ensures that there will be a W boson associated to the ith simple root. However, at weak coupling we would expect massive vector W bosons associated to all roots of the $SU(N)$ algebra, due to Higgsing of the gauge bosons. The set of massive vectors should fill out exactly one adjoint of the $SU(N)$, except for the Cartan elements, which remain massless.

Let us see how these additional vectors come about by first considering $SU(3)$. We seek a vector state corresponding to a representation with dimension vector $(1, 1, 1, 1)$. The superpotential is then

$$\mathcal{W} = X_1 \phi' X_2 \phi - Y_1 \phi' Y_2 \phi, \tag{76}$$

and the resulting F-terms are

$$\phi\phi' X_2 = \phi\phi' Y_2 = \phi\phi' X_1 = \phi\phi' Y_1 = 0\,, \tag{77}$$

$$\phi(X_1 X_2 - Y_1 Y_2) = \phi'(X_1 X_2 - Y_1 Y_2) = 0\,. \tag{78}$$

If both ϕ, ϕ' are zero, the rep is given by X_i, Y_i, and falls apart into the direct sum of two subreps, $b_1 + c_1, b_2 + c_2$. Such a situation is described as a decomposable representation; decomposable reps are never stable, since one of the two subreps must be to the left of decomposable rep in the $\mathcal{Z}$-plane. If ϕ, ϕ' are both nonzero, then X_i, Y_i are all zero by (77), and again the rep is decomposable. We are left with two cases, $\phi = 0, \phi' \neq 0$ and vice versa. Having set one of the ϕ's to zero, there is one more equation in (78) that must be satisfied: $X_1 X_2 = Y_1 Y_2$. Naive dimension counting gives us $6 - 2 - 3 = 1$, so we have a vector. Gauge fixing sets ϕ (or ϕ') $= X_1 = Y_1 = 1$; then the actual moduli space is parameterized by $X_2 = 1/Y_2$, which forms $\mathbb{P}_1$. Lefschetz $SU(2)$ gives exactly one vector of this charge, and no hypers. It remains to check the stability conditions. For $\phi = 0$, there are subreps $c_1, b_1 + c_1, b_1 + c_1 + c_2$; these are *not* destabilizing precisely when, in addition to the weak coupling conditions, we also have $\arg \mathcal{Z}(b_1 + c_1) < \arg \mathcal{Z}(b_2 + c_2)$. On the other hand, when $\arg \mathcal{Z}(b_1 + c_1) > \arg \mathcal{Z}(b_2 + c_2)$, then $c_1 + b_1$ is certainly a destabilizing subrep. Similarly, $\phi_2 = 0$ is

stable precisely for $\arg \mathcal{Z}(b_1 + c_1) > \arg \mathcal{Z}(b_2 + c_2)$. Therefore, at any region in weak coupling, we find precisely one W boson of the desired charge.

Now we consider arbitrary $SU(N)$. By embedding the $SU(3)$ quiver as a subquiver of an arbitrary $SU(N)$ quiver, we see that the specified superpotential (75) guarantees that exactly one W boson vector with charge $(\alpha_i + \alpha_{i+1}, 0)$ appears at weak coupling. It remains to check the W bosons associated to the rest of the roots, which have charges $\left(\sum_{i=j}^{j+k} \alpha_i, 0\right)$ for any $k > 1$. As representations, these are given by $\sum_{i=j}^{j+k} b_i + c_i$. It is clear that, for this analysis, we can simply focus on the subquiver formed by b_i, c_i for $j \leq i \leq j+k$; all other nodes (and maps involving them) are set to zero in this rep, and consequently, any superpotential terms from them are trivial. Thus we can simply study the rep $v = \sum_{i=1}^{k} b_i + c_i$ of the $SU(k+1)$ quiver and superpotential as shown above.

The F-terms are now a bit more subtle.

$$\phi_{i-1}\phi'_{i-1}X_{i-1} + \phi_i\phi'_i X_{i+1} = \phi_{i-1}\phi'_{i-1}Y_{i-1} + \phi_i\phi'_i Y_{i+1} = 0\,, \tag{79}$$

$$\phi_i(X_iX_{i+1} - Y_iY_{i+1}) = \phi'_i(X_iX_{i+1} - Y_iY_{i+1})\,. \tag{80}$$

Again, not both ϕ_i, ϕ'_i can be zero, or else the rep is decomposable. However, it seems that perhaps both ϕ_i, ϕ'_i may be nonzero; since (79) now has two terms, this no longer forces the rep to become decomposable. Nonetheless, we can dispose of this possibility by stability. If both ϕ_i, ϕ'_i are nonzero, then either both ϕ_{i-1}, ϕ'_{i-1} are nonzero or X_{i+1}, Y_{i+1} are zero due to (79). By induction, we will find that X_j, Y_j are zero for some j. This situation cannot be Π-stable; because X_j, Y_j vanish, we have two subreps, b_j (which is now effectively a sink in the quiver), and $v - c_j$, the subrep where we set to zero c_j, (which is now an effective source in the quiver). It must be the case that one of these is destabilizing. If $\arg \mathcal{Z}(c_j) > \arg \mathcal{Z}(v)$, then we have $\arg \mathcal{Z}(b_j) > \arg \mathcal{Z}(c_j) > \arg \mathcal{Z}(v)$ so that b_j is destabilizing; otherwise $\arg \mathcal{Z}(v - c_j) > \arg \mathcal{Z}(v) > \arg \mathcal{Z}(c_j)$, so that $v - c_j$ is destabilizing.

Having dealt with this subtlety, we can continue with the analysis. The remaining case is that exactly one of ϕ_i, ϕ'_i is nonzero for each i; this gives 2^k possibilities. First, we check the dimension of the parameter space: we start with $4k - 2$ maps and $2k - 1$ gauge symmetries; we have set $k - 1$ maps to zero, and we have $k - 1$ remaining constraints (80); thus $(4k - 2) - (2k - 1) - (k - 1) - (k - 1) = 1$. We may gauge fix ϕ_i (or ϕ'_i) $= X_i = Y_i = 1$ for $1 \leq i < N - 1$; then

the moduli space is $\mathbb{P}^1$ parametrized by $X_{N-1} = 1/Y_{N-1}$. Thus we have 2^k vector states. Using stability, we will find that precisely one of these vectors is stable for any region of weak coupling. To see this, fix j and choose $\phi_j \neq 0$. Because of this choice, there is a subrep $\sum_{i=j+1}^{k} b_i + c_i$, which is destabilizing when $\arg \mathcal{Z}\left(\sum_{i=j+1}^{k} b_i + c_i\right) > \arg \mathcal{Z}(v) > \arg \mathcal{Z}\left(\sum_{i=1}^{j} b_i + c_i\right)$. If we had chosen $\phi'_j \neq 0$, we would have a subrep $\sum_{i=1}^{j}(b_i + c_i)$ which is destabilizing in exactly the opposite situation, $\arg \mathcal{Z}\left(\sum_{i=1}^{j} b_i + c_i\right) > \arg \mathcal{Z}(v) > \arg \mathcal{Z}\left(\sum_{i=j+1}^{k} b_i + c_i\right)$.[27] So we have arrived at the desired conclusion, namely, that we obtain precisely one vector for each root of $SU(N)$. With a bit more work it is possible to see that, up to field redefinitions, this is the unique superpotential at quartic order that properly produces exactly one set of W bosons. In principle this leaves the possibility of higher order terms in the superpotential, but the derivation of [33] shows that indeed no such terms arise.

6.2 General ADE-type Gauge Group

Some brief comments will allow us to extend the above analysis to arbitrary ADE-type (ie simply-laced) gauge group G. At weak coupling, we would again expect to be able to decouple the rank G distinct $SU(2)$ subgroups, again with one corresponding to each simple root of the algebra. Then we would again find an $SU(2)$ subquiver for each simple root α_i. If we again make the ansatz of fixing charges $(0, \alpha_i), (\alpha_i, -\alpha_i)$, then we find that, for each line in the Dynkin diagram (ie $\alpha_i \cdot \alpha_j = -1$), we must connect the respective $SU(2)$ subquivers as

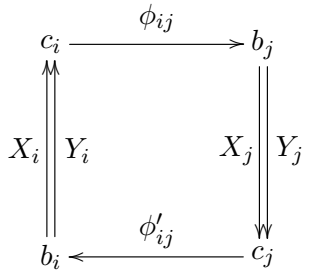

(81)

[27] There are some additional subreps that should be considered, but ultimately play no role. For example, if $\phi_j \neq 0, \phi'_m \neq 0$ for $j < m$, then there is a subrep $\sum_{i=j+1}^{m} b_i + c_i$, which is destabilizing when $\arg \mathcal{Z}\left(\sum_{i=j+1}^{m} b_i + c_i\right) > \mathcal{Z}(v)$. Suppose that neither subreps described above are destabilizing; then $\arg \mathcal{Z}\left(\sum_{i=j+1}^{k} b_i + c_i\right) < \arg \mathcal{Z}(v)$ and $\arg \mathcal{Z}\left(\sum_{i=1}^{m} b_i + c_i\right) < \arg \mathcal{Z}(v)$. Summing these inequalities, we find $\arg \mathcal{Z}\left(\sum_{i=j+1}^{m} b_i + c_i\right) < \mathcal{Z}(v)$, so that this new subrep cannot be destabilizing. Further, if $c_i + b_i$ is a subrep, then so is c_i, but this again gives no additional destabilizing constraints since $\arg \mathcal{Z}(b_i) > \arg \mathcal{Z}(b_i + c_i) > \arg \mathcal{Z}(c_i)$.

with the quartic superpotential $\mathcal{W} = X_i \phi'_{ij} X_j \phi_{ij} - Y_i \phi'_{ij} Y_j \phi_{ij}$.

Thus there is a straightforward graphical prescription for constructing a quiver for pure SYM with simply-laced gauge group G, starting from the Dynkin diagram of G. For every node i of the Dynkin diagram, we draw and $SU(2)$ subquiver with nodes b_i, c_i; for every line in the Dynkin diagram given $i - j$ we connect the $SU(2)$ subquivers as above, with the quartic superpotential. This is exactly the quiver $\widehat{A}_1 \boxtimes G$, which was found to describe these theories via $2d/4d$ in [21]. The superpotential guarantees the existence of some subset of the W bosons, namely those contained in any $SU(N)$ subquiver of the full G quiver; studying the full root system of W bosons becomes quite complicated, and we omit the analysis here. While the quartic terms must be present in the superpotential, there may or may not be some additional higher order terms. For clarity, we draw the Dynkin diagrams along with resulting quivers for D_4, E_6.

(82)

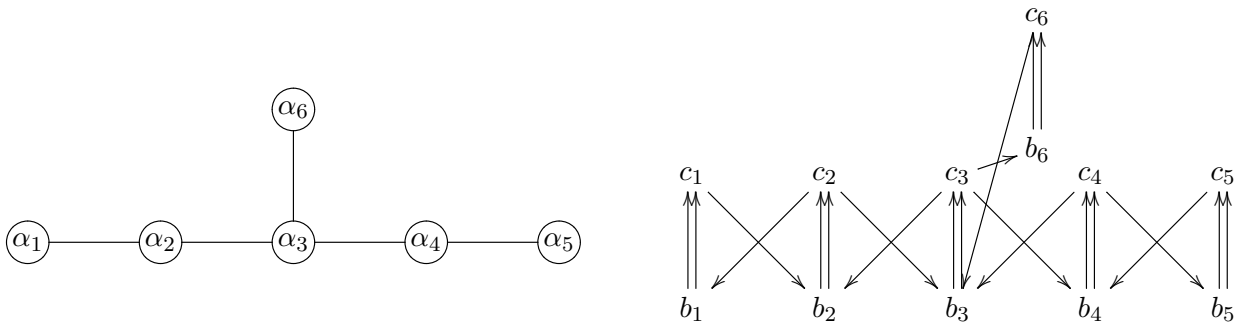

(83)

6.3 BPS Spectra of Pure $SU(N)$ SYM

In the following we will compute the BPS spectra of $SU(N)$ theories using the mutation method. We find a spectrum consisting of $N(N-1)$ BPS particles and their antiparticles at strong coupling, in agreement with the identification of the spectrum in this region with CFT states of [76].

For $N \geq 3$ these theories are not complete, in the sense of section 7, since their charge lattice has rank $2(N-1)$ while there are only N physical moduli that can be varied ($N-1$ Coulomb branch parameters as well as the UV coupling constant). We will therefore not have the freedom to adjust all the central charges we wish. To apply the mutation method, we therefore must find a point in moduli space where the central charges of the basis particles for the quiver we propose (which we must compute from the Seiberg-Witten solution of $SU(N)$) actually lie in a half-plane. We can then tune moduli and maintain a valid quiver description, as long as we perform any necessary mutations.

6.3.1 $SU(3)$

We begin with an analysis of the $SU(3)$ theory starting from the quiver discussed in section 6.1, which was obtained from a weak coupling analysis and which is verified by the $2d/4d$ correspondence [16]. We identify the nodes of the quiver with cycles in the SW geometry and compute their central charges to determine the ordering of the mutations. Furthermore, we track these cycles to the strong coupling region where we produce the full BPS spectrum consisting of 6 particles.

The central charge function is part of the IR data of the theory, and is thus specified by the SW solution. The $SU(N)$ SW curve can be written as [77–79]

$$y^2 = (P_{A_{N-1}}(x,u_i))^2 - \Lambda^{2N}\,, \quad P_{A_{N-1}}(x,u_i) = x^N - \sum_{i=2}^{N} u_i x^{N-i}\,, \tag{84}$$

where the u_i are the Casimirs parameterizing the Coulomb branch and Λ is the strong coupling scale. The SW differential is then given by [77–79]

$$\lambda(u_i) = \frac{1}{2\pi i}\frac{\partial P_{A_{N-1}}(x,u_i)}{\partial x}\frac{x\,dx}{y}\,, \tag{85}$$

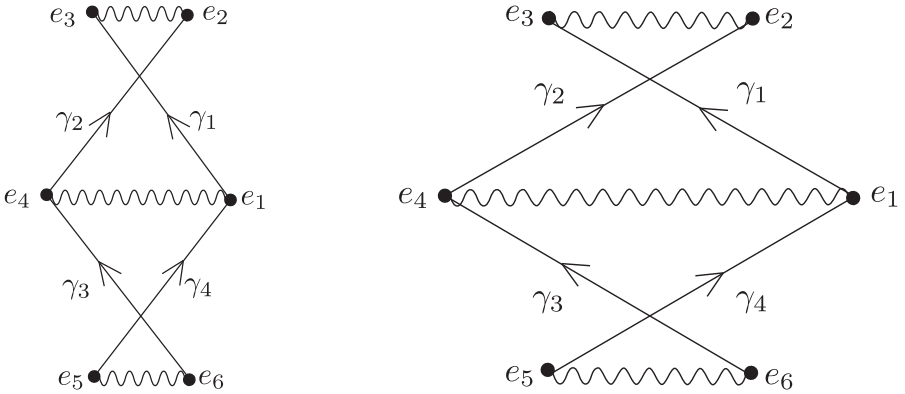

(a) Choice of cycles at weak coupling

(b) Cycles at strong coupling

Figure 6: The choice of cycles in the x-plane at weak and strong coupling is shown in Figs. 6a ,6b respectively. $e_i\,, i = 1, \ldots, 6$ denote the roots of $(x^3 - ux - v)^2 - \Lambda^6$ and become the sixth roots of unity as we tune the moduli to strong coupling and set $\Lambda = 1$.

and a BPS particle which is represented by a cycle γ on the SW curve has charge

$$Z_{u_i}(\gamma) = \int_\gamma \lambda(u_i). \tag{86}$$

Finally, the electric-magnetic inner product of two particles is computed by the intersection product of the associated cycles. We will use γ to refer to both the particle and associated cycle, and $\circ$ to indicate both the electric-magnetic inner product and the intersection product.

We will calculate the central charge configuration for a weakly coupled point of the $SU(3)$ theory. For $SU(3)$ we set $u_2 = u$ and $u_3 = v$. The Casimirs u_i determine the vevs of the Cartan elements of $SU(N)$ semi-classically, and it can be checked that $u \to -\infty$ and $v = 0$ indeed corresponds to a weakly coupled point in $SU(3)$.

The $SU(N)$ theory has an $Sp(2N-2, \mathbb{Z})$ duality which is manifest in the different possible choices of symplectic homology basis that could be identified with electric and magnetic charges. We postpone the charge labeling and identify the nodes of the quiver directly with a choice of cycles in the geometry as shown in Fig. 6a.

The quiver obtained in this way at weak coupling should have a number of properties:

- The intersections of cycles must agree with the electric-magnetic inner product as defined by the quiver

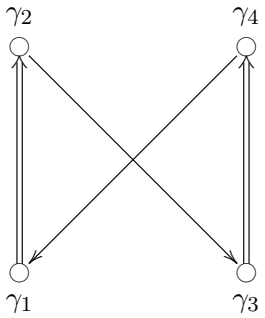

Figure 7: Quiver obtained from the intersections of the cycles in Figs. 6a,6b.

- The central charges of all the nodes must lie in a common half-plane
- The apparent $SU(2)$ subquivers should be weakly coupled
- The central charges of the W bosons of the $SU(2)$ gauge groups should be vanishingly small compared to the central charges of the nodes in the $u \to -\infty$ limit

The last condition follows from the fact that the electrically charged objects should be parametrically light compared to the dyonic states of the theory at weak coupling, since here the electric particles are the fundamental degrees of freedom.

The choice of cycles in Fig. 6a meets these conditions. That the first is met is obvious, and the latter three can be explicitly checked by numerically computing the associated integrals of the SW differential along the given curves. This has been done, and the values of the central charges for large but finite $u < 0$ are as depicted in Fig. 8a. Since the $SU(2)$ subquivers are weakly coupled, we are in an infinite chamber, as expected at weak coupling. To apply the mutation method most efficiently we will tune the moduli to arrive in a chamber with a finite spectrum.

We can track the behavior of the quiver explicitly as we tune moduli. At walls of marginal stability nothing happens at the level of the quiver, while at walls of the second kind we must mutate to find a valid description on the other side. A generic path in the $SU(3)$ moduli space may pass through arbitrarily many - even infinitely many - walls of the second kind, thereby alluding an analysis. For $SU(3)$ there exists a path which takes us from weak coupling to the strongly coupled $u = 0$ point and passes through no walls of the second kind, thereby allowing a quite seamless transition between the understood weak coupling chamber and the strongly coupled chamber containing the $u = 0$ point.

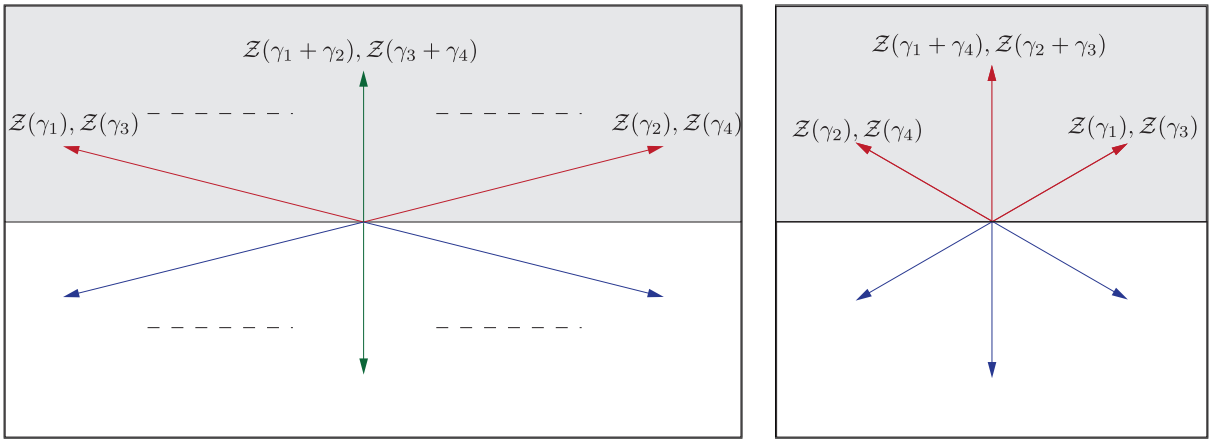

(a) Weak coupling (b) Strong coupling

Figure 8: The central charges of BPS states of $SU(3)$ are depicted at weak (a) and strong (b) coupling respectively. At weak coupling, the left- and right-most nodes, along with the weak coupling W bosons are shown explicitly. The full spectrum at weak coupling is not known, but at least includes two infinite towers of dyons, which are not shown. In the limit of zero coupling, the left- and right-most nodes approach π separation and infinite length. As we tune towards strong coupling, the states γ_1, γ_3 and γ_2, γ_4 approach and cross each other. At strong coupling, the full finite spectrum of BPS states is depicted; the $\mathbb{Z}_6$ symmetry is manifest.

We follow the straight line path with $v = \mathrm{Im}\, u = 0$ from $u = -\infty$ to $u = 0$. The pairs of aligned central charges stay aligned along the entire path, and cross in tandem at a finite value of $u < 0$. All the while, all central charges remain in the upper half-plane. At $u = 0$, both $SU(2)$'s are strongly coupled, and the central charge configuration is as given in Fig. 8b. Now we simply apply the mutation algorithm with the central charges associated to this point in moduli space. What we find is a $N(N-1) = 6$ state chamber with states

$$\gamma_2, \gamma_4, \gamma_2+\gamma_3, \gamma_1+\gamma_4, \gamma_1, \gamma_3\,. \tag{87}$$

Let us note some features of the strong coupling spectrum we have found. First of all, all states in the chamber correspond to vanishing cycles in the Seiberg-Witten geometry. That is, they all correspond to cycles which vanish somewhere on moduli space. This agrees with earlier intuition about the relation between the strong coupling $SU(N)$ spectrum and vanishing cycles of the SW geometry [33, 77, 79, 80].

The second feature, which will become quite important in our $SU(N)$ analysis below, is that the chamber we have found respects the $\mathbb{Z}_{2N} = \mathbb{Z}_6$ symmetry of the IR solution.

In principle one would hope that the same story carried over for the $SU(N)$ case. We would ideally start from weak coupling and tune moduli until we arrived at the strongly coupled $u_i = 0$ point, and then see that this point lied in a finite chamber with $N(N-1)$ states. Unfortunately the situation becomes technically complicated, in a way we will briefly explain. Above, we chose a very particular path between the $u_i = 0$ point and weak coupling, along which the quiver passed through no walls of the second kind, where quiver mutation is necessary. This was a path which deformed the order 1 term in the defining polynomial of the Seiberg-Witten curve.

In the $SU(N)$ case it is always the x^{N-2} deformation which has this nice property. That is, if we deform the coefficient of the x^{N-2} term alone from the $u_i = 0$ point along certain directions in $\mathbb{C}$, the quiver will be extremely well behaved, just as above. The issue is that it is only in the $N = 3$ case that this deformation alone is sufficient to arrive at weak coupling. In all other cases there will be some unbroken subgroup which remains. Thus to get to weak coupling, we must deform lower order terms, but these are not nice in terms of the quiver description. In particular, no simple choice seems to get from strong to weak coupling while only passing through a small number of walls of the second kind. Potentially such a path remains to be found, and the same method can then be generalized to the $SU(N)$ case. At present, we will proceed with a discussion of the $SU(N)$ case at $u = 0$ based on what we've learned in $SU(3)$.

6.3.2 $SU(N)$ at Strong Coupling

We now consider the general case of $SU(N)$ at strong coupling. Our objective is to determine the quiver, charge labels of nodes, and ordering of central charges at some point of strong coupling, and then compute the resulting spectrum via the mutation method. Of course, to honestly produce the quiver we would need to somehow find a basis of BPS states. However, the quiver has already been derived from other considerations, and motivated from a purely $4d$ perspective in 6.1. Here we will infer quiver along with charge labels at strong coupling by generalizing the results above for $SU(3)$.

Fix the moduli $u_i = 0$, so that the Seiberg-Witten curve is given as

$$y^2 = x^{2N} - \Lambda^{2N}, \tag{88}$$

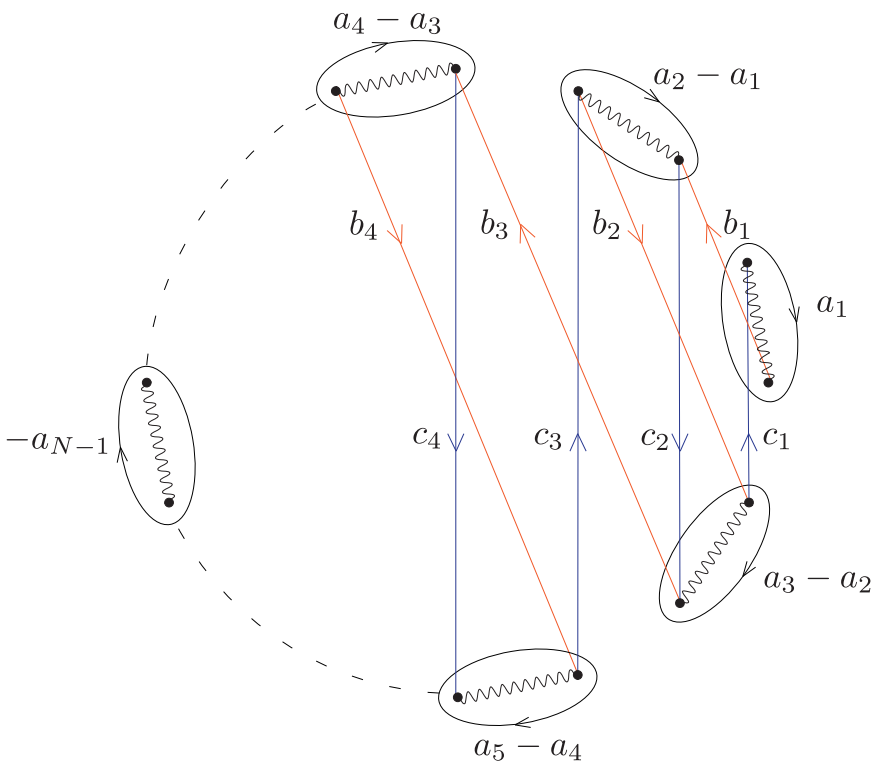

Figure 9: The Seiberg-Witten curve described by (88), shown as a double cover of the x-plane, with branch cuts as indicated. The labeled a_i, b_i cycles give a symplectic homology basis. The action of the $\mathbb{Z}_{2N}$ symmetry rotates the plane by $e^{-i\pi/N}$, and thus rotates b_i into c_i. The b_i, c_i cycles constitute the positive integral basis of states that appear as nodes of the quiver. Note that we have taken a different convention for branch cuts than the one used in Fig. 6a. This choice is more convenient for the strong coupling analysis, and agrees with the conventions used in [79].

with Seiberg-Witten differential

$$\lambda = \frac{1}{2\pi i}\frac{Nx^N dx}{y}. \tag{89}$$

We take a symplectic homology basis, a_i, b_i for $i = 1, \ldots, N-1$, with $a_i \circ a_j = b_i \circ b_j = 0$ and $a_i \circ b_j = \delta_{ij}$. The appropriate choice of cycles is shown in Figure 9. We have chosen the a_i's to be the cycles that collapse as $u_N \to \infty$, since these are pure electric charges. There is still some ambiguity in choosing b cycles, which are pure magnetic monopoles with charges given by simple roots of $SU(N)$. We fix the ambiguity by choosing the b cycles to be ones that vanish somewhere in moduli space. This is a natural choice, since each of the simple roots has a full $SU(2)$ moduli space associated with it contained in the $SU(N)$ moduli space; by the original Seiberg-Witten $SU(2)$ analysis, the monopole associated to each simple root becomes massless at some locus of the $SU(N)$ moduli space.

At the origin of moduli space, the curve has a $\mathbb{Z}_{2N}$ discrete symmetry. If we denote ξ the generator of the symmetry, we have

$$\xi(x) = e^{-i\pi/N} x. \tag{90}$$

The action on the x-plane is simply a $-\pi/N$ rotation; on the central charge function $\mathcal{Z}$, this gives

$$\xi(\lambda) = -e^{-i\pi/N}\lambda \tag{91}$$

$$\xi\left(\mathcal{Z}(\gamma)\right) = -e^{-i\pi/N}\mathcal{Z}(\gamma). \tag{92}$$

This induces an exact symmetry of the quantum theory that will be quite useful. It indicates that BPS states will come in $\mathbb{Z}_{2N}$ orbits; the magnitude of their central charges of cycles in an orbit are all identical, and their phases are distributed $\mathbb{Z}_{2N}$ symmetrically in the complex plane. Again, by $SU(2)$ reasoning, each magnetic monopole with simple root charge will be a BPS state at the origin of moduli space. From Figure 9, it is clear that all the b_i's are in distinct orbits. Thus we have obtained $(N-1)$ distinct orbits, one for each simple root monopole with electric-magnetic charge $(0, \alpha_i)$; each orbit consists of $2N$ BPS states, N of which are particles, and N antiparticles.

To compute the periods, we integrate the Seiberg-Witten differential, to obtain

$$\int \lambda = \frac{1}{2\pi}\frac{N}{N+1} x^{N+1}\, {}_2F_1\left(\frac{1}{2}, \frac{N+1}{2N}, \frac{1}{2N}+\frac{3}{2}, 1\right) = \kappa(N) x^{N+1}, \tag{93}$$

where κ is some proportionality constant that depends on N but is independent of x. Evaluating the definite integral for the b_i's shown in Figure 9, we find

$$\mathcal{Z}(b_j) = 2\kappa(N) i e^{i\pi/N} \sin\frac{j\pi}{N} \tag{94}$$

From the action of the ξ, we see that the full $\mathbb{Z}_{2N}$ orbits of vanishing cycles will fill out all $2N$-roots of unity (up to some overall phase $\arg(ie^{i\pi/N}\kappa(N))$) in the $\mathcal{Z}$-plane. This configuration of central charges is depicted in Figure 10

To continue, we now generalize from the $SU(2)$ and $SU(3)$ results. In those cases, the BPS spectra were precisely equivalent to the set of vanishing cycles of the Seiberg-Witten geometry. It is natural to imagine that for general N it is at least possible to choose a positive integral basis for

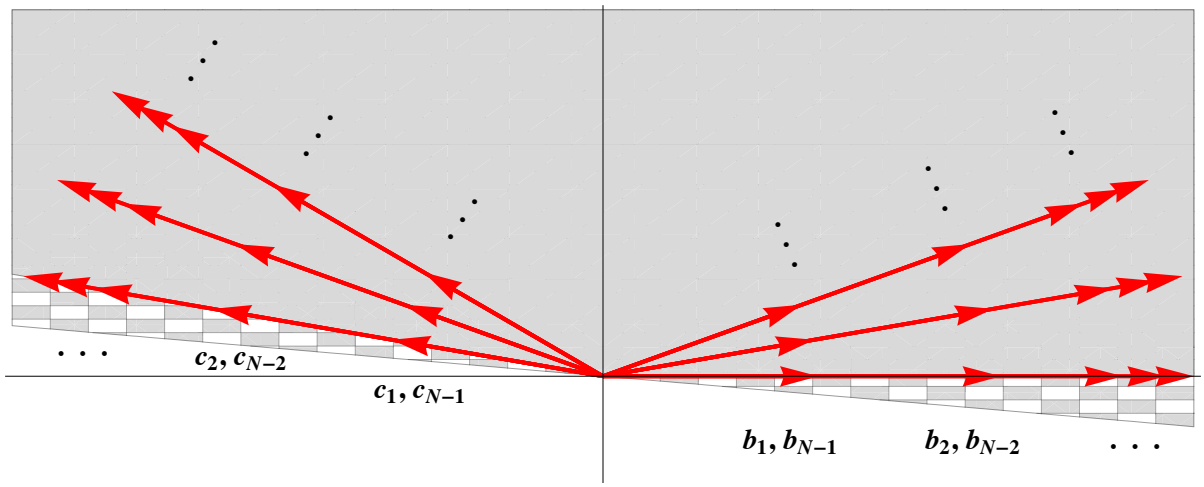

Figure 10: Central charges of vanishing cycles plotted in the $\mathcal{Z}$-plane (where we have rotated by some overall phase $\arg(i\kappa(N))$. The half-plane we use to construct the quiver is shown as the gray region. The b_j cycles have $\mathcal{Z}(b_j) \sim \sin\frac{j\pi}{N}$; note that $\mathcal{Z}(b_j) = \mathcal{Z}(b_{N-j})$. The b_j are therefore $N-1$ distinct collinear states shown on the positive real axis. Each ray of collinear red arrows is a $\mathbb{Z}_{2N}$ rotation of the b_j's. There are N such rays in the half-plane, situated at $2N$-roots of unity. In total we have $N(N-1)$ states depicted in the diagram. The antiparticles in the opposite half-plane are not shown. The half-plane is chosen so that b_j are right-most BPS states, which forces c_j to be left-most BPS states. As explained in the analysis, for such a half-plane to exist, the region checkered in white and gray must be free of BPS states.

BPS states that consists of vanishing cycles. The vanishing cycles do in fact span the homology lattice, so this is sensible assumption. As we will see, this allows us to obtain a quiver that agrees with (73), which was also proposed from other perspectives [16, 33]. Thus, we seek a positive integral basis of vanishing cycles; to do so, we must first choose a half-plane. Since the $N-1$ b_i's have the same phase, we may tune the half-plane to make them right-most vanishing cycles; then the b_i's are forced to appear as $N-1$ nodes of the quiver.[28] Having fixed this choice of half-plane, it is clear from Figure 10 that $c_i \equiv \xi(b_i)$ form $N-1$ right-most vanishing cycles in the half-plane, and therefore must also appear in the quiver. These states are given as

$$c_i \equiv \xi(b_i) = \begin{cases} -a_{i-1} + 2a_i - a_{i+1} + b_i = (\alpha_i, \alpha_i) & \text{if } i \text{ is even} \\ -a_{i-1} + 2a_i - a_{i+1} - b_{i-1} - b_i - b_{i+1} = (\alpha_i, -\alpha_{i-1} - \alpha_i - \alpha_{i+1}) & \text{if } i \text{ is odd} \end{cases} \tag{95}$$

[28] In principle, a bound state of multiple b_i's would also have the same phase, and one might worry that some of these $N-1$ states were actually bound states of the others. However, this is in fact impossible. The b_i are linearly independent cycles, so none can occur as a linear combination of the others; furthermore $b_i \circ b_j = 0$, so there exist no bound states of the form $b_i + b_j$. So *all* of the b_i cycles must appear as nodes of the quiver.

We now have specified $2(N-1)$ nodes of the quiver; in fact, this is exactly the number of nodes in the quiver, by the counting $2r + f = 2(N-1)$. At this point we have fully determined the quiver as follows:

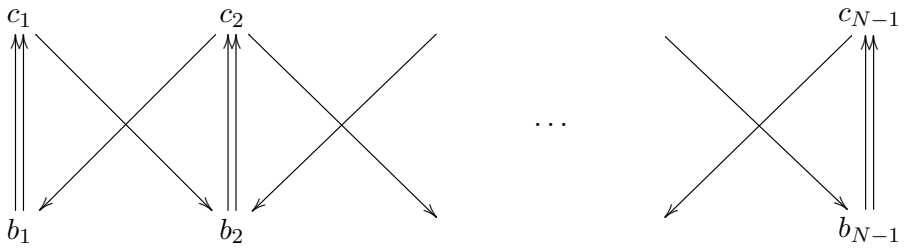

(96)

It is encouraging to note that mutation equivalences will allow us to make contact with the weak coupling discussion of section 6.1. The quiver we have obtained (96) is already of the same form as (73), but with different charge assignments. Mutating to the right on all b_{2i} and to the left on all b_{2i-1} will produce leave the quiver form unchanged, but transform the charges to $b_i = (0, -\alpha_i), c_i = (\alpha_i, \alpha_i)$. These are precisely the weak coupling charges proposed in section 6.1, with some alternative choice of dyon pairs, $n_i = -1$. Note, however, that in order to realize these mutations, we must go through a large number of wall crossings, since we took left-mutations of some b_i, which, in our strong coupling calculation, are not left-most, but instead right-most.

We can use the quiver to compute the full BPS spectrum at this strong coupling chamber of moduli space. We begin by mutating on the left-most states, c_i. This produces a new set of charges, $c_i \to -c_i, b_i \to b_i + c_{i-1} + c_{i+1}$. The new states that replace the b_i are now left-most, again all at the same phase in the central charge plane. Focusing on the central charges of the nodes, we see that the charges of the new quiver are related to those of the original quiver by a rotation of $e^{-i\pi/N}$ (see Fig. 10). So as we continue mutating in phase order, this process of N coincident mutations simply repeats itself. Continuing in this way, a finite spectrum is exhibited by the mutation method with a mutation sequence of length $N(N-1)$,

$$c_1, c_2, \ldots, c_{N-1}, b_1, b_2, \ldots, b_{N-1}, c_1, c_2, \ldots, c_{N-1}, b_1, b_2, \ldots, b_{N-1}, \ldots \tag{97}$$

The states produced in this way are,

$$\begin{array}{ccccc} c_1, & c_2, & c_3, & \ldots, & c_{N-1}, \\ b_1+c_2, & c_1+b_2+c_3, & c_2+b_3+c_4, & \ldots, & c_{N-2}+b_{N-1}, \\ b_2+c_3, & b_1+c_2+b_3+c_4, & c_1+b_2+c_3+b_4+c_5, & \ldots, & c_{N-3}+b_{N-2} \\ b_3+c_4, & b_2+c_3+b_4+c_5, & b_1+c_2+b_3+c_4+b_5+c_6, & \ldots, & c_{N-4}+b_{N-2} \\ \vdots & \vdots & \vdots & \vdots & \vdots \\ b_{N-1}, & b_{N-2}, & b_{N-1} & ,\ldots, & b_1 \end{array} \tag{98}$$

This array of states can be filled out iteratively after the first two rows are computed. The state μ_{ij} in position (i,j) with $i \geq 2$ is given by

$$\mu_{i-1,j-1} + \mu_{i-1,j+1} - \mu_{i-2,j}, \tag{99}$$

where we set $\mu_{ij} = 0$ for $j < 1$ and $j > N-1$. It is slightly more economical to take as the base cases $i = 0, 1$ where we add $\mu_{0,j} = -b_j$, along with $\mu_{1,j} = c_j$ as already given. The resulting states precisely fill out the full set of $N(N-1)$ vanishing cycles,

$$\boxed{|\mathcal{B}_{SU(N)}| = N(N-1).} \tag{100}$$

This result agrees with the computation of strong coupling BPS states via CFT methods [76] and is a strong confirmation of the techniques studied here.

6.4 Adding Matter

Adding arbitrary hypermultiplet matter to pure SYM with ADE-type gauge group is quite analogous to the procedure described in 5.2 for $SU(2)$. Consider adding hypermultiplet matter charged under the gauge group G in a representation R. Again, we tune the mass of the matter to infinity. Here, by similar decoupling reasoning we would expect to add as a node a an electrically charged lowest weight state of the matter representation R; ie we should have electric-magnetic charge $(-d, 0)$ where $-d$ is the lowest weight of R. From this, positive linear combinations may generate the full representation R by adding various W bosons with charge $(\alpha_i, 0)$ to the new state $(-d, 0)$.

Having determined the charge of the new node $f = (-d, 0)$, it is straightforward to compute electric-magnetic inner products to fix the quiver. Explicitly, we may decompose the lowest weight $-d = -\sum_i d_i \omega_i$ where d_i are positive integers. Then $f \circ b_j = (-d, 0) \circ (0, \alpha_j) = -d_i(\omega_i \cdot \alpha_j) = -d_i$ and $f \circ c_j = (-d, 0) \circ (\alpha_j, -\alpha_j) = d_i$. Thus the new node has d_i arrows connected to each node of the ith $SU(2)$ subquiver, forming an oriented three-cycle. Again we run into the subtlety seen in section 8.5: this quiver can certainly generate the matter rep R, but may in fact generate some additional matter representations. In fact, by adding such a node, we actually add the full tensor reducible representation $\otimes_i \mathbf{r_i}^{d_i}$, (where $\mathbf{r_i}$ are the fundamental reps of the gauge group) instead of adding only the irreducible rep, R.

We can propose one very clear consistency check on this procedure. Due to the structure of $\mathcal{N} = 2$ hypermultiplets, adding a hypermultiplet in rep R adds a multiplet of states in $R \oplus \bar{R}$. Thus, in principle, adding matter in rep R is equivalent to adding matter in rep $\bar{R}$. For the fundamental $\mathbf{N}$ of $SU(N)$, the lowest weight of $\mathbf{N}$ is $-\omega_{N-1}$, while the lowest weight of $\overline{\mathbf{N}}$ is $-\omega_1$. This creates some ambiguity in defining the quiver of $SU(N)$ $N_f > 1$.

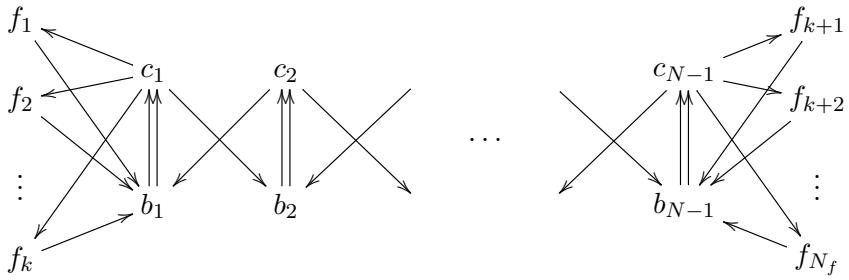

(101)

By the above discussion, any choice of $0 \leq k \leq N_f$ seems to give a possible quiver for this theory. For consistency, the representation theory of all of these quivers must be equivalent. One can easily check that the quivers are in fact mutation equivalent. To move node f_i from the left to the right, apply the following sequence of mutations: $f_i, b_1, c_1, b_2, c_2, \ldots, b_{N-1}, c_{N-1}$; a similar reversed sequence $f_j, b_{N-1}, c_{N-1}, b_{N-2}, c_{N-2}, \ldots, b_1, c_1$ moves node f_j from right to left. We can move the f_i one by one across the quiver, and any two choices of k will be connected via these mutation sequences. Thus by the general reasoning of section 4, these quivers do in fact correspond to identical physical theories.

6.5 BPS States of SQCD

We now wish to extend our analysis of strong-coupling SYM to include arbitrary fundamental quark hypermultiplets coupled to the gauge group. Recall that our rule for coupling matter was valid with all masses tuned parametrically large. With a suitable definition of charges, only the N_f flavor nodes will carry flavor charge,[29] and decouple from the pure gauge theory when masses are scaled up. We again study the origin of the Coulomb branch, and expect the light pure gauge degrees of freedom to reproduce the finite spectrum given above. Finally, we must fix the central charge phases of the flavor nodes; we choose all of them to be to the left of the c_i; for definiteness, let $\arg \mathcal{Z}(f_1) > \arg \mathcal{Z}(f_2) > \cdots > \arg \mathcal{Z}(f_{N_f})$. Having fixed all parameters of the theory, we may use the mutation method to compute a finite spectrum. For each flavor f_k, we find, in phase order

$$f_k, f_k + b_1, f_k + b_1 + c_1, f_k + b_1 + c_1 + b_2, \ldots, f_k \sum_{i=1}^{N-1} b_i + c_i, \tag{102}$$

given by mutation sequence

$$f_k, b_1, c_1, b_2 \ldots c_{N-1}. \tag{103}$$

As discussed in section 5.4, the charges assigned to nodes are dependent on some choice of 'duality frame.' If we take the charge assignments found at weak coupling, $b_i = (0, \alpha_i), c_i = (\alpha_i, -\alpha_i)$, we can see a nice consistency check on this result. With these charges, the flavor states found above contain N pure electric (ie, zero magnetic charge) states with charges forming a fundamental $\mathbf{N}$ of the $SU(N)$, given by $f_k + \sum_{i=1}^{k} b_i + c_i$, $0 \leq k \leq N-1$. The remaining states are then some additional $N-1$ additional flavor dyon states.

Since the flavor nodes are to the left with parametrically large masses, any state with flavor occurs before any of the light pure gauge degrees of freedom; by our choice of central charges, the flavor states occur in order. All states with flavor charge f_1 occur first, and then all states with charge f_2 and so on. Continuing with the mutation method, the set of $N(N-1)$ gauge dyons will be found after all the flavor states described above. The full spectrum is given by $N_f(2N-1)+N(N-1)$

[29] Recall that in our analysis of $SU(2)$ with flavor, the natural assignment of charges gave flavor charge to the nodes of the $SU(2)$ subquiver, along with the additional flavor node. This was simply a familiar choice of convention; by redefining electric and magnetic charges, we can arrange a configuration in which only the additional matter node carries flavor charge.

BPS hypermultiplets, consisting of $2N-1$ flavor states for each fundamental, and $N(N-1)$ pure gauge strong coupling dyons,

$$\boxed{|\mathcal{B}_{\text{SQCD}}| = N_f(2N-1) + N(N-1).} \tag{104}$$

6.6 Further ADE examples

Here, we briefly review some additional finite chambers of ADE-type gauge theories that may be obtained by the mutation method. For these examples, the period computation done in section 6.3.2 becomes much more complicated. We will skip that calculation, and instead simply identify a finite mutation sequence that generalizes the one found there for $SU(N)$.

For pure SYM with DE-type gauge group, the quiver was given in section 6.2. There exists a finite mutation sequence for any of the ADE-type quivers whose number of states is exactly the total number of roots of G,

$$\boxed{|\mathcal{B}_{ADE}| = \dim(\text{adjoint}) - \text{rank}(G).} \tag{105}$$

This spectrum can be interpreted as a monopole-dyon pair for every positive root. The mutation sequence is given as before

$$c_1, c_2, \ldots, c_n, b_1, b_2, \ldots, b_n, c_1, c_2, \ldots, c_n, \ldots \tag{106}$$

We can also study ADE-type groups with additional matter representations, by following the same strategy as 6.5. We fix the pure gauge degrees of freedom at the strong coupling, finite chamber point discussed above, and take large mass limit for the matter. By choosing the phase of the matter nodes to be left-most, we force all states with flavor charge to be further left than the pure gauge states. For an A-type group (ie $SU(N)$), in addition to quarks, we may couple antisymmetric tensor representations, and find a finite chamber. Generalizing from the SQCD result, there is some duality frame for which the flavor states organize into $\frac{1}{2}N(N-1)$ pure electric states whose charges fill out the antisymmetric tensor of $SU(N)$, along with some number of additional dyon states. Note that by contrast, an $SU(N)$ theory with matter in the symmetric tensor rep can never

have a finite chamber. The symmetric tensor is given as a the highest weight representation of the tensor $\mathbf{N} \otimes \mathbf{N}$. By the prescription of section 6.4, the resulting quiver would contain a subquiver of the form studied for the $SU(2)$, $\mathcal{N} = 2^*$ theory. In section 8.5, we showed that this any chamber of this quiver contains at least two vector particles, and thus cannot have finitely many states. Furthermore, the presences of at least two accumulation rays obstructs the mutation method. The larger quiver for $SU(N)$ with a symmetric tensor will produce at least all the states obtained from its subquiver, and thus it will suffer from the same complications.

For a D-type group, $SO(2n)$ with matter in vector representation of $SO(2n)$, we find a finite chamber of $4(n+1)$ flavor states, along with the $2n(n-1)$ gauge states. Here the flavor states contain $2n$ pure electric states whose charges fill out a **2n**-vector of $SO(2n)$, along with $2n+1$ additional flavor dyon states. With N_v vector representations, we find

$$\boxed{|\mathcal{B}_{SO(2n)}| = N_v(4n+1) + 2n(n-1).} \tag{107}$$

We also find a finite chamber for E_6 with matter in the smallest fundamental representation, **27**; the flavor states contain pure electric charges filling out the fundamental representation, along with 46 additional flavor dyon states; a theory with N_f **27**'s yields

$$\boxed{|\mathcal{B}_{E_6}| = 73N_f + 72.} \tag{108}$$

For E_8, one may not expect any finite chamber, since the smallest fundamental is the adjoint, and the resulting theory is $\mathcal{N} = 2^*$, that is, a massive deformation of a conformal $\mathcal{N} = 4$ theory.

7 Complete Gaiotto Theories

In [21], a class of $\mathcal{N} = 2$ theories are singled out - those theories in which one can parametrize the moduli space by the central charges of a basis of BPS particles. These theories are termed complete. In this section we study the BPS quivers for complete theories, and find some remarkable results. In terms of a quiver description, it is clear why completeness is a useful feature: We can vary our central charges as we like, and know that we haven't left the moduli space of the UV theory we're considering. Thus, for example, one can look for a chamber of a complete theory by starting with

the quiver, and mutating on a sequence of positive nodes. As long as one eventually returns to the original quiver (up to sign), it can be shown that there is actually a chamber in the theory that contains precisely the particles mutated on. The key element of this argument is that this sequence of mutations corresponds to the application of the mutation method to the theory with some arrangement of central charges. Since the theory is complete, any arrangement of central charges is accessible, and hence the chamber exists. This is a very powerful line of reasoning, and led to a classification of theories with finite chambers in [24]. In particular, it allows one to avoid the central charge gymnastics we underwent in the discussion of $SU(N)$ theories in section 6.3.

However, there is also an entirely separate reason for studying complete theories. For all but an exceptional few,[30] complete theories correspond to rank 2 Gaiotto theories, of the type discussed in section 2.3. By construction, all such theories are intrinsically determined by a Riemann surface $\mathcal{C}$ decorated by a number of marked points defined by the punctures. We will see something remarkable emerge for the rank 2 case. We find that the BPS quiver, together with its superpotential, is encoded combinatorically in a triangulation of the decorated surface defining the theory. Thus we will have an algorithmic way of writing down quivers for any element of the class of rank 2 Gaiotto theories. Further, this is one of the very few cases where we can explicitly specify a superpotential for our quiver. This construction is unique to the rank two case, because for cases of higher rank the equivalent flow equations leading to the triangulation and combinatorical solution become quite complex, and we must turn to other means of understanding the theories (see section 8).

We will thus specialize to the rank 2 case and construct these theories using geometric engineering [58–60, 75] in type IIB string theory on a non-compact Calabi-Yau threefold. The threefolds in question can be built up starting from a Riemann surface $\mathcal{C}$. We start with a four complex-dimensional space described by a rank three complex vector bundle over $\mathcal{C}$. Explicitly

$$K_{\mathcal{C}} \oplus K_{\mathcal{C}} \oplus K_{\mathcal{C}} \to \mathcal{C}, \tag{109}$$

where in the above $K_{\mathcal{C}}$ denotes the canonical line bundle of holomorphic one-forms on the Riemann surface $\mathcal{C}$. In general the surface $\mathcal{C}$ is punctured at a finite number of points $p_i \in \mathcal{C}$ and thus is non-compact.

[30] For a solution of the exceptional cases, see [24].

Next we select a particular holomorphic quadratic differential ϕ on $\mathcal{C}$. As a quadratic differential, ϕ transforms under holomorphic changes of coordinates on $\mathcal{C}$ as follows

$$\phi'(x') = \phi(x) \left(\frac{dx}{dx'}\right)^2. \tag{110}$$

To completely specify the problem, we must also fix the limiting behavior of ϕ at the ideal boundaries of $\mathcal{C}$, namely the punctures p_i. Near each such puncture the quadratic differential is permitted to have a pole of finite order. We fix the non-normalizable behavior of ϕ as a boundary condition and therefore impose that near p_i

$$\phi(x) \sim \frac{1}{x^{k_i+2}} dx^2 + \text{less singular terms.} \tag{111}$$

The integer $k_i \geq 0$ associated to each puncture is invariant under changes of coordinates. It is an important aspect of the construction, which we return to in section 7.1.[31]

Given this data our Calabi-Yau threefold is then defined by introducing local coordinates (u, v, y) on the fiber of the vector bundle (109) and solving the following equation

$$uv = y^2 - \phi(x). \tag{112}$$

The associated holomorphic three-from Ω is given by

$$\Omega = \frac{du}{u} \wedge dy \wedge dx. \tag{113}$$

It is then known that finite mass strings probing the singularity of this geometry engineer a 4d field theory with $\mathcal{N} = 2$ supersymmetry. The Seiberg-Witten curve Σ of such a theory is given by a double cover of $\mathcal{C}$, and we obtain the Seiberg-Witten differential by integrating Ω over a non-trivial 2-cycle in the fiber.

$$\Sigma = \{(x, y) | y^2 = \phi(x)\}; \qquad \lambda = \int_{S^2(x)} \Omega = y dx = \sqrt{\phi}. \tag{114}$$

[31]The reason for the exclusion of the case $k_i = -1$ is that such fluctuations in ϕ are normalizable, and hence are not fixed as part of the boundary conditions.

By varying the quadratic differential we obtain a family of Seiberg-Witten curves, and in this way the Coulomb branch $\mathcal{U}$ of the theory is naturally identified with the space of quadratic differentials obeying the boundary conditions (111).

It is also known that many of the simplest interesting gauge theories can be geometrically engineered in this fashion. For example taking $\mathcal{C}$ to be a sphere with two punctures p_i, both with $k_i = 1$, constructs the pure $SU(2)$ theory. In general, the class of field theories constructed in this way yields asymptotically free or conformal theories with gauge groups given by a product of $SU(2)$'s, together with various scaling and decoupling limits of such field theories.

For our present purposes, the primary advantage of building an $\mathcal{N} = 2$ quantum field theory in string theory is that the set of supersymmetric objects in string theory, the BPS branes, is known. In our case we seek a brane whose physical interpretation in four-dimensions is a charged supersymmetric particle of finite mass. Thus the worldvolume of the brane should be an extended timelike worldline in Minkowski space times a volume minimizing compact cycle in the Calabi-Yau (112). Since type IIB has only odd dimensional branes, the only possibility is that BPS states are described geometrically by Dirichlet three-branes wrapping special lagrangian three-cycles.

Thus we are reduced to a classical, if difficult, geometric problem of counting special lagrangians [9, 61]. These are compact lagrangian three-manifolds N on which the holomorphic three-form has a constant phase

$$\Omega|_N = e^{i\theta}|\Omega|. \tag{115}$$

The central charge of such a brane is given by

$$\mathcal{Z}_u(N) = \int_N \Omega, \tag{116}$$

and the phase θ in the above is identified with the argument of the central charge of the 4d particle defined by N

$$\theta = \arg \mathcal{Z}(N). \tag{117}$$

Now one of the key observations of [60] is that, in the geometries described by (112), the counting of special lagragians can in fact be phrased entirely as a problem in $\mathcal{C}$. To exhibit this feature we use the fact that all of our special lagrangians are embedded inside the vector bundle (109) and

hence admit a natural projection to $\mathcal{C}$. The image of this projection is a certain one cycle η in $\mathcal{C}$ whose topology depends on the topology of N. Each special lagrangian also wraps a non-trivial S^2 in the fiber, which shrinks to zero at the zeros of ϕ. The possibilities in our examples are as follows, and are illustrated in Figure 11:

- $N \cong S^3$. Such special-lagrangians are discrete. Their quantization yields hypermultiplets in 4d. When this three-sphere is projected to $\mathcal{C}$ we obtain an interval η stretching between two zeros of the quadratic differential ϕ.

- $N \cong S^1 \times S^2$. This class of special-lagrangians always come in one-parameter families. Their quantization yields a vector multiplet in 4d. The projection of any such $S^1 \times S^2$ to $\mathcal{C}$ is a closed loop η.

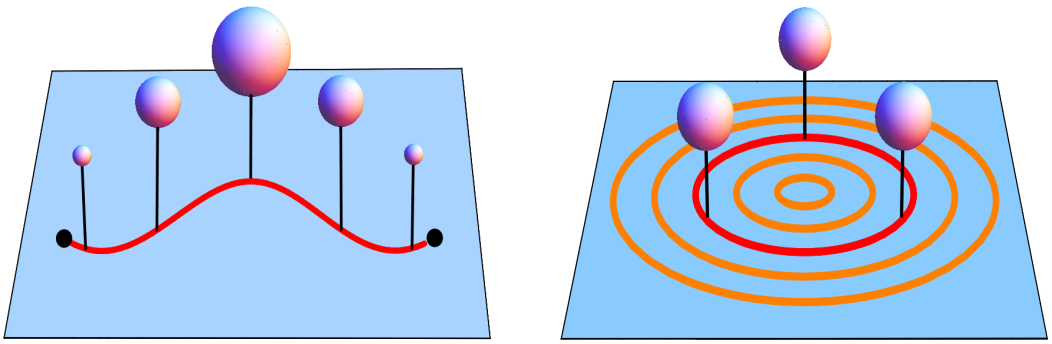

(a) S^3 (b) $S^1 \times S^2$

Figure 11: Special-Lagrangian geometry in the Calabi-Yau. The blue denotes a patch of the surface $\mathcal{C}$. The red trajectory denotes the cycle η and the S^2 fibers are indicated schematically above $\mathcal{C}$. In (a) the topology of the cycle η is an interval which terminates at two zeros of ϕ. The S^2 fibers shrink at these end points yielding a total space of an S^3. In (b), the cycle η has the topology of a circle, and the total space is $S^1 \times S^2$. Such special-lagrangians always come in one parameter families indicated in orange.

The shape of η in $\mathcal{C}$ is constrained by the special Lagrangian condition (115) on N. Explicitly if we let $t \in \mathbb{R}$ parametrize η then the condition of constant phase Ω reduces to

$$\sqrt{\phi}|_\eta = e^{i\theta} dt. \tag{118}$$

The ambiguity in choosing the square root appearing in the above reflects the physical fact that for every BPS particle there is also an associated BPS antiparticle of opposite charge. Choosing

the opposite sign for the square root then sends $\theta \to \theta + \pi$, i.e. it replaces a BPS particle by its antiparticle.

We have now arrived at an elegant statement of the problem of calculating BPS states in this class of quantum field theories. Our goal, however, is not directly to use this structure to compute the BPS states, but rather to extract the BPS quiver of this theory. In the following we will explain a natural way to extract such a quiver from a global analysis of the flow equations (118).

7.1 Triangulations from Special-Lagrangian Flows

Our goal in this section will be to encode certain topological and combinatorial data about the special lagrangian flow in terms of a triangulation of the surface $\mathcal{C}$. Our basic strategy will be to analyze the local and asymptotic properties of the flow on $\mathcal{C}$ defined by (118). This is a problem which is well-studied in mathematics [85] and has received much attention in the present physical context [6, 12, 15, 20, 61]. We will confine ourselves to a brief self-contained review. Since a quiver is constructed from hypermultiplets, our focus will be on the trajectories of this flow which interpolate between the zeros of ϕ. Thus a special role will be played by these trajectories.

To begin, we investigate the local nature of the flow near each zero. We assume that this is a simple zero so that, in some holomorphic coordinate $w(x)$ centered at the zero of ϕ, the flow equation (118) takes the local form

$$\sqrt{w}dw = e^{i\theta}dt \Longrightarrow w(t) = \left(\frac{3}{2}e^{i\theta}t + w_0^{3/2}\right)^{2/3}. \tag{119}$$

Because of the three roots of the right-hand-side of the above, each zero has three trajectories emanating from it. These trajectories make angles of $2\pi/3$ with each other and separate a local neighborhood centered on them into three distinct families of flow lines, as illustrated in Figure 12.

Aside from the zeros, which can serve as endpoints for BPS trajectories, the other distinguished points for the flow are the punctures of $\mathcal{C}$. Since the punctures form ideal boundaries of $\mathcal{C}$, they should be thought of as lying at strictly infinite distance. Thus the behavior of the flow equation near these points governs the asymptotic properties of trajectories at very late and early times. In

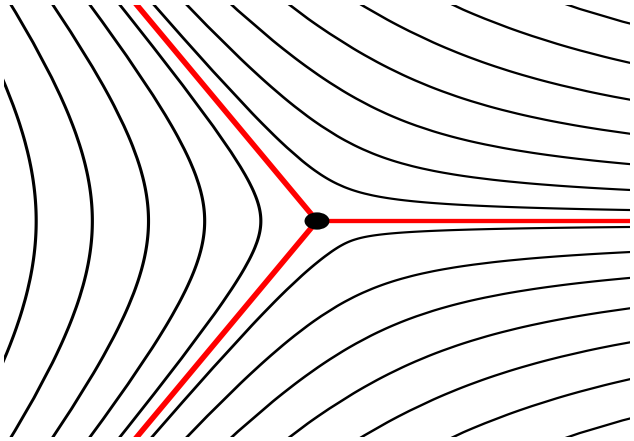

Figure 12: The local structure of the flow near a zero of ϕ shown as a black dot at the center of the diagram. The red trajectories are the three flow lines which pass through the zero. The black trajectories denote other generic flow lines.

a local neighborhood centered on the puncture $p_i \in \mathcal{C}$, the flow equation is asymptotically given by

$$\frac{dw}{w^{1+k_i/2}} = e^{i\theta} dt. \tag{120}$$

We split our analysis of the solutions into two cases depending on the order $k_i + 2$ of the pole in ϕ at the puncture:

- *Regular Punctures*: $k_i = 0$

  The regular punctures in $\mathcal{C}$ are naturally associated to flavor symmetries and hence mass parameters of the engineered field theory [38]. In our analysis this manifests itself in the following way: the residue of the pole in the flow equation is a coordinate invariant complex parameter that is part of the boundary data of the geometry. Restoring this parameter to the asymptotic flow equation we then have.

  $$m\frac{dw}{w} = e^{i\theta} dt. \tag{121}$$

  The parameter m is the residue of a first order pole in the Seiberg-Witten differential and can be interpreted as a bare mass parameter.

  We deduce the behavior of the late time trajectories by integrating (121). The solution with

initial condition w_o takes the form

$$w(t) = w_o \exp\left(m^{-1}e^{i\theta}t\right). \tag{122}$$

Assume that the BPS angle θ has been chosen so that $m^{-1}e^{i\theta}$ is not purely imaginary. Then the solution (122) is a logarithmic spiral. Asymptotically all trajectories spiral in towards the puncture as illustrated in Figure 13.

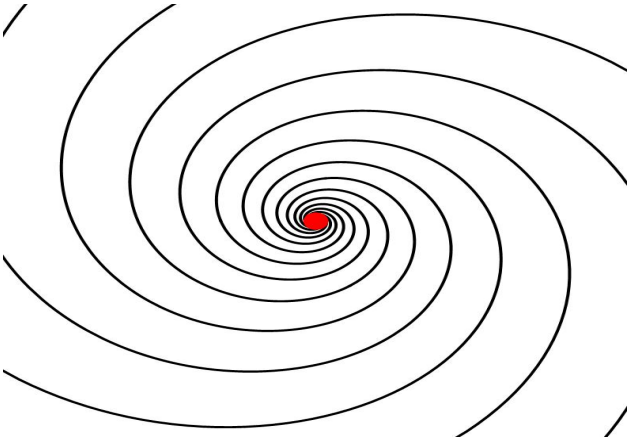

Figure 13: The local flow near a regular puncture indicated in red. The flow lines are spirals terminating at the puncture.

- *Irregular Punctures*: $k_i > 0$

  In the case of irregular punctures, we find power law behavior for the asymptotic trajectories upon integrating (120):

$$w(t) = \left(\frac{-2e^{i\theta}}{k_i}t + \frac{1}{w_o^{k_i/2}}\right)^{-2/k_i}. \tag{123}$$

  A key feature of this solution is that it exhibits Stokes phenomena. For large $|t|$ the trajectories converge to the origin $w = 0$ along k_i distinct trajectories. We account for this behavior of the flows by cutting out a small disk in the surface $\mathcal{C}$ centered on the origin in the w plane. In terms of the metric structure of $\mathcal{C}$ this hole is to be considered of strictly infinitesimal size. The modified surface now has a new ideal boundary S^1, and the k_i limiting rays of the flows are replaced by k_i marked points on this boundary. This procedure is illustrated in Figure 14.

  For each puncture p_i with $k_i > 0$ we perform the operation described above. At the conclusion

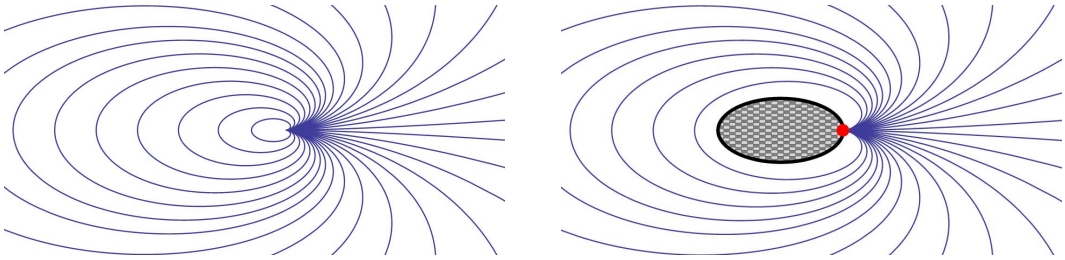

(a) (b)

Figure 14: Asymptotic flows near an irregular puncture with $k = 1$. In (a) the flow lines converge along a single ray, the rightward horizontal direction. In (b), the surface $\mathcal{C}$ is modified by cutting out the small gray checkered region. This surface now has a boundary, depicted by the black curve. On the modified surface with boundary, generic flows terminate at a point, indicated in red, on the boundary.

of this procedure our modified surface $\mathcal{C}$ now has an ideal boundary component S_i^1 for each irregular puncture p_i and further each S_i^1 is decorated with k_i marked points. From now on, when discussing flows with irregular punctures, the symbol $\mathcal{C}$ shall mean this modified surface, equipped with boundary components containing marked points for each irregular puncture.

Armed with the above, it is easy to deduce the global structure of the flow diagram on $\mathcal{C}$, that is, the global picture of the solutions to

$$\sqrt{\phi} = e^{i\theta} dt. \tag{124}$$

We first choose the BPS angle θ *generically*. This means that there are no BPS trajectories in the flow, and hence no finite length trajectories connecting zeros of ϕ as well as no closed circular trajectories. There are then two types of flow lines:

- *Separating Trajectories*

  These are flow lines which have one endpoint at a zero of ϕ and one endpoint at a regular puncture or marked point on the boundary of $\mathcal{C}$. Separating trajectories are discrete and finite in number.

- *Generic Trajectories*

  These are flow lines which have both endpoints at either regular punctures or marked points on the boundary. Generic trajectories always come in one parameter families.

A useful way to encode the topological structure of these flow diagrams is the following. We

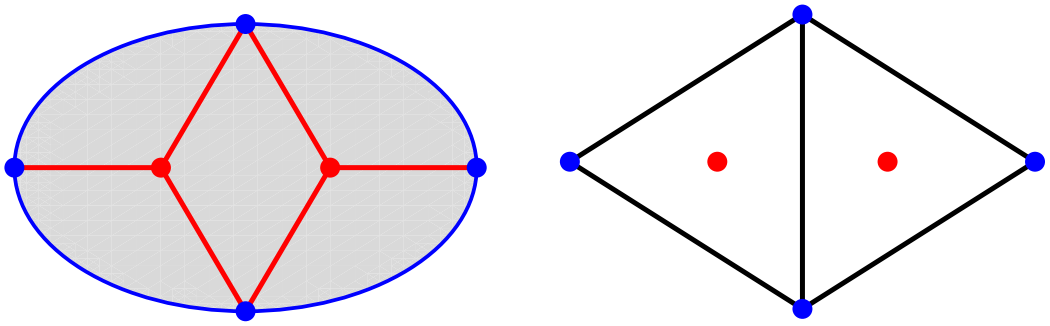

(a) Flow Diagram (b) Triangulation

Figure 15: An example flow diagram and its associated triangulation. In (a) we have a global flow diagram on a disc with four marked points on the boundary. The red dots are the zeros of ϕ and the associated separating trajectories are the red lines. The gray cells denote one parameter families of generic flows. All flow lines end on the four marked blue dots on the boundary. In (b) we have extracted the associated triangulation. Each black line is a generic flow line selected from each one parameter family. The resulting triangles each contain one zero of ϕ by construction.

consider our surface $\mathcal{C}$ with boundary. It has marked points in the interior for each regular puncture, and marked points on the boundary given by the order of the pole of ϕ at the associated irregular puncture. Then, for each one parameter family of generic trajectories, we choose exactly one representative trajectory and draw an arc on $\mathcal{C}$ connecting the indicated marked points. An example is indicated in Figure 15b. This procedure produces an *ideal triangulation* of $\mathcal{C}$ where each diagonal of the triangulation terminates at two marked points. Further, by construction, each triangle contains exactly one zero of ϕ. Generally it is possible for the flow to produce an ideal triangulation with *self-folded* triangles; these result in some technical complications which are addressed in [24].

In summary, for a fixed quadratic differential ϕ and generic angle θ, we have produced an ideal triangulation of $\mathcal{C}$ by studying trajectories of

$$\sqrt{\phi} = e^{i\theta} dt. \tag{125}$$

The combinatorial structure of this triangulation encodes properties of the flow, and we will see in the remainder of this section how to directly extract a BPS quiver and superpotential from this triangulation. Throughout the discussion it will be important to inquire how the triangulation varies as the data (ϕ, θ) varies. The quadratic differential ϕ labels a point in the Coulomb branch of the gauge theories in question, and thus it is natural to fix this data and study the BPS spectrum

at fixed point in moduli space. By contrast, the angle θ is completely arbitrary. Any generic angle θ can be used, and different angles will produce distinct triangulations. Demanding that ultimately our results are independent of θ will give a powerful constraint in the upcoming analysis.

7.2 BPS Quivers from Ideal Triangulations

We have now arrived at the structure of an ideal triangulation on the surface $\mathcal{C}$. From this data there is a simple algorithmic way to extract a quiver [62]. As a preliminary definition, we refer to an edge in the triangulation as a diagonal, δ, if the edge does not lie on a boundary of $\mathcal{C}$. Then proceed as follows:

- For each diagonal δ in the triangulation, draw exactly one node of the quiver.
- For each pair of diagonals δ_1, δ_2 find all triangles for which the specified diagonals are both edges. For each such triangle, draw one arrow connecting the nodes defined by δ_1 and δ_2. Determine the direction of the arrow by looking at the triangle shared by δ_1 and δ_2. If δ_1 immediately precedes δ_2 going counter-clockwise around the triangle, the arrow points from δ_1 to δ_2.

In [21] many aspects of these quivers were explored and it was argued that these are exactly the BPS quivers of the associated quantum field theories. We now provide a full explanation of this proposal.

We first address the identification of the diagonals of the triangulation with the nodes of the quiver. As we have previously explained, our triangulation is constructed at a fixed value of the central charge angle θ appearing in (118). This angle has been chosen such that no BPS states have a central charge occupying this angle. Now let us imagine rotating θ. Eventually we will reach a critical value θ_c where a BPS hypermultiplet occurs and the structure of the flow lines will jump discontinuously. The key observation is that each triangle in the triangulation contains exactly one zero of ϕ. Then, since BPS hypermultiplets are trajectories which connect zeros of ϕ, a BPS hypermultiplet trajectory must cross some number of diagonals in the triangulation to traverse from one zero to another. A simple example of this is illustrated in Figure 16(b).

What the above example illustrates is that each diagonal δ labels an obvious candidate BPS hypermultiplet trajectory, connecting the two zeros in the two triangles which have δ as a common

boundary. Further any hypermultiplet trajectory which crosses multiple diagonals can be viewed homologically as a sum of the elementary BPS trajectories which cross only one diagonal. Therefore, diagonals should be nodes of the BPS quiver.

Next let us justify why arrows in the quiver should be described by triangles in the triangulation. Each elementary hypermultiplet, corresponding to a diagonal in the triangulation, lifts to a three-sphere in the Calabi-Yau. Since these three spheres form nodes of the quiver, the lattice generated by their homology classes is naturally identified with the charge lattice Γ of the theory. Further the symplectic pairing given by the electric magnetic inner-product is precisely the intersection pairing on these homology classes. Thus for each intersection point of the three-spheres, we should put an arrow connecting the associated nodes. On the other hand it is clear that this intersection number can be calculated by projecting the three-spheres to $\mathcal{C}$ and then simply counting the signed number of endpoints that the associated trajectories share. Each shared endpoint is naturally associated to the triangle containing it; so the triangles correspond to arrows between nodes.

The result of this section is that, given a Riemann surface $\mathcal{C}$ defining a 4d, $\mathcal{N} = 2$ quantum field theory, we have produced a natural candidate BPS quiver. It is quite interesting to note that as a result of recent mathematical work [62], these quivers are all of *finite mutation type*. In other words, repeated mutations of vertices produce only a finite number of distinct quiver topologies. In fact this property is equivalent to the more physically understandable property of completeness [21]. The set of finite mutation type quivers (or equivalently, the set of complete theories) consists precisely of the quivers associated to triangulated surfaces, as described above, along with a finite number of exceptional cases, discussed in [21, 63].

We can give one strong consistency check on our proposal for the BPS quivers as follows. Observe that, to a given Riemann surface theory $\mathcal{C}$ we have in fact produced not one quiver but many. Indeed our quivers are constructed from the triangulation produced from a fixed value θ of the BPS angle where there are no BPS states. So in fact our assignment is

$$(\mathcal{C}, \theta) \longrightarrow Q_\theta = \text{BPS Quiver}. \tag{126}$$

As the central charge phase θ varies over a small region, the flow evolves continuously and the incidence data of the triangulation encoded in Q_θ remains fixed. However, as θ varies past a BPS

state, the flow lines and triangulation will jump discontinuously, as illustrated in the basic example of Figure 16. This results in a new quiver $Q_{\theta'}$, distinct from Q_θ. Both of these quivers Q_θ and $Q_{\theta'}$ are natural candidates for the BPS quiver of theory defined by $\mathcal{C}$, and hence we should expect that the quantum mechanics theories they define are equivalent. In other words consistency of our proposal demands that all quivers of the from Q_θ for any given θ are mutation equivalent. Happily, a simple theorem [62] shows that this is indeed the case: the set of quivers obtained from triangulations of a given surface precisely forms a mutation class of quivers.

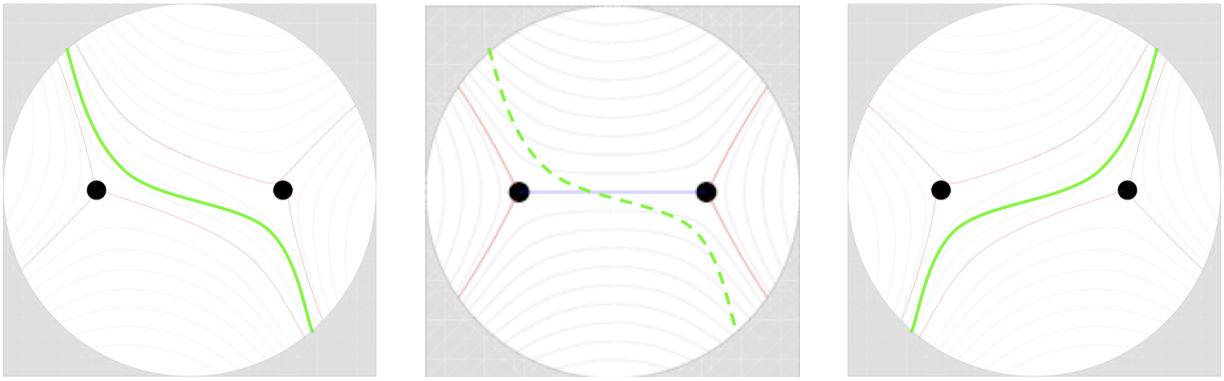

(a) $\theta < \theta_{critical}$ (b) BPS State $\theta = \theta_{critical}$ (c) $\theta > \theta_{critical}$

Figure 16: Evolution of the special lagrangian flows with the BPS angle θ. In each picture the black dots indicate the branch points of the cover where flows emerge. Red trajectories are flows that emerge from the branch points and terminate on the boundary at $|x| = \infty$, while gray trajectories indicate generic flow lines. The green trajectory denotes a representative of a generic flow line which can serve as an edge in the triangulation. In (b) the BPS angle of the flow aligns with the phase of the central charge and a new kind of trajectory, shown in blue, traverses between branch points. Afterwards in (c) the green line has flipped.

Actually, we can say more. If we tune θ from 0 to 2π, we will see that every BPS hypermultiplet corresponds to a jump of the triangulation, and gives a new choice of quiver. This approach to computing BPS spectra was studied in [12]. As was described there, the discontinuous jump of triangulation, or *flip*, at each BPS state γ is given by simply removing the diagonal crossed by γ, and replacing it with the unique *other* diagonal that gives an ideal triangulation.[32] As argued in [62], at the level of the quiver, this flip corresponds precisely to a mutation at the associated node. Thus, if we forget about the surface $\mathcal{C}$ and triangulation, and instead focus on the quiver itself, we

[32]To clarify, once we remove the diagonal of the appropriate BPS state, we are left with some quadrilateral in our 'triangulation.' To produce a true triangulation, we may add one of the two possible diagonals that would cut the quadrilateral into a triangle. A flip is simply given by taking the choice that differs from the original triangulation.

see that we are simply applying the mutation method to compute Π-stable representations! This seems to be a deep insight into how the naively unrelated problems of finding special lagrangians and computing Π-stable quiver representations are in fact equivalent. Recall, however, that the mutation method made no reference to completeness of the theory. While the triangulations and flips exist for some set of complete theories, the mutation method is more general, and can be applied any BPS quiver.

In later sections of this paper we will see further evidence for this proposal by recovering the BPS quivers of well-known quantum field theories. However, before reaching this point let us illustrate one important subtlety which we have glossed over in the above. Consider the possible structure in an ideal triangulation of some Riemann surface $\mathcal{C}$, as illustrated in Figure 17. According to the rules

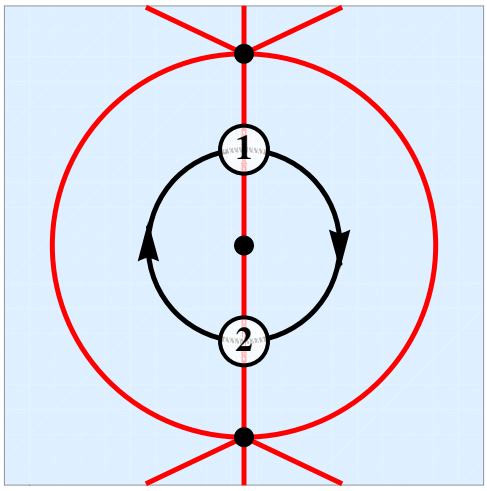

Figure 17: A bivalent puncture in the triangulation gives rise to a two-cycle in Q. The blue denotes a patch of $\mathcal{C}$. Red lines indicate diagonals and marked points are punctures. The nodes of the quiver for the two indicated diagonals are drawn. The bivalent puncture implies that there is a two cycle in the quiver indicated by the black arrows.

of this section, for each bivalent puncture in the triangulation we will obtain, as indicated, a cycle of length two in the quiver. These are fields in the quiver theory which could, in principle, admit a gauge invariant mass term in the superpotential. As mentioned in subsection 3, the quantum mechanics described by the quiver will be rather complicated if no such mass term is generated. In the next section we will argue that the natural potential for these theories does indeed generate all possible gauge invariant mass terms and therefore simplifies the resulting quivers considerably.

7.3 The Superpotential

The previous subsection identified a quiver associated to any ideal triangulation, and further suggested that this quiver is naturally the BPS quiver of the associated gauge theory. In this subsection we will complete this picture by describing a natural superpotential for such a quiver, recently developed in the mathematics literature [81–83]. We will then argue on general grounds, essentially as a consequence of completeness, that this superpotential yields the necessary F-flatness conditions for the quiver quantum mechanics theory.

We will build up the superpotential starting from the elementary case of an acyclic quiver. Since such a quiver has no cycles, there are simply no gauge invariant terms to be written and $\mathcal{W} = 0$.

Next we consider an arbitrary quiver Q which, by a sequence of mutations, is connected to an acyclic quiver. Since Q is the quiver of a complete theory, all of its central charges are free parameters that can be varied arbitrarily as one scans over parameter space. It follows that the sequence of mutations connecting Q to its dual acyclic form is in fact realizable by physical variation of parameters. Hence, following the mutation rules of section 4, the superpotential for the quiver Q is completely fixed by the acyclic quiver with trivial potential.

The argument of the previous paragraph shows that the $\mathcal{W}$ assigned to any such quiver Q is completely fixed, however complicated the sequence of mutations leading from the acyclic form to Q may be. Surprisingly, there exists an elementary description of this superpotential in terms of the local incidence data of the triangulation of $\mathcal{C}$ which gives rise to Q. This description has been developed in [81]. For any quiver Q mutation equivalent to an acyclic quiver, the superpotential $\mathcal{W}$ is computed as follows:

- Let T denote a triangle in $\mathcal{C}$. We say T is *internal* if all of its edges are formed by diagonals, that is none of the sides of T are boundary edges in $\mathcal{C}$. Then each edge of T represents a node of the quiver and the presence of the internal triangle T implies that these nodes are connected in the quiver in the shape of a three-cycle. For each such triangle T we add the associated three-cycle to $\mathcal{W}$. This situation is illustrated in Figure 18a.

- Next let p be an internal, regular puncture in $\mathcal{C}$. Then some number n of edges in the triangulation end at p. Further since p is an internal puncture which does not lie on the boundary of $\mathcal{C}$ it follows that each such edge terminating at p is in fact a diagonal and hence

a node of the quiver. The n distinct nodes are connected in an n-cycle in the quiver and we add this cycle to $\mathcal{W}$. This situation is illustrated in Figure 18b.

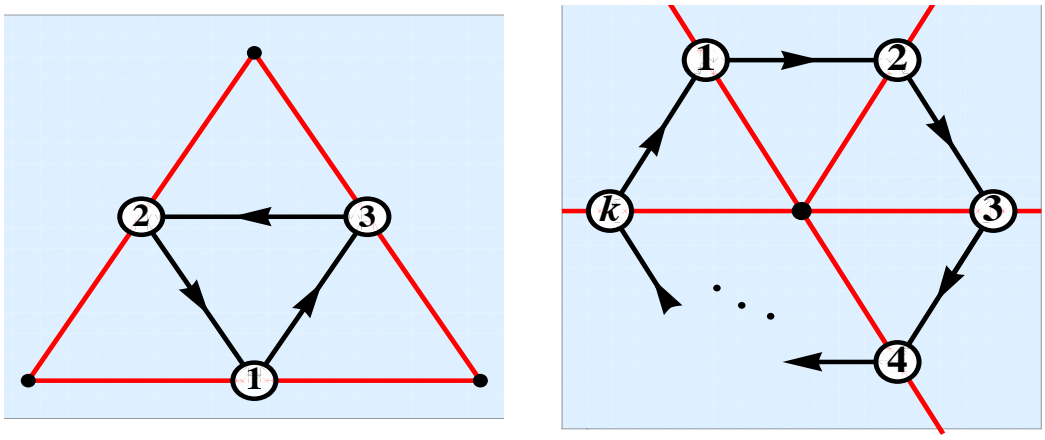

(a) Internal Triangle

(b) Internal Puncture

Figure 18: The two distinct structures in the triangulation which contribute to the potential. The blue region denotes a patch of $\mathcal{C}$, the red edges are diagonals in the triangulation. These correspond to nodes of the quiver which we have indicated on the triangulation. The black arrows connecting the nodes are the arrows in the quiver induced by the shared triangles shown in the diagram. In (a) an internal triangle gives rise to a three-cycle in $\mathcal{W}$ in (b) an internal puncture of valence k gives rise to a k-cycle in $\mathcal{W}$.

For quivers with multiple arrows between two given nodes, it is important to keep track of which triangle the arrow arises from when writing down the superpotential. The superpotential must be written with a fixed, consistent assignment of arrows to triangles; inconsistent choices are *not* equivalent, and will generally give the wrong answer.

The observation that the superpotential can be determined in such an elementary way from the incidence data of the triangulation is striking. It strongly suggests that $\mathcal{W}$ is a local object that can be determined patch by patch on $\mathcal{C}$. Granting for the moment that this is so allows us to immediately generalize to any theory determined by an arbitrary Riemann surface $\mathcal{C}$. We can simply extend the simple rules given above to all quivers.

One important consequence of this extension is that the it automatically ensures that all of our superpotentials will be compatible with mutation. That is, just as in equation (126), we have now constructed a map from a Riemann surface $\mathcal{C}$ and an angle θ to a quiver Q and superpotential $\mathcal{W}$. However the angle θ is arbitrary. As θ rotates, in general the triangulation $\mathcal{T}$ of $\mathcal{C}$ will undergo a

series of flips and arrive at a new triangulation $\widetilde{\mathcal{T}}$. From this new triangulation we can determine the quiver $(\widetilde{Q}, \widetilde{\mathcal{W}})$. On the other hand we have previously noted that flips in the triangulation are the geometric manifestation of quiver mutation. Thus we have two independent ways of determining the dual quiver and superpotential:

- Compute $(\widetilde{Q}, \widetilde{\mathcal{W}})$ from $(Q, \mathcal{W})$ by performing a sequence of mutations.
- Compute $(\widetilde{Q}, \widetilde{W})$ from the new triangulation $\widetilde{\mathcal{T}}$

A necessary condition for a consistent superpotential is that the two computations yield the same answer. In [81] it was proved that this is the case.

The above argument shows that our proposal for the superpotential is consistent with the quiver dualities described by mutation. However, it depends fundamentally on our locality hypothesis for the superpotential. As we will now argue, using the completeness property of the field theories in question, we can give a strong consistency check on this assumption.

All of our arguments thus far involve constraints on $\mathcal{W}$ that arise from mutation. As we mentioned in section 4 mutations may be forced when, as we move around in moduli space, the central charges rotate out of the chosen half-plane. Most importantly, all these rotations are physically realized, since in a complete theory all central charges are free parameters.

Of course the central charges of the theory come not just with phases but also with magnitudes. In a complete theory we are also free to adjust these magnitudes arbitrarily. Let us then consider the limit in parameter space where the magnitude of the central charge associated to a node δ becomes parametrically large compared to all other central charges

$$|\mathcal{Z}(\delta)| \longrightarrow \infty. \tag{127}$$

In this limit, the BPS inequality implies that all particles carrying the charge δ become enormously massive and decouple from the rest of the spectrum. At the level of the quiver Q this decoupling operation is described as follows: simply delete from the quiver the node δ and all arrows which start or end at δ. This produces a new quiver $\widetilde{Q}$ with one node fewer than Q. The superpotential for the resulting quiver theory $\widetilde{Q}$ is then determined simply by setting to zero all fields transforming under the gauge group indicated by δ.

Following our interpretation of nodes of the quiver as diagonals in a triangulation, it is possible to describe this decoupling operation at the level of the Riemann surface $\mathcal{C}$ itself. Consider the diagram of Figure 19a which depicts the local region in $\mathcal{C}$ containing a diagonal δ traversing between two punctures or marked points p_i. The decoupling operation to destroy the node δ is then realized by excising a small disc containing δ as a diameter and no other diagonals. The result of this procedure is shown in Figure 19b. It is clear from our construction of BPS quivers from triangulations that

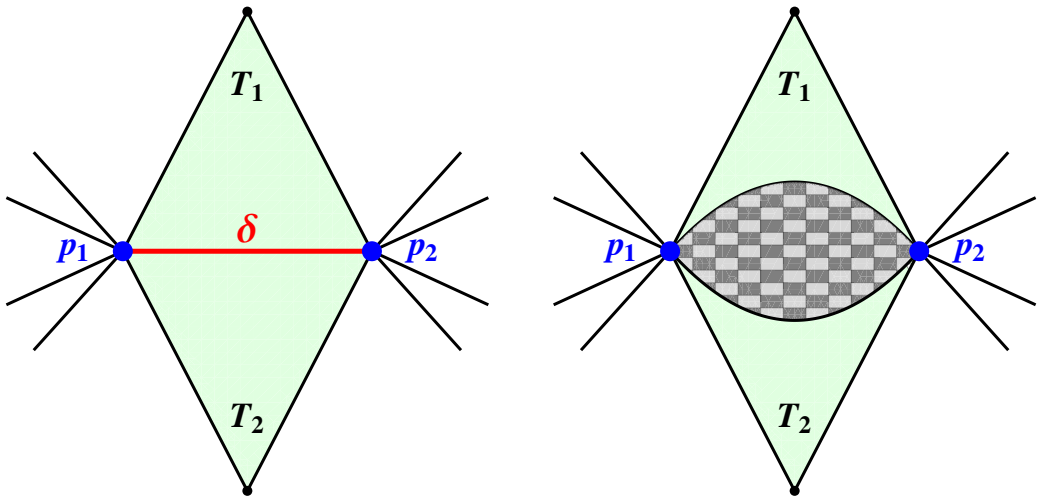

(a) $\mathcal{C}$ pre-surgery (b) δ Decoupled

Figure 19: The node decoupling surgery for a typical diagonal δ. In (a) we see a patch of $\mathcal{C}$ focused on the region involving a typical diagonal δ. In (b) δ has decoupled leaving a new a new Riemann surface $\widetilde{\mathcal{C}}$ which differs from $\mathcal{C}$ by the addition of a new boundary component which encloses the checkered region and has two marked points p_i.

this decoupling operation produces a new surface $\widetilde{\mathcal{C}}$, whose BPS quiver is exactly $\widetilde{Q}$, the quiver with the node δ decoupled. We may therefore determine the superpotential $\mathcal{W}$ for $\widetilde{Q}$ by applying the incidence rules described in this section to the new surface $\widetilde{\mathcal{C}}$.

In summary, we see that there are two distinct ways for computing the superpotential for the quiver $\widetilde{Q}$:

- Determine from $\mathcal{C}$ the superpotential for the quiver Q. Then reduce to $\widetilde{Q}$ by deleting the node δ.
- Determine directly from the surface $\widetilde{\mathcal{C}}$ the superpotential for the quiver $\widetilde{Q}$.

Consistency of our proposal demands that the two methods give rise to the same superpotential. It

is easy to see directly that this is the case. Indeed the effect of the surgery operation illustrated in Figure 19 is to change the two triangles T_i to external ones, and to change the points p_i to marked points on the boundary. Clearly this eliminates from the superpotential exactly those terms in which fields charged under the node δ appear.

By completeness, the decoupling limit argument can be applied to an arbitrary node in a BPS quiver and yields a strong consistency check on the locality hypothesis and thus our proposal for the superpotential.

Let us remark that the superpotential we have constructed naturally resolves the headache proposed at the end of section 7.2. By construction, every two-cycle in a quiver arises from a bivalent puncture of the corresponding triangulation. For each bivalent puncture there is now a quadratic term in the superpotential that lifts the fields involved in the associated two-cycle. Thus we may integrate out and cancel all possible two-cycles to produce a two-acyclic quiver.

Finally, before turning to examples, we point out that it would be interesting to calculate this superpotential directly from a string theory construction. While several plausibility and consistency arguments have been given, a direct calculation may certainly lead to further insight.

7.4 $SU(2)$ Revisited

In this section we will return to some simple theories with a single $SU(2)$ gauge group that we have seen previously, and find their quivers in our new, general rank 2 framework. Consistent with our previous discussion, for those examples involving irregular punctures, we will present triangulations of surfaces with boundary.

Before enumerating the examples, we take a moment to fix conventions. Throughout, in all triangulations, red labeled lines denote diagonals, which appear as nodes of the quiver, while black lines denote boundary components. Both regular punctures and marked points on the boundary are indicated by black dots. Bifundamental fields corresponding to arrows in the quiver will be denoted by X_{ij} and Y_{ij} where i and j label the initial and final vertex of the arrow respectively.

7.4.1 Asymptotically Free Theories

We first study quivers for $SU(2)$ theories with asymptotically free gauge coupling.

- $SU(2)$

  This theory is constructed on an annulus with one marked point at each boundary.

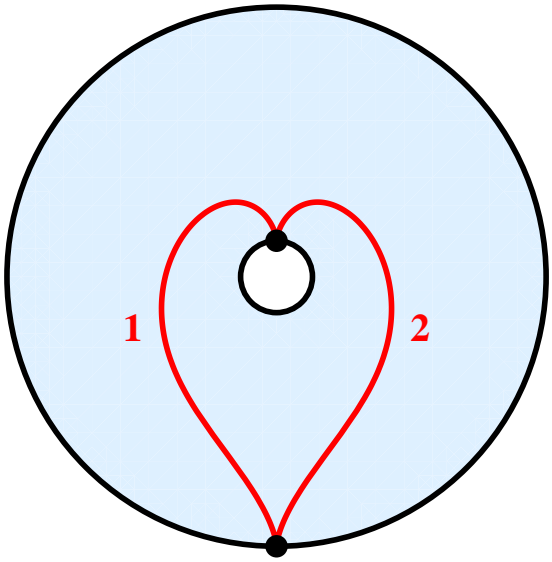

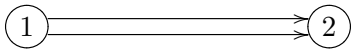

$$\mathcal{W} = 0.$$

  Of course this is exactly the quiver for $SU(2)$ Yang-Mills.

- $SU(2)$ $N_f = 1$

  This theory is constructed on an annulus with one marked point on one boundary component, and two marked points on the remaining boundary component.

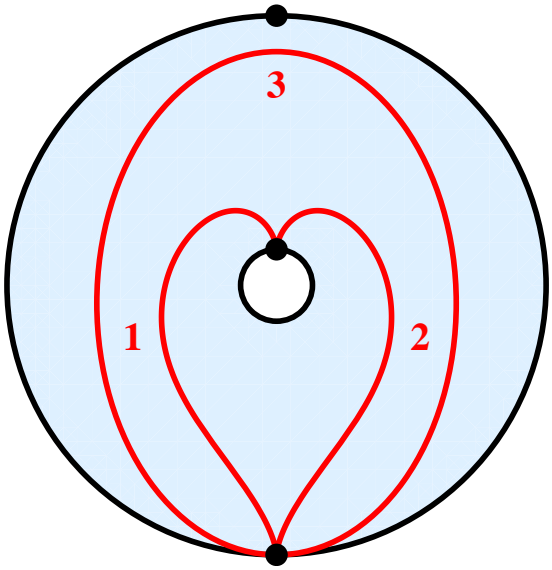

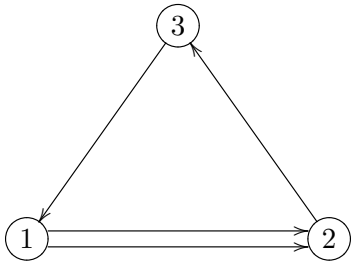

$$\mathcal{W} = X_{12}X_{23}X_{31}.$$

- $SU(2)$ $N_f = 2$

  This theory is constructed on an annulus with two marked points on each boundary component.

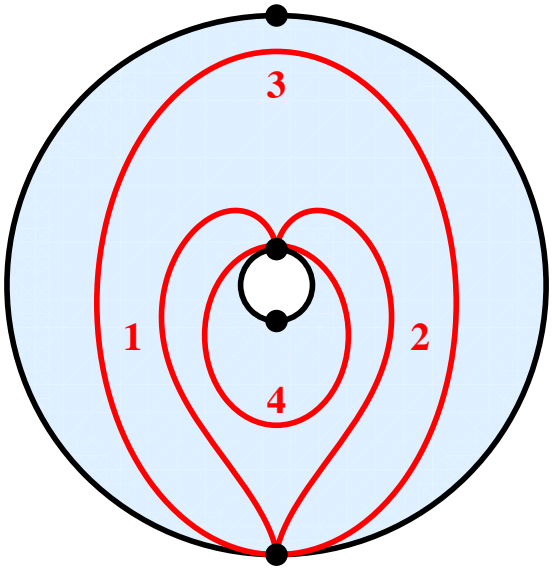

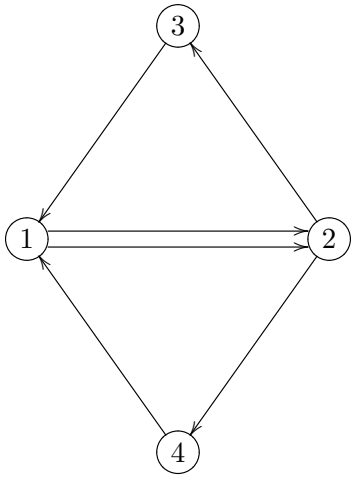

$$\mathcal{W} = X_{12}X_{23}X_{31} + Y_{12}X_{24}X_{41}.$$

- $SU(2)$ $N_f = 3$

  This theory is constructed on a disc with two marked points on the boundary and two punctures.

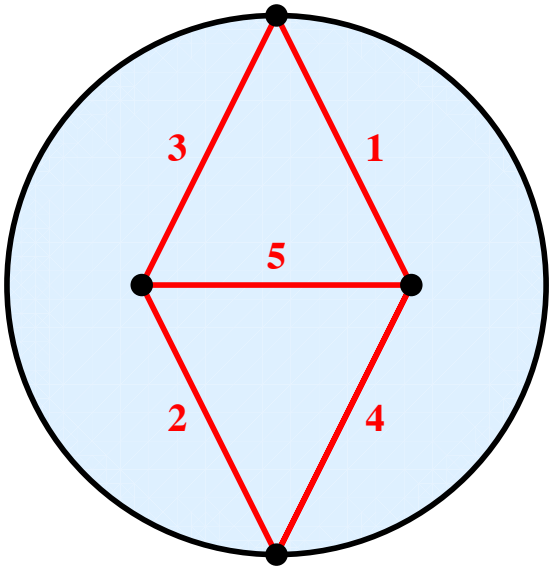

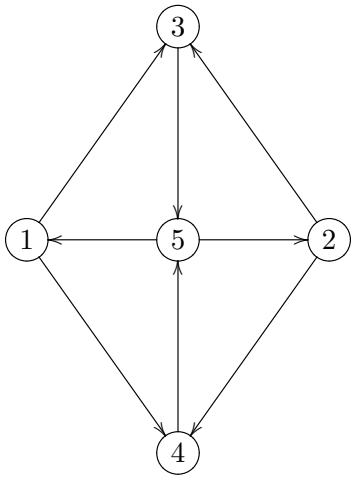

$$\begin{aligned}\mathcal{W} &= X_{13}X_{35}X_{51} + X_{23}X_{35}X_{52} \\ &+ X_{14}X_{45}X_{51} + X_{24}X_{45}X_{52}.\end{aligned}$$

7.4.2 Conformal Theories

While the previous examples illustrate many general features, all the quivers given there are mutation equivalent to quivers without oriented cycles. Thus for those cases the potential is completely

fixed by the mutation rules of section 4. Now we will consider the case of $SU(2)$ Yang-Mills theories with vanishing beta functions where the conformal invariance is broken only by mass terms. Such quivers arise from triangulations of closed Riemann surfaces and never have acyclic quivers. As such, our proposal for the superpotential is the only known way of constructing $\mathcal{W}$.

- $SU(2)$ $N_f = 4$

  This theory is constructed on a sphere with four punctures. We draw the associated triangulation on a plane omitting the point at infinity.

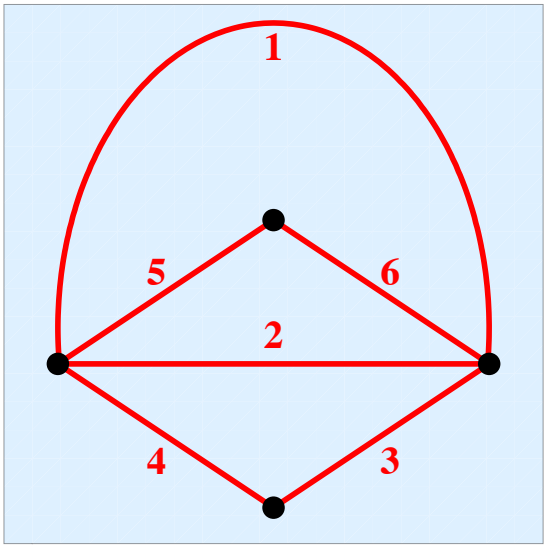

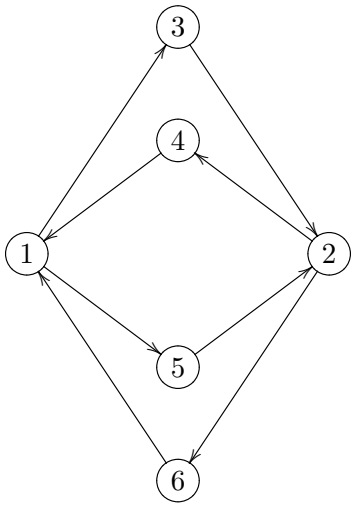

$$\begin{aligned}\mathcal{W} &= X_{15}X_{52}X_{24}X_{41} + X_{13}X_{32}X_{26}X_{61} \\ &+ X_{15}X_{52}X_{26}X_{61} + X_{13}X_{32}X_{24}X_{41}.\end{aligned}$$

  Notice that this triangulation contains two bivalent punctures; the quiver and superpotential above are obtained after integrating out the corresponding two-cycles.

- $SU(2)$ $\mathcal{N} = 2^*$.

  This theory is constructed on a torus with one puncture. We draw the triangulation on a quadrilateral where opposite sides are identified.

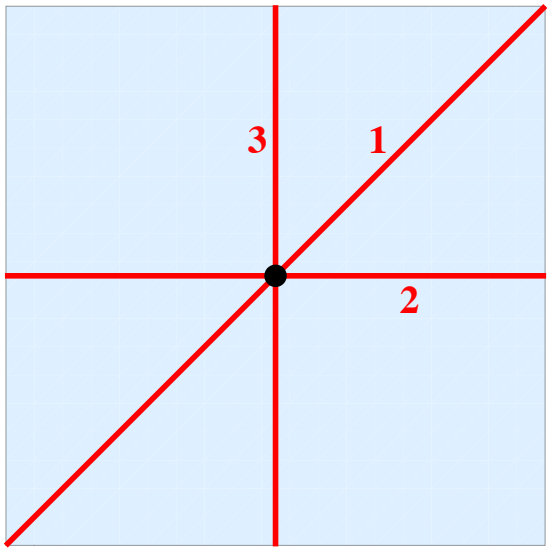

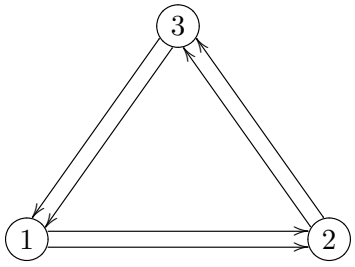

$$\begin{aligned}\mathcal{W} &= X_{12}X_{23}X_{31} + Y_{12}Y_{23}Y_{31} \\ &+ X_{12}Y_{23}X_{31}Y_{12}X_{23}Y_{31}.\end{aligned}$$

It is amusing to note that the this quiver for the $\mathcal{N} = 2^*$ theory is in fact invariant under mutation and, consistent with our general discussion, our potential is also mutation invariant.

Building from the examples in this section the reader can easily construct the BPS quiver for a complete theory associated to any arbitrary Riemann surface.

8 Quiver Gauging and Non-Complete Gaiotto

Near the beginning of this work, in section 2, we described a very general class of theories given by wrapping n M5-branes on a punctured Riemann surface. Then, after introducing our quiver framework, we went on to investigate the BPS spectra of many individual gauge theory examples. It's very prudent to realize, at this point, that the majority of the gauge theory examples we have studied are of the Gaiotto type (as long as one includes decoupling limits). Thus, it is obvious that we stand to gain a lot of insight if we can understand, in a general way, the prescription for deducing a quiver for any theory in the Gaiotto class.

In fact, we have already accomplished this for the rank two case. These are precisely the class of theories we solved using triangulations of Riemann surfaces in section 7. The triangulations came about as a result of studying flows on the Riemann surface. However, for the case of n M5-branes, the relevant surface becomes a multi-sheeted cover, and the flow problem becomes intractable. Thus, to discover a method of constructing quivers for $n \geq 2$, we need to go back to the drawing board.

The essential feature that Gaiotto theories of any rank share is that they can be built up step by step from a set of simple building blocks, by diagonally gauging flavor symmetries, as we described in section 2.3. Thus, if we can understand how the quiver for a diagonally gauged pair of theories relates to their individual BPS quivers, we have a hope of building up the quiver for an arbitrary Gaiotto theory simply by constructing the BPS quiver from the building block BPS quivers, in parallel to the construction of the theory itself. Thus, in section 8.1, we consider what happens to the quiver of an $\mathcal{N} = 2$ theory when one gauges a flavor symmetry in 4d.

For a theory with n M5-branes, there are many kinds of punctures that can decorate the Riemann surface; indeed, there is a classification of punctures by Young tableaux [38–41]. However, there is a distinguished type of puncture: the kind that appears as the degeneration limit of surfaces, and correspondingly the ones which we can use to glue surfaces together. This is the puncture which corresponds to an $SU(n)$ flavor symmetry. In turn, there is a special building block, namely the sphere with three maximal punctures, corresponding to the theory with (at least) $SU(n)^3$ flavor symmetry, called $\mathcal{T}_n$.

Thus, after discussing how to gauge a flavor symmetry, we propose quivers for the $\mathcal{T}_n$ theories, for all n. We consider a very interesting consistency check on our proposals in the rank 3 case, which is related to the Argyres-Seiberg duality discussed in section 2.3. We then go on to describe how one can build a general quiver for a rank 3 surface, by considering how two $U(1)$ type punctures collide to give an $SU(3)$ puncture, and comment on the generalization to the rank n case.

Finally, we conclude with an example of a rank 2 theory which cannot be completely solved - namely, the $\mathcal{N} = 2^*$ theory which is a deformation of $\mathcal{N} = 4$ SYM - and comment on the novel features this case presents.

8.1 Flavor Symmetries and Gauging

We begin by studying the relationship between global symmetries of our 4d quantum field theory and the discrete symmetries of its BPS quiver. Suppose a physical theory has some known global symmetry. Generally speaking, turning on various deformations of the theory will break the global symmetry, so here we consider studying the theory at the precise point of parameter space that preserves the full global symmetry of interest. Of course, the BPS spectrum should reflect this symmetry. The first question we wish to explore is how this symmetry should be encoded in the

BPS quiver.

It is possible that every state in the BPS spectrum might be singlet under the global symmetry; then it would be very difficult to find evidence for the symmetry in either the quiver or the full BPS spectrum. So we should refine the question a bit. Let us restrict to a global $SU(n)$ symmetry, and further, let us study the case in which there is some BPS hypermultiplet in the fundamental of $SU(n)$. In this case we can give a very straightforward answer to the question. The full fundamental multiplet of BPS states must have identical central charges. We simply choose our quiver half-plane so that this multiplet is left-most in the $\mathcal{Z}$-plane.[33] Since they carry distinct flavor charges spanning the weight space, all n states of fundamental must occur in the quiver.[34] These states of course have different global charges, but identical electric-magnetic charges. Since the quiver is only sensitive to electric-magnetic charges, we will find n identical nodes in the resulting quiver, and thus an S_n permutation symmetry that exchanges these identical nodes.

The $SU(2)$ examples in section 5 with massless matter illustrate this fact. For $N_f = 2$, we had an $SO(4) = SU(2) \times SU(2)$ flavor symmetry, which manifests as two S_2 discrete symmetries in the quiver, given by exchanging γ_1, γ_2 and γ_3, γ_4. For $N_f = 3$, we had an $SO(6) = SU(4)$ symmetry, manifested as an S_4 on $\gamma_1, \gamma_2, \gamma_3, \gamma_4$. For $N_f = 4$, there should be a full $SO(8)$ flavor symmetry; however, it is only preserved at the massless conformal point, where we have no quiver description. For any mass deformation, the maximal symmetry is $SU(4)$, which corresponds to the obvious S_4 acting on $\gamma_3, \gamma_4, \gamma_5, \gamma_6$.

From these observations, we can suggest a powerful rule for constructing quivers of new theories by gauging global symmetries of a theory with a known quiver. For now, let us focus on gauging a global $SU(2)$ symmetry that is manifested as an S_2 symmetry in the quiver acting on a pair of identical nodes. We will later extend our results to the general $SU(n)$ case. Physically, to gauge a symmetry, we add gauge degrees of freedom and couple them appropriately to the matter

[33]This choice of half-plane will be impossible when the phase of central charge of the fundamental of hypermultiplets occurs at some accumulation ray of BPS states. In fact, this exact situation occurs in the case of $SU(2), \mathcal{N} = 2^*$. This theory has an enhanced $SU(2)$ flavor symmetry at the massless point. However, we are never able to see the symmetry in the quiver (which has a single mutation form (147)). The massless theory is conformal, and the spectrum is dense; hence there is no half-plane that admits a positive integer basis. Barring this complication, there exists a half-plane that yields a mutation form of the quiver which explicitly presents the symmetry.

[34]The weight space is only $n-1$-dimensional, so one may worry that only $n-1$ of the states appear. However, the weights obey $\sum_i f_i = 0$ so that the last weight is given by a *negative* integer linear combination of the others. As long as the multiplet carries some non-zero electric-magnetic charge, the last state be linearly independent from the others. Then, to fill out the n states of the fundamental, all n states must appear in the quiver.

already present in the theory. At the level of the quiver, the procedure is quite analogous. We should add two nodes of an $SU(2)$ subquiver to add the gauge degrees of freedom. Then we must couple to the existing pair of identical nodes to this subquiver to form a fundamental of the $SU(2)$. Recall that when we added a flavor to $SU(2)$, we added only one state of the doublet fundamental representation, because bound states would generate the second. Here we must do the same thing - we delete one of the nodes, and connect the other to the $SU(2)$ subquiver in an oriented triangle. The deleted state will now be generated by a bound state with the $SU(2)$ nodes.

To give an example, we can consider gauging one of the $SU(2)$ flavor symmetries of $SU(2)$, $N_f = 2$, which exchanges γ_1, γ_2.

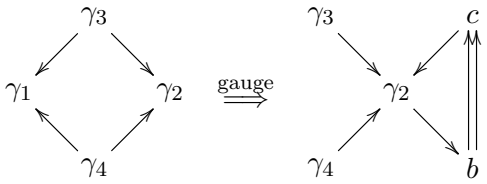

(128)

We have added an $SU(2)$ subquiver b, c and charged the flavor node γ_2 under it; now we have two $SU(2)$ gauge groups with a bifundamental matter field. In this case, we can actually see the weak coupling description of the resulting theory from the quiver, if we apply some mutations. Mutating on γ_1, γ_2, b, c in that order produces

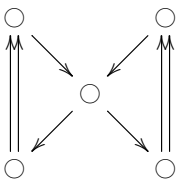

(129)

in which there are two $SU(2)$ subquivers, each coupled to the same node as a fundamental matter state, producing a bifundamental.

As another example, consider glueing the $SU(2)$, $N_f = 4$ quiver to itself other by gauging the diagonal subgroup $SU(2)_d \subset SU(2) \times SU(2) \subset SU(4)$. The original quiver presents $S_2 \times S_2 \subset S_4$ symmetries given by exchanging γ_3, γ_4 and γ_5, γ_6 respectively. The gauging procedure looks as

follows

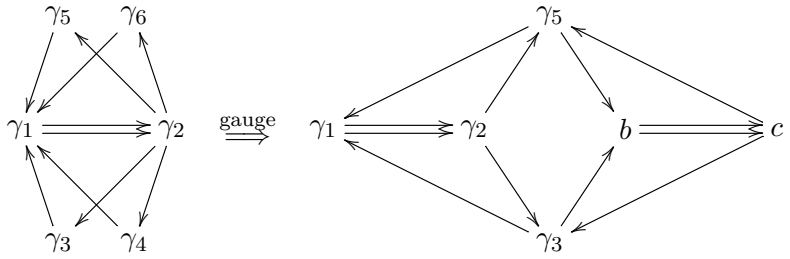

(130)

For these rank 2 theories, there is actually a more systematic way to generate quivers for all surfaces via triangulations from special lagrangian flows, as discussed in section 7. The quiver gauging rule just described can in fact be understood from this triangulation view point, as explained in [21]. For example, the theory $SU(2)$, $N_f = 4$ corresponds to a sphere with 4 punctures; the gauged quiver shown above is known from that analysis to correspond to a torus with 2 punctures, which is precisely the surface produced after glueing two punctures from the 4-punctured sphere. Notice that, since the resulting surface contains 2 punctures, we would expect there to be two more $SU(2)$'s available for gauging. In fact, a mutation sequence can produce one S_2 in the quiver, but there is no way to produce two such symmetries. The analysis from the triangulation perspective shows that we can produce all but one S_2 in the quiver; that is, we can realize one fewer S_2 than the total number of punctures. Actually, there is a very good reason that we are unable to gauge the last $SU(2)$. If we did so, we would remove all punctures from the surface, and produce a quiver for a punctureless surface. However, a punctureless surface supports an exactly conformal theory - all mass deformations have been turned off. Hence the BPS spectrum would exhibit some duality, and in general be dense in the central charge plane, obstructing the existence of a quiver. Thus for consistency, it is necessary that we not be able to gauge the $SU(2)$ symmetry of a once-punctured surface. Nonetheless, we can be able to build up a quiver for any surface with at least one puncture, and these all agree with the quivers obtained from triangulations. For higher rank theories, the analog of the triangulation approach is not known; however, the gauging rules will allow us to construct quivers for a large class of theories whose quiver descriptions were previously unknown.

8.2 Quivers for Gaiotto Building Blocks

We now want to use our gauging technology to construct the quivers for Gaiotto theories. To do this, we must know the quivers for the building blocks of these theories. In particular, we are interested

in the theories described by spheres with three punctures of the maximal type. These are the so-called $\mathcal{T}_n$ theories. One reason why this theory is simple to study is that it is known to be related to M-theory on the Calabi-Yau singularity $\mathbb{C}^3/\mathbb{Z}_n \times \mathbb{Z}_n$ [40]. Specifically, upon compactification along a circle we recover the $\mathcal{T}_n$ theory. The quiver for the Calabi-Yau singularity can be computed by standard methods [27], and indeed the result is known:

- The quiver has n^2 nodes. We arrange them in a grid and index them accordingly as A_{ij} where the indices i, j run from 1 to $n+1$ and are cyclically identified so that 1 is equal to $n+1$.
- There are the following arrows
  - Horizontal arrows: $A_{ij} \to A_{i+1,j}$
  - Vertical arrow: $A_{ij} \to A_{i,j+1}$
  - Diagonal arrows: $A_{ij} \to A_{i-1,j-1}$

An example of this structure for the case of $n = 4$ is shown in below.

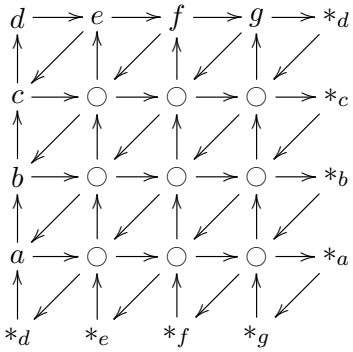

(131)

When we further compactify on a circle, the states carrying momentum along the circle become parametrically heavy. As a result, the charge lattice of the theory has its rank reduced by one. A natural way to achieve this is simply to delete a node of the above quiver, in which all nodes are identical. This is our proposal for the general $\mathcal{T}_n$ quiver. In the following we will provide two explicit checks on this procedure by studying $\mathcal{T}_2$ and $\mathcal{T}_3$ cases in more detail.

8.3 Rank 2 Quivers

All we need to construct the quiver for any rank 2 Gaiotto theory is

- The quiver for the $\mathcal{T}_2$ theory, the theory of two M5-branes on a thrice punctured Riemann surface
- A diagonal gauging rule for connecting two quivers associated with arbitrary punctured surfaces

We constructed the quiver for $\mathcal{T}_2$ in section 8.2. The gauging rule is just as described in section 8.1, except if one of the two theories we are glueing happens to be $\mathcal{T}_2$ itself. Obviously since we plan on constructing everything by starting with $\mathcal{T}_2$ quivers, this difficulty must be overcome, and we will do so below.

In the case of $\mathcal{T}_2$ the quiver takes the form:

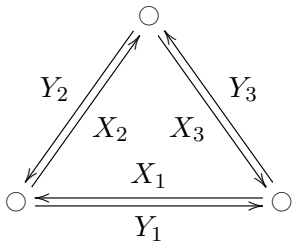

(132)

Further, the general methods of [24, 81, 82] determine the superpotential

$$W = X_1Y_1 + X_2Y_2 + X_3Y_3 + X_1X_2X_3 + Y_1Y_2Y_3. \tag{133}$$

This quiver is novel in that it provides our first example of a quiver with canceling arrows where the potential is not strong enough to integrate out the corresponding fields.

As described in section 2.3, this theory has a BPS spectrum given by a half-hypermultiplet trifundamental of the flavor group $SU(2)^3$. For generic values of the central charges of the nodes, this flavor symmetry is broken. However, the number of states, namely eight, is the same. Of these eight, only half are particles, and of these four particles, three are manifest as nodes of the quiver. Thus, consistency demands that our $\mathcal{T}_2$ quiver, together with its given superpotential, supports exactly one hypermultiplet bound state.

The existence of this single state can be checked explicitly using quiver representation theory. The unique representation with the required charges is a bound state of one of each of the three

node particles. The F-term equations of motion in this case are

$$\begin{aligned} X_1 + Y_2 Y_3 &= 0, && (134)\\ X_2 + Y_3 Y_1 &= 0, && (135)\\ X_3 + Y_1 Y_2 &= 0, && (136)\\ Y_1 + X_2 X_3 &= 0, && (137)\\ Y_2 + X_3 X_1 &= 0, && (138)\\ Y_3 + X_1 X_2 &= 0. && (139) \end{aligned}$$

The solution of interest to us has all fields non-vanishing with

$$X_1 X_2 X_3 = Y_1 Y_2 Y_3 = -1. \quad (140)$$

The moduli space can easily be determined by noting that, since X_1 and X_2 are non-zero, we can eliminate all gauge redundancy by setting $X_1 = X_2 = 1$. Then all remaining field values are fixed by the F-term equations and hence the moduli space is a point. Thus this representation results in a single hypermultiplet. Noting that this representation admits no non-trivial subrepresentations, we further conclude that this hypermultiplet is always stable and provides the required state in the spectrum.

Now that we have examined the $\mathcal{T}_2$ quiver itself, the next step is to begin glueing copies of it together by diagonally gauging $SU(2)$ flavor symmetries, as described above. We found a way to gauge generic quivers in section 8.1. However, that analysis in fact does not apply to gauging a factor of the $\mathcal{T}_2$ quiver itself, as we will see. It does apply to quivers associated with any other pair of rank 2 surfaces, so once we find how to gauge $\mathcal{T}_2$, the procedure for constructing a general rank 2 surface will be clear, and indeed agree with the results found by alternative methods in section 7.

The obvious obstruction to gauging $\mathcal{T}_2$ in the naive way can be seen by considering the charges of the quiver's nodes under the $SU(2)^3$ flavor symmetry. Recall that the content of the theory is a half-hypermultiplet transforming in the $2 \otimes 2 \otimes 2$ representation of $SU(2)^3$. We will see that no $SU(2)$ action can be made manifest on nodes of the quiver, something which is required to use the gauging procedure of section 8.1. Suppose it could. Then, without loss of generality, we can take

two of the nodes to have charges $(\frac{1}{2}, \frac{1}{2}, \frac{1}{2})$ and $(-\frac{1}{2}, \frac{1}{2}, \frac{1}{2})$. Further, we can without loss of generality assign the third node charge $(\frac{1}{2}, -\frac{1}{2}, \frac{1}{2})$. Then clearly neither the state $(\frac{1}{2}, \frac{1}{2}, -\frac{1}{2})$ nor the state $(-\frac{1}{2}, -\frac{1}{2}, \frac{1}{2})$ is a positive integral combination of the nodes. Thus indeed no $SU(2)$ symmetry can be made manifest in the quiver, and so we can't simply apply the rules of section 8.1.

Why is this example at odds with the general framework? We note that for a generic quiver, to make the states associated with some symmetry appear as nodes, we could simply go to the symmetric point in the theory and then rotate the half-plane so that they were all left-most. Usually we have such freedom because of mass parameters which accompany flavor symmetries. However, in this case the charges of the states associated with the symmetry are not independent directions in the charge lattice, and can't be independently tuned. This is related to the fact that the $SU(2)$ symmetries mix particles and anti-particles, as the symmetry acts on half-hypermultiplets.

While our general analysis does not apply here, we can still gauge an $SU(2)$ "by hand," since we know very clearly the content of this theory. After a single $SU(2)$ is gauged, the difficultly above disappears and all the subsequent quivers arrived at can be gauged in the naive way. Let us start with the $\mathcal{T}_2$ quiver with charges $(-\frac{1}{2}, -\frac{1}{2}, -\frac{1}{2})$, $(\frac{1}{2}, \frac{1}{2}, -\frac{1}{2})$ and $(-\frac{1}{2}, \frac{1}{2}, \frac{1}{2})$. The bound states of this quiver fill out, with anti-particles, the trifundamental of $SU(2)^3$.

Say we gauge the first $SU(2)$ factor. Then our quiver should be the quiver for an $SU(2)$ gauge group coupled to a basis for those states with first $SU(2)$ charge $-\frac{1}{2}$ (since the $SU(2)$ will produce the $\frac{1}{2}$ states as bound states in the usual way).[35] Thus we can simply take $(-\frac{1}{2}, -\frac{1}{2}, -\frac{1}{2})$ in addition to $(-\frac{1}{2}, \frac{1}{2}, -\frac{1}{2})$. Since the $SU(2)_1$ electromagnetic charges of these states will be identical, they couple only to the $SU(2)$ factor in the usual way, and we are left with the quiver

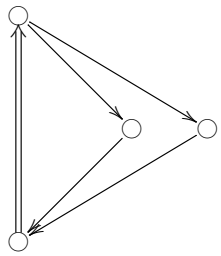

Again, once the first $SU(2)$ factor has been gauged, the methods of section 8.1 apply. Thus, we've defined a procedure for building up the quiver for any rank 2 Gaiotto theory from its pair

[35] Of course we may find additional bound states now that we have an interacting theory.

of pants decomposition. Quivers obtained via this method indeed agree with the results found in section 7. However, as we'll now see, our new method also works for cases of higher rank.

8.4 Rank 3 Quivers

In the case of $\mathcal{T}_3$ the quiver takes the form:

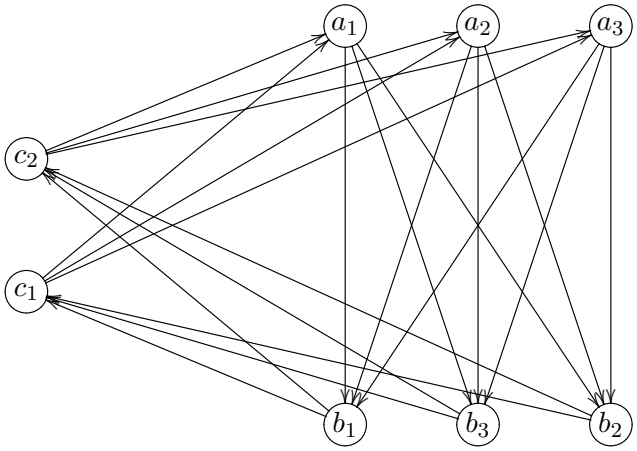

(141)

The quiver's structure can be better understood by grouping the nodes into three sets labeled above as $\{a_1, a_2, a_3\}$, $\{b_1, b_2, b_3\}$, $\{c_1, c_2\}$. In terms of the quiver there is a permutation symmetry on the a-type nodes, and similarly on the b and c-type nodes. Thus for the purposes of illustrating the general structure we can simply draw one member of each group, in which case the quiver appears as:

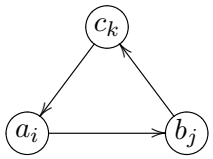

(142)

We first find a finite chamber of this quiver using the mutation method. In decreasing phase order, we find the 24 state chamber:

$$\begin{aligned}
&c_1, c_1+a_1, c_1+a_2, c_1+a_3, b_1, b_2, b_3, c_2+b_1+b_2+b_3, 2c_1+a_1+a_2+a_3,\\
&c_1+a_1+a_2, c_1+a_2+a_3, c_1+a_1+a_3, c_2+b_1+b_2, c_2+b_2+b_3, c_2+b_1+b_3,\\
&c_1+a_1+a_2+a_3, 2c_2+b_1+b_2+b_3, a_1, a_2, a_3, c_2+b_1, c_2+b_2, c_2+b_3, c_2.
\end{aligned} \tag{143}$$

We can provide a strong consistency check on our proposal for this quiver by recalling that

the $\mathcal{T}_3$ theory coincides with the E_6 Minahan-Nemeschansky theory [45]. In particular, the flavor symmetry group $SU(3)^3$ sits inside a full E_6 flavor group. The E_6 theory enjoys an Argyres-Seiberg type duality [44], which we explored in section 2.3. In particular, there is an equivalence between the E_6 theory with an $SU(2)$ subgroup of its flavor symmetry gauged and coupled to an additional fundamental, and $SU(3)$ SYM coupled to 6 fundamentals.

This duality has a strict implication for our T_3 quiver. On one side, we can gauge an $SU(2)$ global symmetry in the $\mathcal{T}_3$ quiver following the considerations of section 8.1, and couple to it and additional fundamental in the obvious way; on the other side, we have proposed and studied quivers of arbitrary $SU(N)$ SQCD theories in section 6.4. Since these theories are to be connected by a single moduli space, there must exist some mutation equivalence between their quivers.

Indeed, in the process of checking this duality, we find an additional check that we can perform. The $\mathcal{T}_3$ quiver exhibits $S_2 \times S_3 \times S_3$ discrete symmetries, acting on the c, b, and a-type nodes which by the reasoning of section 8.1 indicates a global $SU(2) \times SU(3) \times SU(3)$ of the resulting physics. The actual theory admits a full E_6 symmetry, which contains three identical $SU(3)$s; however, we only see the $SU(2)$ subgroup of one of these $SU(3)$'s. The physics, on the other hand, does not distinguish between the three $SU(3)$'s, and thus applying the quiver gauging rules to any of the three $SU(2)$'s available should give mutation equivalent results. It is a nontrivial fact that the quivers obtained from these three gauging procedures,

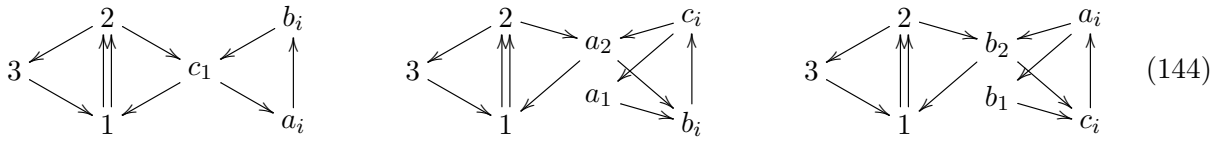

(144)

are all mutation equivalent, and hence describe the same 4d field theory.[36] In these quivers, we have represented the triplets of identical nodes as a_i, b_i, $i = 1, 2, 3$, and the pair of identical nodes c_i, $i = 1, 2$. The arrows incident on these duplicated nodes of course indicate sets of arrows, one incident on each of the duplicated nodes. Beginning with the quiver on the left, we can obtain the middle quiver by the following mutation sequence:

$$3, c, b_1, a_1, c, 3, 2, 1, b_1, b_2, c,$$

[36] In view of what's to come, we have already coupled additional fundamentals to our $SU(2)$s.

and we obtain the quiver on the right via:

$$3, c, b_1, a_1, c, 3, 2, 1, b_1, b_2, 1.$$

Now we return to our check of Argyres-Seiberg duality. Since the three quivers obtained by gauging an $SU(2)$ subgroup are mutation equivalent, we now focus on the left-most quiver. Argyres-Seiberg duality indicates that this quiver should be mutation equivalent to:

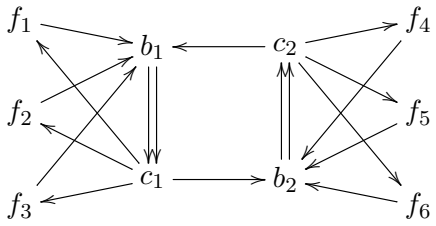

(145)

Beginning again with the left-most quiver above, we find a mutation equivalence given by

$$3, c, b_1, a_1, 2, a_1, a_2, a_3, b_2, b_3.$$

This is a very robust check. Argyres-Seiberg duality is manifest at the level of quivers by a non-trivial sequence of mutation dualities.

Now we consider how one would write the quiver for a general rank 3 Gaiotto theory. First we recall the new punctures on Riemann surfaces that arise in the rank 3 case. For rank 2, there was a single type of puncture, which indicated an $SU(2)$ flavor symmetry of the theory. In rank 3, we have two types of punctures; punctures of the first kind indicate $U(1)$ flavor symmetries, and punctures of the second kind indicate $SU(3)$ flavor symmetries.

We require two quiver gauging rules to build up new theories. The first is the analog of the glueing/gauging rule developed in section 8.1. We consider glueing two Riemann surfaces along punctures of the second kind. This again corresponds to gauging the diagonal subgroup $SU(3)_d \subset SU(3)_1 \times SU(3)_2$ of two flavor symmetries associated with the two punctures. At the level of the quiver, we have a straightforward rule - identify the two $SU(3)$ flavor symmetries as S_3 discrete symmetries of the respective quivers, delete two of the three symmetric nodes from each quiver, add a $SU(3)$ SYM subquiver, and couple the remaining nodes from each triplet as

fundamental **3**'s of the new $SU(3)$ subquiver. The other operation on Riemann surfaces we must understand is that of splitting punctures. The prototypical example of this operation is exactly the Argyres-Seiberg duality just discussed. Argyres-Seiberg duality related the Gaiotto theory on a sphere with two punctures of each kind (which gives $SU(3)$, $N_f = 6$) to the theory on a sphere with three punctures of the second kind (the $\mathcal{T}_3$ theory), with a gauged $SU(2)$ flavor symmetry. We may interpret this as splitting a puncture of the second kind into two punctures of the first kind. The effect on the resulting physics is to gauge an $SU(2)$ subgroup of the $SU(3)$ flavor symmetry corresponding to the split puncture, and couple a fundamental to the gauged $SU(2)$. Again we have a straightforward gauging procedure for the quiver.

Although we have described quite explicit rules, we must now face some limitations in implementing them. Recall from section 8.1 that in the rank 2 case, for a surface with p punctures, there exists a mutation form with $p-1$ global $SU(2)$ symmetries visible in the quiver. Because of this fact, we can gauge all but one $SU(2)$, and thus build up any surface with at least one puncture. In the rank 3 case, all of the quivers have infinite mutation classes [21]. As a result, there is no easy way to systematically search the mutation classes and identify a quiver that makes the maximal number of symmetries visible. As we glue quivers, we actually are losing visible symmetries. For example, consider glueing two $\mathcal{T}_3$ theories to form the sphere with four punctures of the second kind. We start with two visible $SU(3)$ symmetries in each quiver; after the glueing, the resulting theory has only two remaining visible $SU(3)$'s. In order to find the maximal three $SU(3)$'s, we would need to go through some mutation sequence, which could involve arbitrarily many mutations. Finding such a mutation sequence is quite a difficult computational problem that scales as $(\text{number of nodes})^{(\text{length of sequence})}$. Unfortunately, this is an obstruction to implementing this procedure in practice if one wants to obtain surfaces of genus two or higher.

Nonetheless, these techniques allow us to propose quivers for spheres and tori with sufficient punctures. Let (p_1, p_2) denote the number of punctures of the first and second kind respectively. Glueing a $\mathcal{T}_3$ surface to an existing theory takes $(p_1, p_2) \to (p_1, p_2 + 2)$, and the splitting rule takes $(p_1, p_2) \to (p_1 + 2, p_2 - 1)$. We take as our base cases the $\mathcal{T}_3$ theory (a sphere with $(0, 3)$ punctures). The latter theory has a weak coupling description as an $SU(3)^2$ gauge theory with a bifundamental

and three fundamental quarks for each $SU(3)$. This leads to a proposal for the associated quiver,

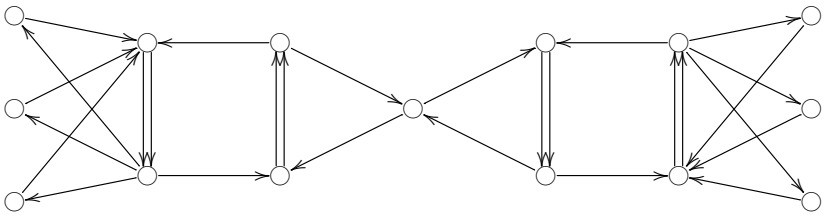

(146)

From these two base cases it is relatively easy to see that the glueing and splitting rules will allow us to construct spheres satisfying $p_1 + 2p_2 \geq 6$ and tori satisfying $p_1 + 2p_2 \geq 2$.

8.5 $\mathcal{N} = 2^*$

We conclude with an example of a theory which gives our methods difficulty, but is nonetheless interesting. This is the $\mathcal{N} = 2^*$ theory, a massive deformation of conformal $\mathcal{N} = 4$, where we give the adjoint hypermultiplet some non-zero mass. Alternatively, it is simply a gauge theory with a massive hypermultiplet charged under the adjoint of the gauge group. For $SU(2)$ this is given, following the discussion in section 5.2, by the following quiver:

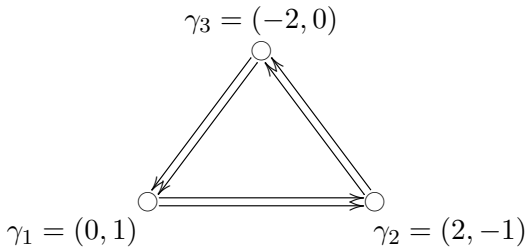

(147)

As indicated in section 5.2, this quiver indeed turns out to generate matter content of the full $\mathbf{2} \otimes \mathbf{2} = \mathbf{3} \oplus \mathbf{1}$. Thus it gives the $\mathcal{N} = 2^*$ theory plus an uncharged singlet hypermultiplet. In section 7.4.2, this quiver was obtained in studying the rank two Gaiotto theory on a torus with one puncture. We can understand this matter content from the point of view of [38]. We start with a pair of pants, corresponding to a half-hypermultiplet charged as a trifundamental under three $SU(2)$ flavor groups, represented by the three boundary components. Glueing together two boundary components of the pair of pants identifies the two $SU(2)$'s and gauges them. To form the punctured torus, we glue two legs together, producing an $SU(2)$ gauge group, and matter content $\mathbf{2} \otimes \mathbf{2} = \mathbf{3} \oplus \mathbf{1}$.

This fact can be checked from the BPS spectrum as follows. Consider the rep $\gamma_1 + \gamma_2 + \gamma_3$ of this quiver. This rep has charge $(0, 0)$ meaning that it is a pure flavor state. For $\mathcal{N} = 2^*$ we would expect such a hypermultiplet, corresponding to the state inside the **3** that is uncharged under the $U(1) \subset SU(2)$; if we add an uncoupled singlet, we would then expect this site of the charge lattice to be occupied by two BPS particles. Quiver representation theory finds the latter situation, as we now demonstrate.

The superpotential for this quiver was worked out in [24]. The result was

$$\mathcal{W} = X_{12}X_{23}X_{31} + Y_{12}Y_{23}Y_{31} + X_{12}Y_{23}X_{31}Y_{12}X_{23}Y_{31}. \tag{148}$$

Here, X_{ij}, Y_{ij} correspond to the two maps between nodes i, j in the representation. The resulting F-terms are of the form

$$X_{23}X_{31} + Y_{23}X_{31}Y_{12}X_{23}Y_{31} = 0, \tag{149}$$

$$X_{12}X_{23} + Y_{12}X_{23}Y_{31}X_{12}Y_{23} = 0, \tag{150}$$

$$X_{31}X_{12} + Y_{31}X_{12}Y_{23}X_{31}Y_{12} = 0, \tag{151}$$

$$Y_{23}Y_{31} + X_{23}Y_{31}X_{12}Y_{23}X_{31} = 0, \tag{152}$$

$$Y_{12}Y_{23} + X_{12}Y_{23}X_{31}Y_{12}X_{23} = 0, \tag{153}$$

$$Y_{31}Y_{12} + X_{31}Y_{12}X_{23}Y_{31}X_{12} = 0. \tag{154}$$

We are studying the rep $\gamma_1 + \gamma_2 + \gamma_3$, so all gauge groups are $U(1)$, and the bifundamental fields here are simply 1×1 matrices. In this example, we can solve the full equations by just truncating to the quadratic pieces and solving those, since setting the quadratic pieces to zero also sets the

quintic terms to zero.[37].

$$X_{23}X_{31} = 0 \tag{155}$$

$$X_{12}X_{23} = 0 \tag{156}$$

$$X_{31}X_{12} = 0 \tag{157}$$

$$Y_{23}Y_{31} = 0 \tag{158}$$

$$Y_{12}Y_{23} = 0 \tag{159}$$

$$Y_{31}Y_{12} = 0 \tag{160}$$

These will set two of the X's and two of the Y's equal to zero. We will focus on the two non-zero fields, X_i, Y_j, with $i, j \in \{(12), (23), (31)\}$. Before going on, we pause to consider what the possible moduli spaces may be. For any choice of i, j, there is enough gauge symmetry to set both X_i, Y_j to one; thus the moduli space is at most 9 points, one for each choice of (i, j). Some of these points will be eliminated by the stability analysis. Note that Π-stability does not distinguish between X, Y, so if $X_i, Y_j \neq 0$ is stable, then $X_j, Y_i \neq 0$ is also stable. We will show below that the stability analysis always yields a moduli space of 2 points.

The simplest way to proceed is a case-by-case analysis of the possible orderings of central charges. For each choice of orderings, we will consider the following cases of (i, j): (a) $(12, 23)$, (b) $(23, 31)$, (c) $(31, 12)$, (d) $(12, 12)$, (e) $(23, 23)$, (f) $(31, 31)$. There are three more cases obtained by exchanging (i, j). A simple study of commutative diagrams shows that, for (a) the subreps are $\gamma_3, \gamma_2 + \gamma_3$. By cyclic symmetry, (b) has subreps $\gamma_1, \gamma_3 + \gamma_1$, and for (c), $\gamma_2, \gamma_1 + \gamma_2$. For (d) we find subreps $\gamma_2, \gamma_3, \gamma_2 + \gamma_3, \gamma_1 + \gamma_2$; (e) and (f) have subreps given by cyclic symmetry. We can choose γ_1 to be the left-most node without loss of generality. Automatically, (e) and (f) are unstable due to the subrep γ_1 which has $\arg \mathcal{Z}(\gamma_1) > \arg \mathcal{Z}(\gamma_1 + \gamma_2 + \gamma_3)$. Suppose $\arg \mathcal{Z}(\gamma_1) > \arg \mathcal{Z}(\gamma_2) > \arg \mathcal{Z}(\gamma_3)$. Then rep (b) is destabilized by subrep γ_1, and reps (c,d) are destabilized by subrep $\gamma_1 + \gamma_2$. Rep (a), on the other hand, is stable since its subreps have $\arg \mathcal{Z}(\gamma_1 + \gamma_2 + \gamma_3) > \arg \mathcal{Z}(\gamma_2 + \gamma_3) > \arg \mathcal{Z}(\gamma_3)$. So here the moduli space is 2 points, $X_{12}, Y_{23} \neq 0$ and $X_{23}, Y_{12} \neq 0$. Next, we consider

[37]There is also a solution given by nontrivial cancellation between the quadratic and quintic terms. However, the resulting moduli space is non-compact, so its cohomology contains no normalizable forms, and as such it does not contribute to the particle spectrum

$\arg \mathcal{Z}(\gamma_1) > \arg \mathcal{Z}(\gamma_1+\gamma_2) > \arg \mathcal{Z}(\gamma_3) > \arg \mathcal{Z}(\gamma_2)$. Rep (a) is again stable, while rep (b) is destabilized by γ_1 and reps (c,d) are destabilized by $\gamma_1+\gamma_2$. The final case we must study is $\arg \mathcal{Z}(\gamma_1) > \arg \mathcal{Z}(\gamma_3) > \arg \mathcal{Z}(\gamma_1+\gamma_2) > \arg \mathcal{Z}(\gamma_2)$. Now we find that rep (c) is stable, while reps (a,d) are destabilized by γ_3 and rep (b) is destabilized by γ_1. The conclusion is that the moduli space of the rep $(\gamma_1+\gamma_2+\gamma_3)$ is simply two points for any choice of parameters. Therefore, at all values in the parameter space of this theory, we find *two* hypermultiplets with no electric-magnetic charge. This confirms that the quiver is describing the Gaiotto construction, $\mathcal{N}=2^*$ plus a single uncharged hypermultiplet.

The spectrum of this theory is extremely intricate for any chamber of the moduli space. We will demonstrate the existence of at least two vector particles for any choice of central charges. Without loss of generality, we take γ_1 to be leftmost. Then we should consider two cases. If $\arg \mathcal{Z}(\gamma_1) > \arg \mathcal{Z}(\gamma_2) > \arg \mathcal{Z}(\gamma_3)$, then the Π-stability analysis yields $\gamma_1+\gamma_2 = (2,0)$ and $\gamma_1+\gamma_3 = (-2,1)$ as stable vector particles. Alternatively, if $\arg \mathcal{Z}(\gamma_1) > \arg \mathcal{Z}(\gamma_3) > \arg \mathcal{Z}(\gamma_2)$, then $\gamma_1+\gamma_2$ is a stable vector particle, along with either $(n+1)\gamma_1+n\gamma_2+\gamma_3$ or $n\gamma_1+(n+1)\gamma_2+\gamma_3$ for some choice of n. In any of the cases, the two vector particles identified have non-zero electric-magnetic inner product. Consequently, the stable vector states could form a highly complicated spectrum of bound states. The presence of multiple accumulation rays (one at each vector) obstructs the mutation method as defined from producing an unambiguous result for the spectrum. We can use left and right mutation to identify some set of dyons, along with the left-most and right-most vector states; however, the region of the $\mathcal{Z}$-plane between the two vectors could be arbitrarily wild. The problem awaits further insight.

References

[1] N. Seiberg and E. Witten, "Electric - magnetic duality, monopole condensation, and confinement in N=2 supersymmetric Yang-Mills theory," *Nucl.Phys.* **B426** (1994) 19–52, `arXiv:hep-th/9407087 [hep-th]`.

[2] N. Seiberg and E. Witten, "Monopoles, duality and chiral symmetry breaking in N=2 supersymmetric QCD," *Nucl.Phys.* **B431** (1994) 484–550, `arXiv:hep-th/9408099 [hep-th]`.

[3] F. Ferrari and A. Bilal, Nucl. Phys. B **469**, 387 (1996) [hep-th/9602082].

[4] F. Denef, "Supergravity flows and D-brane stability," *JHEP* **0008** (2000) 050, arXiv:hep-th/0005049 [hep-th].

[5] F. Denef and G. W. Moore, "Split states, entropy enigmas, holes and halos," arXiv:hep-th/0702146 [hep-th].

[6] D. Gaiotto, G. W. Moore, and A. Neitzke, "Four-dimensional wall-crossing via three-dimensional field theory," *Commun.Math.Phys.* **299** (2010) 163–224, arXiv:0807.4723 [hep-th].

[7] D. Joyce and Y. Song, "A Theory of generalized Donaldson-Thomas invariants," arXiv:0810.5645 [math.AG].

[8] D. Joyce and Y. Song, "A theory of generalized Donaldson-Thomas invariants. II. Multiplicative identities for Behrend functions," arXiv:0901.2872 [math.AG].

[9] D. Joyce, "On counting special Lagrangian homology 3-spheres," *Contemp. Math.* **314** (2002) 125–151, arXiv:hep-th/9907013.

[10] M. Kontsevich and Y. Soibelman, "Stability structures, motivic Donaldson-Thomas invariants and cluster transformations," *ArXiv e-prints* (Nov., 2008) , arXiv:0811.2435 [math.AG].

[11] T. Dimofte and S. Gukov, "Refined, Motivic, and Quantum," *Lett.Math.Phys.* **91** (2010) 1, arXiv:0904.1420 [hep-th].

[12] D. Gaiotto, G. W. Moore, and A. Neitzke, "Wall-crossing, Hitchin Systems, and the WKB Approximation," arXiv:0907.3987 [hep-th].

[13] S. Cecotti and C. Vafa, "BPS Wall Crossing and Topological Strings," arXiv:0910.2615 [hep-th].

[14] T. Dimofte, S. Gukov, and Y. Soibelman, "Quantum Wall Crossing in N=2 Gauge Theories," *Lett.Math.Phys.* **95** (2011) 1–25, arXiv:0912.1346 [hep-th].

[15] D. Gaiotto, G. W. Moore, and A. Neitzke, "Framed BPS States," arXiv:1006.0146 [hep-th].

[16] S. Cecotti, A. Neitzke, and C. Vafa, "R-Twisting and 4d/2d Correspondences," arXiv:1006.3435 [hep-th].

[17] E. Andriyash, F. Denef, D. L. Jafferis, and G. W. Moore, "Wall-crossing from supersymmetric galaxies," arXiv:1008.0030 [hep-th].

[18] E. Andriyash, F. Denef, D. L. Jafferis, and G. W. Moore, "Bound state transformation walls," arXiv:1008.3555 [hep-th].

[19] J. Manschot, B. Pioline, and A. Sen, "Wall Crossing from Boltzmann Black Hole Halos," *JHEP* **1107** (2011) 059, arXiv:1011.1258 [hep-th].

[20] D. Gaiotto, G. W. Moore, and A. Neitzke, "Wall-Crossing in Coupled 2d-4d Systems," arXiv:1103.2598 [hep-th].

[21] S. Cecotti and C. Vafa, "Classification of complete N=2 supersymmetric theories in 4 dimensions," arXiv:1103.5832 [hep-th].

[22] S. Cecotti and M. Del Zotto, "On Arnold's 14 'exceptional' N=2 superconformal gauge theories," *JHEP* **1110** (2011) 099, arXiv:1107.5747 [hep-th].

[23] M. Alim, S. Cecotti, C. Cordova, S. Espahbodi, A. Rastogi, and C. Vafa, "N=2 Quantum Field Theories and Their BPS Quivers," arXiv:1112.3984 [hep-th].

[24] M. Alim, S. Cecotti, C. Cordova, S. Espahbodi, A. Rastogi, and C. Vafa, "BPS Quivers and Spectra of Complete N=2 Quantum Field Theories," arXiv:1109.4941 [hep-th].

[25] M. Del Zotto, "More Arnold's N = 2 superconformal gauge theories," *JHEP* **1111** (2011) 115, arXiv:1110.3826 [hep-th].

[26] A. Sen, "Equivalence of Three Wall Crossing Formulae," arXiv:1112.2515 [hep-th].

[27] M. R. Douglas and G. W. Moore, "D-branes, Quivers, and ALE Instantons," arXiv:hep-th/9603167.

[28] H. Derksen, J. Weyman, and A. Zelevinsky, "Quivers with potentials and their representations I: Mutations," arXiv:0704.0649 [math.RA].

[29] D.-E. Diaconescu and J. Gomis, "Fractional branes and boundary states in orbifold theories," *JHEP* **0010** (2000) 001, arXiv:hep-th/9906242 [hep-th].

[30] M. R. Douglas, B. Fiol, and C. Römelsberger, "Stability and BPS branes," *JHEP* **0509** (2005) 006, arXiv:hep-th/0002037 [hep-th].

[31] M. R. Douglas, B. Fiol, and C. Römelsberger, "The Spectrum of BPS branes on a noncompact Calabi-Yau," *JHEP* **0509** (2005) 057, arXiv:hep-th/0003263 [hep-th].

[32] B. Fiol and M. Marino, "BPS states and algebras from quivers," *JHEP* **0007** (2000) 031, arXiv:hep-th/0006189 [hep-th].

[33] B. Fiol, "The BPS spectrum of N = 2 SU(N) SYM and parton branes," arXiv:hep-th/0012079.

[34] S. Fomin and A. Zelevinsky, "Cluster algebras I: Foundations," arXiv:math/0104151.

[35] F. Denef, "Quantum quivers and Hall / hole halos," *JHEP* **0210** (2002) 023, arXiv:hep-th/0206072 [hep-th].

[36] P. C. Argyres and M. R. Douglas, "New phenomena in SU(3) supersymmetric gauge theory," *Nucl.Phys.* **B448** (1995) 93–126, arXiv:hep-th/9505062 [hep-th].

[37] E. Witten, "Solutions of four-dimensional field theories via M theory," *Nucl.Phys.* **B500** (1997) 3–42, arXiv:hep-th/9703166 [hep-th].

[38] D. Gaiotto, "N=2 dualities," arXiv:0904.2715 [hep-th].

[39] D. Gaiotto and J. Maldacena, "The Gravity duals of N=2 superconformal field theories," arXiv:0904.4466 [hep-th].

[40] F. Benini, S. Benvenuti, and Y. Tachikawa, "Webs of five-branes and N=2 superconformal field theories," *JHEP* **0909** (2009) 052, arXiv:0906.0359 [hep-th].

[41] O. Chacaltana and J. Distler, "Tinkertoys for Gaiotto Duality," *JHEP* **1011** (2010) 099, arXiv:1008.5203 [hep-th].

[42] O. Chacaltana and J. Distler, "Tinkertoys for the D_N series," arXiv:1106.5410 [hep-th].

[43] D. Xie, "*work in progress*".

[44] P. C. Argyres and N. Seiberg, "S-duality in N=2 supersymmetric gauge theories," *JHEP* **0712** (2007) 088, arXiv:0711.0054 [hep-th].

[45] J. A. Minahan and D. Nemeschansky, "An N=2 superconformal fixed point with E(6) global symmetry," *Nucl.Phys.* **B482** (1996) 142–152, arXiv:hep-th/9608047 [hep-th].

[46] N. Seiberg, "Electric - magnetic duality in supersymmetric nonAbelian gauge theories," *Nucl.Phys.* **B435** (1995) 129–146, arXiv:hep-th/9411149 [hep-th].

[47] P. S. Aspinwall, T. Bridgeland, A. Craw, M. Douglas, M. Gross, A. Kapustin, G. W. Moore, G. Segal, B. Szendrői, and P. Wilson, *Dirichlet Branes and Mirror Symmetry, (Clay mathematics monographs. Volume 4)*. American Mathematical Society, Clay Mathematics Institute, 2009.

[48] D.-E. Diaconescu, M. R. Douglas, and J. Gomis, "Fractional branes and wrapped branes," *JHEP* **9802** (1998) 013, arXiv:hep-th/9712230 [hep-th].

[49] S. Cecotti and C. Vafa, "On classification of N=2 supersymmetric theories," *Commun. Math. Phys.* **158** (1993) 569–644, arXiv:hep-th/9211097.

[50] K. Hori, A. Iqbal, and C. Vafa, "D-branes and mirror symmetry," arXiv:hep-th/0005247 [hep-th].

[51] F. Cachazo, B. Fiol, K. A. Intriligator, S. Katz, and C. Vafa, "A Geometric unification of dualities," *Nucl.Phys.* **B628** (2002) 3–78, arXiv:hep-th/0110028 [hep-th].

[52] B. Feng, A. Hanany, Y. H. He, and A. Iqbal, "Quiver theories, soliton spectra and Picard-Lefschetz transformations," *JHEP* **0302** (2003) 056, arXiv:hep-th/0206152 [hep-th].

[53] B. Feng, A. Hanany, and Y.-H. He, "D-brane gauge theories from toric singularities and toric duality," *Nucl.Phys.* **B595** (2001) 165–200, arXiv:hep-th/0003085 [hep-th].

[54] B. Feng, A. Hanany, and Y.-H. He, "Phase structure of D-brane gauge theories and toric duality," *JHEP* **0108** (2001) 040, arXiv:hep-th/0104259 [hep-th].

[55] A. Hanany and K. D. Kennaway, "Dimer models and toric diagrams," arXiv:hep-th/0503149 [hep-th].

[56] S. Franco, A. Hanany, K. D. Kennaway, D. Vegh, and B. Wecht, "Brane dimers and quiver gauge theories," *JHEP* **0601** (2006) 096, arXiv:hep-th/0504110 [hep-th].

[57] B. Feng, Y.-H. He, K. D. Kennaway, and C. Vafa, "Dimer models from mirror symmetry and quivering amoebae," *Adv.Theor.Math.Phys.* **12** (2008) 3, arXiv:hep-th/0511287 [hep-th].

[58] A. Klemm, P. Mayr, and C. Vafa, "BPS states of exceptional non-critical strings," arXiv:hep-th/9607139.

[59] S. H. Katz, A. Klemm, and C. Vafa, "Geometric engineering of quantum field theories," *Nucl. Phys.* **B497** (1997) 173–195, arXiv:hep-th/9609239.

[60] A. Klemm, W. Lerche, P. Mayr, C. Vafa, and N. P. Warner, "Selfdual strings and N=2 supersymmetric field theory," *Nucl.Phys.* **B477** (1996) 746–766, arXiv:hep-th/9604034 [hep-th].

[61] A. D. Shapere and C. Vafa, "BPS structure of Argyres-Douglas superconformal theories," arXiv:hep-th/9910182 [hep-th].

[62] S. Fomin, M. Shapiro, and D. Thurston, "Cluster algebras and triangulated surfaces. Part I: Cluster complexes," *Acta Mathematica* **201** (Aug., 2006) 83–146, arXiv:math/0608367.

[63] A. Felikson, M. Shapiro, and P. Tumarkin, "Skew-symmetric cluster algebras of finite mutation type," arXiv:0811.1703 [math.CO].

[64] A. King, "Moduli of representations of finitedimensional algebras," *Quart. J. Mat. Oxford* **45** (1994) 515–530.

[65] P. Gabriel, "Unzerlegbare Darstellungen," *Manuscripta Mathematica* **6** (1972) 71–103.

[66] I. N. Bernstein, I. M. Gel'fand, and V. A. Ponomarev, "Coxeter Functors and Gabriel's Theorem," *Russian Mathematical Surveys* **28** (Apr., 1973) 17–32.

[67] C. E. Beasley and M. Plesser, "Toric duality is Seiberg duality," *JHEP* **0112** (2001) 001, arXiv:hep-th/0109053 [hep-th].

[68] B. Feng, A. Hanany, Y.-H. He, and A. M. Uranga, "Toric duality as Seiberg duality and brane diamonds," *JHEP* **0112** (2001) 035, arXiv:hep-th/0109063 [hep-th].

[69] D. Berenstein and M. R. Douglas, "Seiberg duality for quiver gauge theories," arXiv:hep-th/0207027.

[70] B. Keller, "Cluster algebras, quiver representations and triangulated categories," arXiv:0807.1960 [math.RT].

[71] B. Keller, "On cluster theory and quantum dilogarithm identities," *ArXiv e-prints* (Feb., 2011) , arXiv:1102.4148 [math.RT].

[72] F. Ferrari and A. Bilal, "The Strong coupling spectrum of the Seiberg-Witten theory," *Nucl.Phys.* **B469** (1996) 387–402, arXiv:hep-th/9602082 [hep-th].

[73] A. Bilal and F. Ferrari, "Curves of marginal stability, and weak and strong coupling BPS spectra in N=2 supersymmetric QCD," *Nucl.Phys.* **B480** (1996) 589–622, arXiv:hep-th/9605101 [hep-th].

[74] A. Bilal and F. Ferrari, "The BPS spectra and superconformal points in massive N=2 supersymmetric QCD," *Nucl.Phys.* **B516** (1998) 175–228, arXiv:hep-th/9706145 [hep-th].

[75] S. Katz, P. Mayr, and C. Vafa, "Mirror symmetry and exact solution of 4-D N=2 gauge theories: 1.," *Adv.Theor.Math.Phys.* **1** (1998) 53–114, arXiv:hep-th/9706110 [hep-th].

[76] W. Lerche, "On a boundary CFT description of nonperturbative N=2 Yang-Mills theory," arXiv:hep-th/0006100 [hep-th].

[77] A. Klemm, W. Lerche, S. Yankielowicz, and S. Theisen, "Simple singularities and N=2 supersymmetric Yang-Mills theory," *Phys.Lett.* **B344** (1995) 169–175, arXiv:hep-th/9411048 [hep-th].

[78] P. C. Argyres and A. E. Faraggi, "The vacuum structure and spectrum of N=2 supersymmetric SU(n) gauge theory," *Phys.Rev.Lett.* **74** (1995) 3931–3934, arXiv:hep-th/9411057 [hep-th].

[79] A. Klemm, W. Lerche, and S. Theisen, "Nonperturbative effective actions of N=2 supersymmetric gauge theories," *Int.J.Mod.Phys.* **A11** (1996) 1929–1974, arXiv:hep-th/9505150 [hep-th].

[80] W. Lerche, "Introduction to Seiberg-Witten theory and its stringy origin," *Nucl.Phys.Proc.Suppl.* **55B** (1997) 83–117, arXiv:hep-th/9611190 [hep-th].

[81] D. Labardini-Fragoso, "Quivers with potentials associated to triangulated surfaces," arXiv:0803.1328 [math.RT].

[82] D. Labardini-Fragoso, "Quivers with potentials associated to triangulated surfaces, Part II: Arc representations," arXiv:0909.4100 [math.RT].

[83] G. Cerulli Irelli and D. Labardini-Fragoso, "Quivers with potentials associated to triangulated surfaces, Part III: tagged triangulations and cluster monomials," arXiv:1108.1774 [math.RT].

[84] D. Gaiotto, G. W. Moore, and A. Neitzke, "*S-wall networks*, talk given by A. Neitzke at KITP and *Surface defects and spectral networks*, talk given by G. Moore at Harvard".

[85] K. Strebel, *Quadratic Differentials*. Springer Verlag, 1984.

[86] A. Bakke Buan and I. Reiten, "Cluster algebras associated with extended Dynkin quivers," arXiv:math/0507113.

[87] H. Derksen and T. Owen, "New Graphs of Finite Mutation Type," arXiv:0804.0787 [math.CO].

[88] S. Ladkani, "Mutation classes of certain quivers with potentials as derived equivalence classes," arXiv:1102.4108 [math.RT].

[89] A. Strominger, "Special geometry," *Communications in Mathematical Physics* **133** (1990) 163–180. http://dx.doi.org/10.1007/BF02096559.

[90] P. C. Argyres and A. E. Faraggi, Phys. Rev. Lett. **74**, 3931 (1995) [hep-th/9411057].

[91] P. C. Argyres, M. R. Plesser and A. D. Shapere, Phys. Rev. Lett. **75**, 1699 (1995) [hep-th/9505100].

[92] P. C. Argyres and A. D. Shapere, Nucl. Phys. B **461**, 437 (1996) [hep-th/9509175].

[93] P. C. Argyres, M. R. Plesser, N. Seiberg and E. Witten, Nucl. Phys. B **461**, 71 (1996) [hep-th/9511154].

[94] W. Lerche, Nucl. Phys. Proc. Suppl. **55B**, 83 (1997) [Fortsch. Phys. **45**, 293 (1997)] [hep-th/9611190].